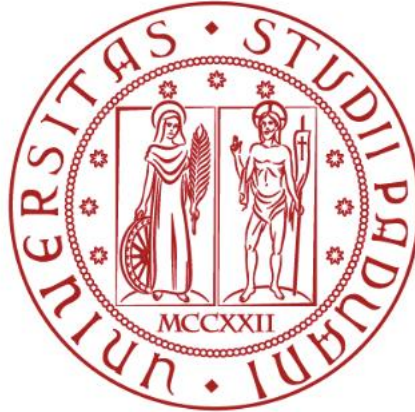


UNIVERSITÀ DEGLI STUDI DI PADOVA

DIPARTIMENTO DI BIOLOGIA

Corso di Laurea magistrale in Marine Biology



TESI DI LAUREA

**Modelling the impact of Climate Change on
the habitat distribution of the fin whale in the
Mediterranean Sea**

Relatore: Prof Gianfranco Santovito (Dipartimento di Biologia)

**Correlatore: Prof Eduardo Jorge Belda Perez (Dipartimento de
Ciencia Animal, Universitat Politcnica de Valencia)**

**Fondazione CIMA- Centro Internazionale in Monitoraggio
Ambientale**

Laureanda: Maria Giovanna Gavin

ANNO ACCADEMICO 2024/2025

Acknowledgements

I wish to express my profound gratitude to my parents, Gianfranco and Maria Cristina, whose tireless support and constant encouragement throughout my years of study have been the foundation of my academic journey and have inspired me to pursue my university career with determination.

I am deeply indebted to Universitat Politècnica de Valencia and in particular, to Professor Eduardo Jorge Belda Pérez for his invaluable guidance and support during all the stage of this work. My sincere thanks also go to the distinguished researcher Víctor Gallego, whose passion and expertise have been a true source of inspiration.

I extend my heartfelt appreciation to Professor Gianfranco Santovito for his supervision of this internship and to Professor Alberto Barausse for his generous assistance and mentorship during my internship.

Finally, I reserve a special thank you for Elena, Naira, Giovanni and Moisés, whose closeness, encouragement, and unconditional support in these months have meant more to me than words can express.

TABLE OF CONTENTS

Abstract

INDEX

1. INTRODUCTION	7
<i>1.1 Fin whale biology and ecology</i>	7
1.1.1 Mediterranean population and distribution area	10
1.1.2 Movements and migratory behaviour	13
1.1.3 Feeding ecology and prey-driven distribution	16
<i>1.2 Fin whale anthropogenic threats</i>	17
1.2.1 Historical whaling	18
1.2.2 Vessel collision	19
1.2.3 Underwater noise	21
1.2.4 Chemicals and plastic pollution	22
<i>1.3 The Mediterranean sea: oceanographic characteristics and habitat features</i>	25
1.3.1 Western Mediterranean	26
1.3.2 Catalano-Balearic Sea	27
1.3.3 Gulf of Lion	27
1.3.4 Ligurian Sea	27
<i>1.4 Climate change</i>	29
1.4.1 Climate change in the Mediterranean Sea	30
1.4.2 Effects of climate change on plankton	31
<i>1.5 Protected areas and conservation frameworks in the Mediterranean Sea</i>	33
1.5.1 IUCN red list and other protecting organization	33
<i>1.6 Aim and structure of this study</i>	39
2. MATERIAL AND METHODS	40
<i>2.1 Ecological modelling for species distribution</i>	40
2.1.1 Species Distribution Models (SDMs)	40
2.1.2 Generalized Additive Models	41
2.1.3 Random Forest	42
<i>2.2 Study area</i>	43
<i>2.3 Environmental variables selected</i>	46
2.3.1 Sea Surface Temperature (SST)	48
2.3.2 Phytoplankton	49
2.3.3 Zooplankton	49
<i>2.4 Data collection</i>	51
2.4.1 Opportunistic data	53
2.4.2 Pseudo-Absence Generation	54
<i>2.5 Workflow of ecological models</i>	55
2.5.1 Workflow of presence and pseudo absence data	55
2.5.1 Workflow of GAM	57
2.5.2 Workflow of Random Forest	60
2.5.3 Workflow of future prediction	62
<i>2.6 Software and Computational Details</i>	64
3. RESULTS	64
<i>3.1 GAM</i>	64

3.2 <i>Random Forest</i>	67
3.2.2 Sea Surface Temperature	72
3.2.3 Phytoplankton	73
3.2.4 Zooplankton	76
3.3 <i>Future prediction</i>	79
3.3.1 RCP 4.5	79
3.3.2 RCP 8.5	81
4. DISCUSSION	83
4.1 <i>GAM</i>	83
4.2 <i>Random Forest</i>	84
4.3 <i>SST</i>	85
4.5 <i>Phytoplankton</i>	89
4.6 <i>Zooplankton</i>	90
4.7 <i>Future prediction</i>	92
4.7.1 RCP 4.5 year 2050	92
4.7.2 RCP 4.5 for year 2099	93
4.7.3 RCP 8.5 for year 2050	95
Under the RCP 8.5 high-emissions scenario for 2050, the western Mediterranean fin whale habitat undergoes pronounced decreasing trend.	95
4.7.4 RCP 8.5 for year 2099	96
5. CONCLUSION	98
6. BIBLIOGRAPHY	100

ABSTRACT

The Mediterranean Sea, despite covering less than 1% of the global ocean surface, hosts a disproportionately high level of marine biodiversity, including a genetically distinct and endangered subpopulation of fin whales (*Balaenoptera physalus*). As the only regularly occurring mysticete in the basin, the Mediterranean fin whale is increasingly exposed to rapid oceanographic changes driven by climate change, which may alter prey availability, disrupt migratory patterns, and modify the distribution of suitable habitat. Understanding how environmental change influences fin whale presence is therefore critical for developing effective conservation strategies.

This study investigates the relationship between fin whale occurrence and key environmental variables, and models future distribution suitability under projected climate scenarios. Presence data from 2006 to 2022 were compiled from ACCOBAMS and OBIS databases, while pseudo-absences were generated using occurrences of striped dolphins (*Stenella coeruleoalba*) recorded in locations where fin whales were not detected. Environmental predictors were sourced from the Copernicus Climate Data Store and included sea surface temperature (SST), phosphate concentration, phytoplankton biomass, and zooplankton biomass, variables known to influence euphausiid availability, the primary prey of Mediterranean fin whales.

Two species distribution modelling approaches were applied: Generalized Additive Models (GAMs) and Random Forest (RF). Model performance was assessed through cross-validation and comparison of predictive accuracy. The Random Forest model outperformed GAMs, capturing non-linear responses and complex interactions among variables; SST emerged as the most influential predictor. Phosphate, phytoplankton, and zooplankton contributed to model performance but exhibited weaker or more variable relationships with fin whale presence.

Future projections were developed using two Representative Concentration Pathways (RCPs), RCP 4.5 and RCP 8.5, to estimate habitat changes for mid-century (2050) and late-century (2099). Under the RCP 4.5 scenario, the predicted probability of occurrence remains generally higher than under RCP 8.5, highlighting a progressive deterioration of suitable habitat under more severe warming conditions.

Overall, this study highlights the vulnerability of Mediterranean fin whales to climate-driven oceanographic change and underscores the urgency of integrating climate projections into conservation planning. Identifying future habitat refugia will be essential for mitigating risks to this already fragile and isolated population.

1. INTRODUCTION

1.1 Fin whale biology and ecology

Fin whale (*Balaenoptera physalus* L. 1758) is the largest animal in the Mediterranean Sea, while globally the blue whale is the largest animal (*Balaenoptera musculus*) (Espada et al., 2024). It is a species with global distribution and significant ecological importance, making it a key animal in the marine environment. As a filter-feeding species within the *Balaenopteridae* family, it uses fringed baleen plates to consume vast quantities of small schooling fish and plankton, particularly krill, such as *Meganyctiphanes norvegica* and *Nyctiphanes couchi* in the Mediterranean (Mizroch et al., 1984; Canese et al., 2006). This species exhibits remarkable adaptations that allow it to thrive across diverse oceanic environments, from temperate to subpolar waters. However, its Mediterranean subpopulation faces unique challenges due to its genetic isolation and increasing anthropogenic pressures (Panigada et al., 2021). As an apex predator, the fin whale plays a critical role in marine ecosystems, yet its ecological significance has been understudied due to historical population declines and a focus on resource limitation and bottom-up controls, such as prey availability (Roman et al., 2014). These traits and challenges underscore the need for ecological modelling to predict its distribution and inform conservation strategies in the Mediterranean Sea.



Figure 1. Fin whale (*Balaenoptera physalus*) at the surface off Denia (Alicante, Spain), 2025. Photograph by Victor Gallego (Universitat Politècnica de València).

Fin whales display slight sexual dimorphism, with females typically measuring a few meters longer than males to support the substantial energy demands of pregnancy and lactation (Aguilar et al., 2018). Adult fin whales can reach lengths of up to 25 meters and weigh approximately 80,000 kg, making them one of the fastest baleen whales reaching 55km/h due to their streamlined bodies (Aguilar et al., 2018; Panigada et al., 2006). These morphological traits, combined with their baleen plates, enable efficient filter-feeding on dense aggregations of prey, a

behaviour that shapes their distribution and movements (Aguilar et al., 2018; Mizroch et al., 1984).

The species is genetically closely related to the humpback whale (*Megaptera novaeangliae*) but cases of hybridisation with blue whales (*Balaenoptera musculus*) have been documented, highlighting their evolutionary proximity within the *Balaenopteridae* family (Aguilar et al., 2018). Globally, fin whales are classified into two subspecies based on their geographic and temporal separation: *Balaenoptera physalus physalus* in the Northern Hemisphere and *Balaenoptera physalus quoyi* in the Southern Hemisphere (Aguilar et al., 2018; Notarbartolo di Sciara et al., 2003). These subspecies are distinguished by slight differences in body proportions, with *B. p. quoyi* exhibiting a larger body and shorter pectoral fins compared to *B. p. physalus* (Aguilar et al., 2018). Their migratory cycles are offset by six months, preventing interbreeding and resulting in reproductively isolated populations (Mizroch et al., 1984). Mediterranean fin whales are comparable in size to those in the northeastern North Atlantic but are generally larger than those along the northeastern U.S. continental shelf, reflecting regional adaptations to environmental conditions (Notarbartolo di Sciara et al., 2003).

Fin whales are a cosmopolitan species, inhabiting major ocean basins worldwide while avoiding extreme polar latitudes near ice edges due to limited prey availability in these regions (Aguilar et al., 2018). Their presence is scarce in equatorial waters and enclosed seas such as the Baltic Sea, Persian Gulf, Red Sea, eastern Mediterranean, and absent in the Black Sea (Aguilar et al., 2018). Globally, the fin whale population is estimated at approximately 100,000 mature individuals, reflecting their widespread distribution (Panigada et al., 2021).

In the North Atlantic, the population is estimated at around 53,000 individuals, distributed across distinct regions: 25,800 in the central North Atlantic (East Greenland, Iceland, Jan Mayen, and the Faroe Islands); 17,400 in the Spain–Portugal and the British Isles; 4,100 in the northeastern North Atlantic (Norway, both north and west); 2,800 along the east coast of North America southward from the Gulf of Saint Lawrence; 1,700 off in West Greenland and 1,000 off in Newfoundland (Aguilar et al., 2018). The International Whaling Commission (International Whaling Commission et al., 2020) has classified North Atlantic fin whales into seven management units based on tagging and genetic data: Nova Scotia, Newfoundland-Labrador, West Greenland, East Greenland-Iceland, North Norway, West Norway-Faroe Islands, and British Isles-Spain-Portugal (Castellote et al., 2011). Yet there be proofs that certain whales do stray beyond the bounds of these managing domains, showing that the said domains be not totally parted one from another (Castellote et al., 2011).

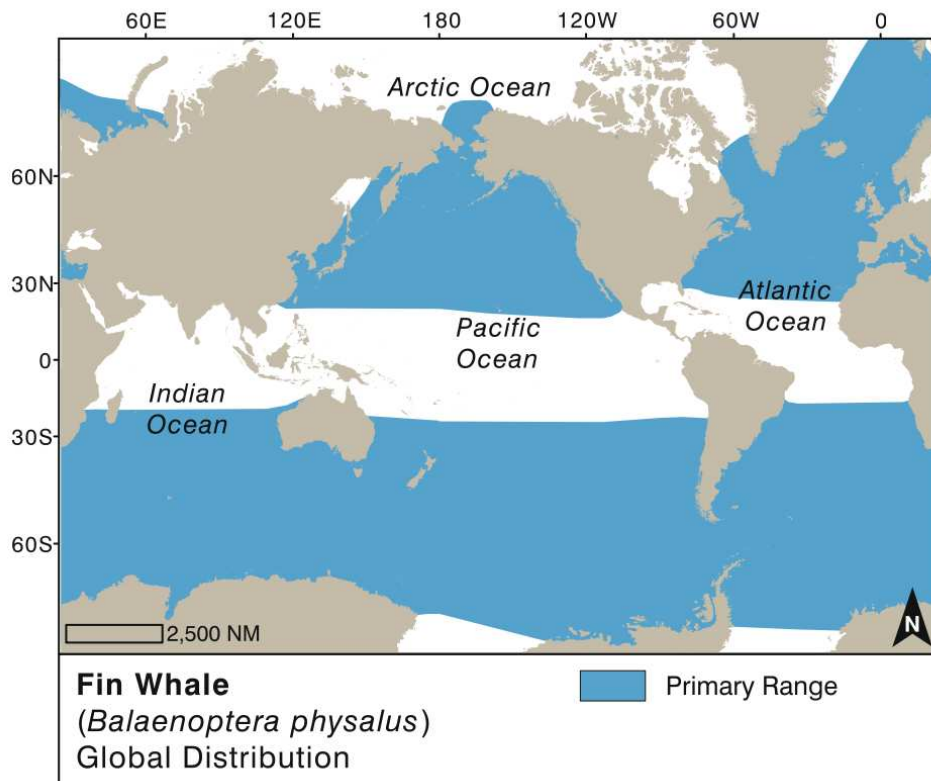


Figure 2. Global distribution of fin whale (*Balaenoptera physalus*). Adapted from Aguilar et al., 2018.

Fin whales exhibit a general migratory pattern driven by prey availability, moving to higher-latitude feeding grounds in summer and dispersing to lower-latitude regions in winter for breeding (Mizroch et al., 1984). However, in the Mediterranean Sea, this migratory pattern is less pronounced and remains under investigation due to the region's semi-enclosed nature and unique oceanographic conditions (Notarbartolo Di Sciara et al., 2016). The Mediterranean's high primary productivity in areas like the Ligurian-Corsican-Provençal Basin supports year-round feeding for some individuals, complicating the traditional migration model observed in open-ocean populations (Notarbartolo Di Sciara et al., 2016).

The Mediterranean fin whale population is recognized as a distinct subpopulation, genetically and geographically isolated from its North Atlantic counterparts. Mitochondrial DNA analyses have revealed significant differences between Mediterranean fin whales and those in the Atlantic coastal waters of Canada, Greenland, Iceland, and Spain, indicating limited gene flow between these populations (Castellotte et al., 2011). Satellite tagging studies have provided critical insights into the movements of Mediterranean fin whales, revealing that a small percentage migrate seasonally into the Atlantic Ocean through the Strait of Gibraltar (Castellotte et al., 2011). However, most of the population is considered resident, exploiting productive feeding grounds such as the Ligurian-Corsican-Provençal Basin and Gulf of Lion year-round (Notarbartolo di Sciara et al., 2003). The Mediterranean subpopulation is estimated to comprise fewer than 2,500 mature individuals, a number that is declining due to increasing anthropogenic pressures (Panigada et al., 2021). These pressures include intensified marine

traffic, which increases the risk of ship collisions, underwater noise pollution that disrupts communication and navigation, and intrusive activities such as whale watching, which can disturb feeding and breeding behaviours (Panigada et al., 2021). The combination of a small population size limited genetic exchange with other populations, and ongoing decline has led to the classification of the Mediterranean fin whale subpopulation as Endangered under IUCN Criterion C2, in contrast to the global population's Vulnerable status (Panigada et al., 2021).

1.1.1 Mediterranean population and distribution area

The fin whale inhabiting the Mediterranean Sea shares several physical characteristics with those in the North-west Atlantic: both the lips and the third apical fanon of the right side have a white color, a whitish patch extending dorsally and caudally on the head; and a V-shaped spot with its apex curving downwards towards the blowholes (Notarbartolo di Sciara et al., 2003). The Mediterranean fin whale (MED) population is genetically and ecologically distinct from the Northeast North Atlantic (NENA) population (Notarbartolo di Sciara et al., 2003). Stable isotope analyses of nitrogen (^{15}N) and carbon (^{13}C) in baleen plates reveal differences between the two subpopulations, with Atlantic fin whales exhibiting higher isotopic values than their Mediterranean counterparts (Gimenez et al., 2013). These isotopic signatures in Mediterranean fin whales reflect the diet dominated by the local krill species *Meganyctiphanes norvegica* (Bentaleb et al., 2011). Additionally, higher levels of organochlorine contaminants, such as PCBs and DDT, are found in the blubber of Mediterranean fin whales compared to Atlantic individuals, likely due to greater pollution in the Mediterranean Sea (Espada et al., 2024). The fin whales present in the Mediterranean Sea can be divided into the 'true' Mediterranean individuals (called MED) that remain in this sea all year, therefore considered a small resident population (Panigada et al., 2017). Meanwhile there is a population that will migrate outside the Mediterranean Sea reaching the North Atlantic Ocean, this population is called NENA (Northeast North Atlantic) (Panigada et al., 2017).

Fin whales are present in almost the entire Mediterranean Sea with a patchy distribution, excluding the Black Sea and the Sea of Marmara. (Notarbartolo di Sciara et al., 2003). The highest concentration is in the Ligurian-sea and Gulf of Lions, followed by Gulf of Cádiz, Tyrrhenian, Ionian Sea. (Tepsich et al., 2020; International Whaling Commission et al., 2020). The presence of these whales decreases from west to east (Espada et al., 2024). The most important area is the French coast and the island of Corsica and Sardinia (Espada et al., 2024). The movement of the fin whales MED are driven by feeding and breeding reasons, for this reason this population is considered nomadic, showing seasonal movements related to prey availability (Gauffier et al., 2018; Stephens et al., 2021). Based on the regional delineation of the Mediterranean Sea shown in Figure 3, the Mediterranean Sea can be partitioned into the following zones:

- A. The Western Mediterranean includes an area between Spain, Morocco and Algeria. Historical whaling industry killed more than 4000 of fin whales

nearly leading to local extinction of this species (Notarbartolo Di Sciara et al., 2003). Fortunately, recent sightings and strandings confirm the current presence of some individuals use Balearic Sea as feeding (Panigada et al., 2021; Tort et al., 2023). This area are also hosts fin whales belonging to the NENA population, which use this area to migrate to (and then return from) the Atlantic Ocean.

- B. Ligurian-Corsican-Provençal Basin, Gulf of Lions and north- western of Corsica and Sardinia. This is the primary habitat for the fin whales in the Mediterranean Sea thanks to its high primary productivity and the only area where there are recurring blooms (Notarbartolo di Sciara et al., 2003). The offshore waters of the basin lead this area to have a permanent Ligurian-Provençal Front structure with a large biomass of krill *Meganyctiphanes norvegica* (Notarbartolo di Sciara et al., 2003; Tepsich et al., 2020). In this region, fin whales are primarily found in deep offshore waters of 2,000 m in depth, where upwelling system enhance productivity (Aissi et al., 2007). An annual presence of the whale has been observed but follows a seasonal distribution: peaks of presence from late spring to late summer due to the favourable conditions that make this area rich in krill (Notarbartolo di Sciara et al., 2003; Aissi et al., 2007). The rest of the year, especially in winter, there is a decrease in krill biomass which however supports some individuals (Notarbartolo di Sciara et al., 2003); most whales during the winter will disperse through the western and central basin. (Panigada et al., 2021).
- C. The Tyrrhenian Basin hosts abundant presence of fin whales with peaks in spring and autumn reflecting migratory movements: reaching the feeding ground in the Ligurian sea in summer period (Notarbartolo Di Sciara et al., 2003). While in autumn they move to areas further south, including the Lampedusa Island. The submarine canyon called ‘Cuma’ between the islands of Ischia, Procida and the coast of Italy, supports high productivity attracting whales for feeding (Notarbartolo Di Sciara et al., 2003).
- D. In the Adriatic Basin, fin whale presence is scarce due to the absence of favourable feeding habitat. (Notarbartolo Di Sciara et al., 2003).
- E. The Ionian/ Central Basin. This area expands from eastern/southern Sicily, southern Italy, Malta, eastern Tunisia, Libya, and the eastern/ southern coasts of Greece. The presence of the fin whales in this basin is throughout the year, with peaks during spring and summer. (Sciacca et al., 2015). Unlike other zone, the area surrounding the island of Lampedusa the feeding behaviour is at the surface and there is present cooperative feeding behaviour with two or more whales. (Canese at al., 2006; Sciacca et al., 2015). This surface feeding behaviour suggests a different prey: here dominates the presence of a small Euphausiid *Nyctiphanes couchi* (Canese at al. 2006).
- F. Aegean Basin includes eastern, northern Greece and the western coast of Turkey, extending south to the islands of Crete, Karpathos, and Rhodes. In this area fin whales presence is rare, with few reported strandings and observations. (Notarbartolo di Sciara et al., 2003).

- G. Levantine Basin covering the southern coast of Turkey, Cyprus, Syria, Lebanon, Israel, Egypt, and the southern shores of Crete. Here rarely were observed fin whales. (Notarbartolo di Sciara et al., 2003).

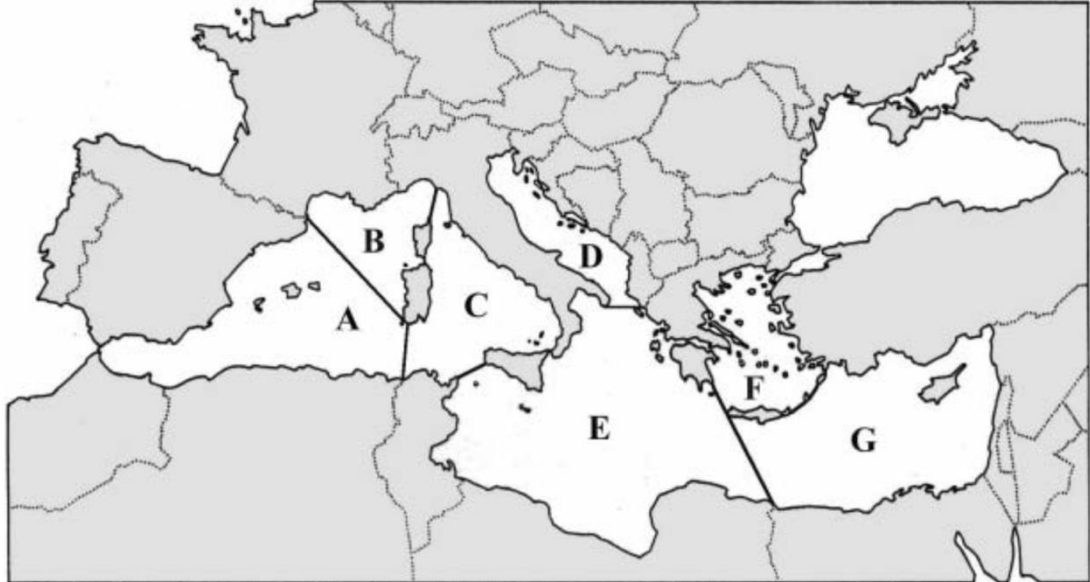


Figure 3. Biogeographic subdivision of the Mediterranean Sea into seven major basins. Key fin whale distribution areas are highlighted: (A) Western Mediterranean, (B) Ligurian-Corsican-Provençal Basin and Gulf of Lion, (C) Tyrrhenian Basin, (D) Adriatic Basin, (E) Ionian/Central Basin, (F) Aegean Basin, (G) Levantine Basin. Adapted from Notarbartolo di Sciara et al. (2003).

Fin whales in the Mediterranean primarily inhabit deep pelagic waters (400–2500 m), though some individuals are observed in shallow coastal areas, such as bays and harbours (Notarbartolo Di Sciara et al., 2003; Panigada et al., 2021).

According to the 2021 IUCN, the Mediterranean fin whale subpopulation is classified by presence in national waters as follows (Panigada et al., 2021):

- Native and resident year-round: Gibraltar, Spain (Balears Island), France (Corsica), Monaco and Italy Island. (Figure 3. Upper Area A, B, C)
- Regular seasonal presence: Albania, Algeria, Greece, Malta, Montenegro, Morocco, northern Spain, Tunisia. (Figure 3. Lower area A and C, upper E)
- Irregular presence: Croatia, Cyprus, Egypt, Greece, Israel, Lebanon, Libya, Slovenia, Syrian Arab Republic, Turkey, Bosnia and Herzegovina and Palestine. (Figure 3. Area G, F, lower E)

1.1.2 Movements and migratory behaviour

The migratory behaviour of fin whales (*Balaenoptera physalus*) in the Mediterranean Sea is notably complex, diverging significantly from the well-defined latitudinal migrations observed in other oceanic populations.

Unlike their counterparts in the open Atlantic, Mediterranean fin whales exhibit a combination of resident and nomadic behaviours, with movements largely driven by prey availability rather than strictly seasonal patterns (Gauffier et al., 2018; Geijer et al., 2015; Mizroch et al. 1984). The Mediterranean population is considered to follow a deviation from the traditional paradigm of migration (Geijer et al., 2015).

The resident Mediterranean fin whales depart from the classic migratory pattern of baleen whales in three key aspects (Geijer et al., 2015):

1. They stay year-round within the semi-enclosed, mid- to low-latitude Mediterranean basin, with only a subset staying in the broader northwestern feeding zones during winter.
2. They forage actively in both summer and winter, rather than restricting feeding to the warmer months.
3. They disperse widely from summer concentration areas, exploiting nearly the entire basin for feeding, mating, and calving across different seasons.

Two distinct subpopulations of fin whales are present in the Mediterranean Sea (Notarbartolo Di Sciara et al., 2016):

- the Mediterranean (MED) population, considered largely resident in the Mediterranean Sea, more eastern
- the Northeast North Atlantic (NENA) population, which shows seasonal exchanges with the Mediterranean through the Strait of Gibraltar reaching the Atlantic Ocean

These populations overlap in certain regions, particularly between the Balearic Sea and the Ligurian Sea, complicating efforts to delineate clear migratory pathways (Notarbartolo Di Sciara et al., 2016). Thanks to their massive size and high cruising speed, these whales can traverse the full length of the Mediterranean in just a few days (Geijer et al., 2015)

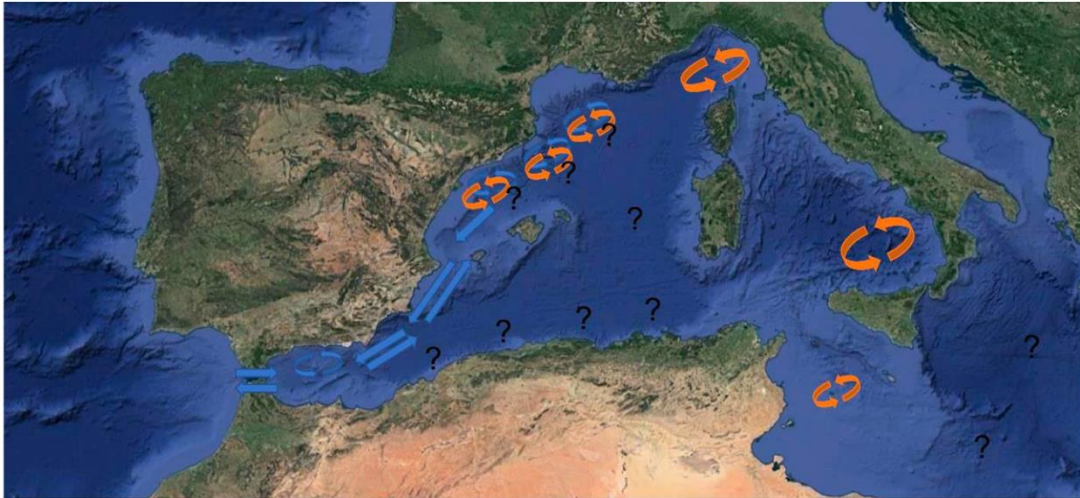


Figure 4. Migration patterns of fin whales in the Mediterranean Sea. The Mediterranean resident subpopulation is represented in orange, while the North-East North Atlantic (NENA) subpopulation entering through the Strait of Gibraltar is shown in blue; question marks indicate a lack of information. Adapted from Tort et al., (2023).

During years of low primary productivity, Mediterranean fin whales exhibit remarkable adaptability, shifting their distribution toward short-lived productive zones where prey is temporarily abundant (Espada et al., 2024). This flexibility underscores their opportunistic feeding strategy, which prioritizes prey availability over fixed migratory routes. In autumn and winter, many individuals disperse southward across the Mediterranean basin, with stranding data along the North African coast indicating a concentration in southern waters during these months (Espada et al., 2024). Key winter foraging areas include the coastal waters of Lampedusa Island and the Strait of Messina, where fin whales target *Nyctiphanes couchi* through surface-feeding behaviours, often in cooperative groups (Canese et al., 2006).

Some individuals remain in the Ligurian-Corsican-Provençal Basin year-round, exploiting the persistent productivity of this region, which is characterized by the Ligurian-Provençal Front and recurrent blooms of *Meganyctiphanes norvegica* (Tepsich et al., 2020). This variability in movement patterns complicates the identification of a uniform migratory strategy for the MED population, suggesting that their behaviour is highly responsive to local environmental conditions and prey dynamics (Espada et al., 2024).

The NENA population exhibits a more pronounced migratory behaviour, with a subset of individuals entering the Mediterranean Sea through the Strait of Gibraltar, the only natural corridor connecting the Mediterranean to the Atlantic Ocean. These movements are primarily observed between November and April, often involving whales accompanied by calves, which suggests that the Mediterranean may serve as a winter breeding ground (Gauffier et al., 2018). Conversely, between May and October, many NENA fin whales return to the

Atlantic; Gauffier et al. (2018) report 185 individuals moving from the Mediterranean to the Atlantic during this period, compared to 38 individuals entering the Mediterranean during other months.

In summer, NENA fin whales are frequently observed along the continental shelf (100–300 m depth) off the Galician coast (Spain) with peak migrations recorded from late June to early July (Tort et al., 2023). During winter, NENA individuals tend to concentrate in the Alboran Sea and the Strait of Gibraltar, which serve as both migratory and foraging zones (Espada et al., 2024).



Figure 5. Summer migration of North-East North Atlantic (NENA) fin whales along the Spain continental shelf. The green arrow indicates the migrations towards Galicia coast (represented by a big green circle). Adapted from Tort et al., (2023).

The region spanning the Balearic Sea to the Ligurian Sea represents a critical overlap zone where the MED and NENA populations coexist, particularly during periods of high primary productivity (Espada et al., 2024). This overlap is driven by oceanographic features, such as upwellings and thermal fronts, which create nutrient-rich environments conducive to krill blooms. The Ligurian-Corsican-Provençal Basin is a reliable summer feeding ground for both populations due to its persistent productivity, with studies consistently reporting high densities of fin whales in this area from late spring to early autumn (Tepsich et al., 2020). In contrast, winter foraging grounds, such as Lampedusa Island and the Strait of Messina, are more significant for the MED population, with *Nyctiphanes couchi* serving as a primary prey species in these southern regions (Canese et al., 2006).

1.1.3 Feeding ecology and prey-driven distribution

The fin whale is a filter-feeding mysticete, exhibits complex feeding and behavioural patterns in the Mediterranean Sea, driven primarily by the availability and distribution of its prey, notably euphausiid krill species such as *Meganyctiphanes norvegica* and *Nyctiphanes couchi* (Mizroch et al., 1984; Canese et al., 2006).



Figure 6. *Meganyctiphanes norvegica*, the northern krill, primary prey of Mediterranean fin whales. Photograph by U. Kils (2005), licensed under CC BY-SA 3.0. Source: Wikimedia Commons.

Unlike the more predictable migratory and foraging behaviours observed in open-ocean populations, Mediterranean fin whales display opportunistic and nomadic strategies, adapting to the region's dynamic oceanographic conditions (Gauffier et al., 2018; Espada et al., 2024). Fin whales in the Mediterranean are primarily planktonophagous, targeting dense aggregations of euphausiids, with *Meganyctiphanes norvegica* identified as the dominant prey species in the northwestern Mediterranean, as confirmed by faecal and stomach content analyses (Notarbartolo di Sciara et al., 2003). In specific regions, such as the Strait of Sicily and around Lampedusa Island, *Nyctiphanes couchi* serves as a significant prey item, particularly during late winter and early spring (Canese et al., 2006). The Mediterranean's high primary productivity, driven by phytoplankton blooms, supports large biomasses of zooplankton, creating ideal feeding grounds (Notarbartolo di Sciara et al., 2003).

The Mediterranean fin whale population's nomadic and opportunistic behaviour is driven by the patchy distribution of prey, particularly euphausiids, which influences both feeding strategies and group dynamics (Gauffier et al., 2018). Low group sizes may reflect dispersed prey availability, reducing competition (Bauer et al., 2015). The Mediterranean population deviates from the traditional mysticete model of distinct summer feeding and winter breeding grounds (Geijer et al., 2015; Notarbartolo di Sciara et al., 2016).



Figure 7. Fin whales feeding in the Mediterranean Sea. Photograph by Tort et al., (2023), from the Fin Whale Project Report, EDMAKTUB.

Fin whales play a key role in marine ecosystems as top consumers, exerting both direct predation and indirect effects on the trophic chain (Roman et al., 2014). In their absence, productivity would shift toward other species, altering food-web dynamics and biogeochemical cycles, particularly the transport of nitrogen and iron. Throughout their lifetime, fin whales sequester substantial biomass, contributing to carbon retention; upon death, their carcasses representing the largest organic inputs to the seafloor sink and dramatically enhance local food availability. During decomposition, they release high concentrations of proteins and lipids, while also serving as a critical resource for scavengers such as sharks, hagfish, and other necrophagous organisms (Roman et al., 2014).

Various models demonstrate that removing whales and other apex predators would not increase fishery yields for humans; instead, it would disrupt ecosystem stability, as whale faeces are rich in nutrients that sustain the food chain (Gerber et al., 2009). Beyond faeces, whale urine and flatus (farts) also release substantial nutrients, creating localized enrichment plumes that fertilize surface waters and stimulate primary production. Collectively, these processes position whales as biological nutrient pumps, driving vertical and horizontal redistribution of essential elements in the marine environment (Roman et al., 2014).

As air-breathing marine mammals that must surface outside the water column, whales further contribute to vertical mixing and influence primary production. When diving to various depths in pursuit of prey, they impart mechanical energy through their movements, promoting the mixing of water layers and the upwelling of nutrients from deeper strata (Roman et al., 2014).

1.2 Fin whale anthropogenic threats

Over the years, the primary causes of mortality for fin whales in the Mediterranean Sea have shifted from direct hunting by humans to vessel

collisions. Additional anthropogenic threats include underwater noise disturbance, chemical and plastic pollution, intrusive whale watching, and research activities, alongside natural factors such as parasites and predation.

A population study reveals that the most vulnerable life stage for fin whales is their first year, with a 77% mortality risk for calves. Therefore, many individuals fail to reach sexual maturity, by limiting the number of mature fin whales in the Mediterranean Sea significantly threatens population sustainability (Arrigoni et al., 2010). In contrast, mature adult whales face a mortality risk below 20%, confirming that juveniles are the most at-risk stage (Arrigoni et al., 2010).

The coastal migration patterns of Mediterranean fin whales expose them to human activities, including chemical and noise pollution, maritime traffic, and a high risk of vessel collisions, making them one of the most impacted cetaceans in the Mediterranean Sea. The Gulf of Lion, west of the Pelagos Sanctuary, experiences the highest frequency of ship strikes involving large cetaceans, such as fin whales and sperm whales (Espada et al., 2024). This region, a critical summer habitat with high fin whale density, is intersected by busy shipping routes connecting Italian, France, and Spanish ports to various islands. With global maritime traffic expected to increase significantly in the future, pressures on marine environments will likely intensify, threatening the welfare and survival of vulnerable species like fin whales in key habitats. (Espada et al., 2024)

1.2.1 Historical whaling

The historical presence of fin whales in the Strait of Gibraltar and adjacent waters is confirmed by the whaling industry, which began in 1921 to extract oil, with each whale yielding over 19 000 barrels of oil. In the following year, two additional companies were established in North Africa, collectively killing at least 4,149 fin whales over six years, leading to a population almost collapse (Gauffier et al., 2018; Notarbartolo di Sciara et al., 2003). The catch per unit effort (CPUE) declined from 54 whales per month to 6 whales per month (Notarbartolo di Sciara et al., 2003). Whaling continued with lower catches throughout the year, interrupted by the Spanish Civil War, and persisted until the 1960s (Notarbartolo di Sciara et al., 2003). Illegal whaling in the Iberian Peninsula until the 1970s resulted in an estimated total of 4,535 fin whales killed (Gauffier et al., 2018; Notarbartolo di Sciara et al., 2003). The primary goal was to obtain oil and other valuable products, though carcass processing was often inefficient, with many bodies discarded. In the 19th century, fin whales were also killed for museum collections, research, military target practice, and by whalers. It is believed that the whales hunted in the Strait of Gibraltar belonged to a non-Mediterranean population (Notarbartolo di Sciara et al., 2003). Whaling is still permitted in Greenland, Iceland, and Antarctica, and genetic studies indicate that historical whaling reduced fin whale populations by up to 90% (Espada et al., 2024; Roman et al., 2014).

1.2.2 Vessel collision

The Mediterranean Sea is one of the most navigated areas in the world, hosting about 30% of global merchant shipping within just 0.8% of the global ocean surface (Notarbartolo di Sciara et al., 2003). Annually, 220,000 ships weighing over 100 tons navigate the Mediterranean, alongside approximately 2,000 smaller vessels, including ferries, military boats, fishing vessels, and pleasure crafts, with traffic peaking in summer (Panigada et al., 2006).

Vessel collisions are a primary cause of mortality for Mediterranean fin whales, particularly in high-traffic areas like the Pelagos Sanctuary and the Strait of Gibraltar (Espada et al., 2024). Despite their high swimming speed of up to 55 km/h, which could allow evasion of vessels if detected in time, behavioural factors and noise interference often limit avoidance in busy shipping areas (Panigada et al., 2006). Behaviours such as feeding or resting reduce attention to the ship, increasing collision risk (Panigada et al., 2006). In areas like the Ligurian-Corsican-Provençal Basin, fin whales undertake deep foraging dives, limiting their ability to detect approaching vessels. During ascent, they often glide, restricting their capacity to change trajectory to avoid ships (Panigada et al., 2006).

Fin whales in the Mediterranean experience high ship collision rates, increasing from ~ 1 fatal collision per year in the 1970s to ~1.7 in the 1990s (Panigada et al., 2021). The areas with favourable whale habitats, where fin whale presence is high, overlap with regions of intense maritime traffic (Espada et al., 2024). The Pelagos Sanctuary and adjacent waters in the Gulf of Lion account for over 82.2% of reported fatal strikes, particularly during summer (July–November), when both whale density and vessel traffic are elevated (Panigada et al., 2021). It is estimated that at least 22.5% of fin whale strandings on the French coast are due to vessel strikes (Panigada et al., 2021). This area serves as a critical trade route connecting French, Italian, and Spanish ports to various islands, with intensified traffic in summer (Espada et al., 2024). A study found that almost the 30% of fatal ship strikes were caused by ferries and fast ferries due to their high speed and size; followed by cargo and container ships (Panigada et al., 2006).

A study revealed that disturbed Mediterranean fin whales in the presence of boats shift from localized foraging to broader traveling patterns, increasing swimming speed as an avoidance response in high-traffic areas (Jahoda et al., 2003). This shift is accompanied by a notable decrease in blow rate and surface time compared to undisturbed periods, indicating both an interruption of foraging and a deliberate avoidance reaction (Jahoda et al., 2003). Even whales already engaged in wide-ranging movement show significantly reduced surface time during disturbances, further suggesting avoidance behaviour. These changes may reduce foraging efficiency and alter habitat suitability, highlighting the need to incorporate noise and shipping density as covariates in ecological models to predict impacts on fin whale distribution in the Mediterranean (Jahoda et al., 2003).



Figure 8. Anthropogenic threats to Mediterranean fin whales: vessel collision and disturbance.

(a - e) Overlapping route between a fin whale and commercial ferry; (b - d) Propeller strike scars on a fin whale; (c) Fin whale surrounded by recreational vessels failing to maintain minimum approach distances. Imagine adapted from Espada et al., (2024).

Estimating ship strike rates for Mediterranean fin whales remains challenging, as collisions often occur far offshore and may go unnoticed by ship crews. Various vessel types can be involved, including tankers, cargo ships, cruise ships, ferries,

whale-watching boats, and sailing vessel. Physical evidence of ship strikes includes deep propeller cuts, extensive bruising, swelling, internal bleeding from impact sites, fractures, and paint marks from ships (Peltier et al., 2019).

1.2.3 Underwater noise

Over recent decades, commercial shipping and marine activities have doubled background noise levels in the Mediterranean Sea, now recognized as a habitat-level stressor (Weilgart et al., 2007; Williams et al., 2020). Maritime traffic, beyond causing direct mortality through collisions and contributing to chemical pollution, generates significant underwater noise that disrupts cetacean behaviour and may have long-term consequences for fin whale populations in the Mediterranean (Notarbartolo di Sciara et al., 2003).

Only male fin whales produce their typical calls during the breeding season (late fall to early spring) to attract females over great distances (Castellote et al., 2011). Fin whales, as large mysticetes, produce low-frequency calls (10–2000 Hz) that can travel approximately 100 km in the Mediterranean Sea (Weilgart et al., 2007; Erbe et al., 2019). These short, high-intensity sounds, typically in the 15–28 Hz range, form songs lasting over 24 hours. Unlike odontocetes, mysticetes like fin whales do not use echolocation but may gather environmental information from their low-frequency vocalizations. Ships produce a broad range of frequencies, overlapping with those used by fin whales for communication (Notarbartolo di Sciara et al., 2003; Weilgart et al., 2007; Erbe et al., 2019; Castellote et al., 2011).

Marine activities produce chronic underwater noise that disrupts cetacean hearing, communication, navigation, prey detection and reproduction (Williams et al., 2020; Bhagarathi et al., 2024). Underwater noise characteristics vary by frequency, amplitude, duration, rise time, directionality, cycle time, and repetition rate (Weilgart et al., 2007). Anthropogenic underwater noise primarily originates from underwater explosions, seismic exploration for oil and gas, geophysical studies, naval sonar operations, and shipping activities. Chronic noise is primarily generated by watercraft (Erbe et al., 2019). The strongest ship-generated noise comes from propeller during cavitation, producing a broadband spectrum. This noise can be reduced by lowering vessel speed, using smaller boats, or operating at greater depths (Erbe et al., 2019). High-intensity impulsive noise comes from sonar and seismic surveys, while lower-intensity continuous noise is generated by shipping vessels (Castellote et al., 2011). Seismic surveys for offshore oil and gas exploration generate intense underwater noise, covering areas up to 300,000 km² and elevating ambient noise levels for days, significantly impacting Mediterranean fin whales (Kavanagh et al., 2019). Acute and chronic noise affects cetaceans through behavioural responses, temporary or permanent hearing threshold shifts, spatial displacement, habitat exclusion, and acoustic interference (Weilgart et al., 2007).

Underwater noise from various type of boats prompts behavioural changes in fin whales, including a 23% increase in swimming speed, a 37% reduction in surface time, a 27% decrease in surfacing frequency, an 18% reduction in blow rate, and a

29% decrease in blows per surfacing compared to undisturbed conditions (Notarbartolo di Sciara et al., 2003). These behavioural changes reduce the time spent on the surface by reducing it and increasing speed (Notarbartolo di Sciara et al., 2003).

High-intensity impulsive noise from seismic vessels or military sonar can cause permanent tissue damage, leading to strandings and death (Erbe et al., 2019). To compensate for high underwater noise, fin whales modify their song activity and characteristics, which reduces communication efficiency and increases energy costs (Castellote et al., 2011). Such acoustic changes may reduce the masking effects of background noise but could decrease song effectiveness, particularly by altering note intervals and bandwidth, which are linked to population identity and reproduction, potentially impacting communication and mating success (Castellote et al., 2011).

Vessels contributing significantly to underwater noise in the Mediterranean Sea should be prioritized for replacement or equipped with ship-quieting technologies to reduce noise impacts. Mitigation strategies, such as rerouting ships or imposing speed limits, may involve trade-offs, such as displacing shipping efforts or balancing noise amplitude against exposure duration, particularly in high-traffic areas like the Pelagos Sanctuary (Rob et al., 2020).

1.2.4 Chemicals and plastic pollution

Thousands of marine species worldwide are negatively affected by marine litter pollution, with persistent debris impacting cetaceans through ingestion and entanglement (Panti et al., 2019). Fin whales as mysticetes, ingest marine litter during feeding by filtering the water, including microplastics, which interact with biota and may cause physiological issues due to associated chemical contaminants (Panti et al., 2019). Over 80% of marine litter in the Mediterranean is plastic, predominantly small-sized microplastics (Fossi et al., 2017). Mysticetes, due to their filter-feeding strategy, are more likely to ingest microplastics than larger debris (Fossi et al., 2015).

Fin whales are also affected by high-toxicity substances that persist and bioaccumulate in their tissues. As marine predators with low excretion rates and high metabolic rates, they experience significant toxic effects from contaminant accumulation (Fossi et al., 2015; Panti et al., 2019). Also persistent organic pollutants (POPs) associated with undigested floating microplastics are increasing (Fossi et al., 2012).

Skin biopsy results reveal a correlation between organochlorine contamination and biomarker responses, with low levels of DDT metabolites causing endocrine disruption and anti-androgenic effects (Fossi et al., 2015). These effects may impair the reproductive system, with contaminants transferred to calves during pregnancy and lactation, potentially leading to premature births (Panti et al., 2019).

Microplastics refer to particles smaller than 5 mm, while mesoplastics are particles smaller than 25 mm, primarily resulting from the fragmentation of larger plastic objects (Fossi et al., 2015). An estimated 100,000 microplastics and 62 million macro-litter items float on the Mediterranean Sea surface, with constant exchange with the Atlantic Ocean (Fossi et al., 2015).

Unlike the open ocean, the Mediterranean lacks permanent gyres, but seasonal patterns concentrate microplastics in specific areas, increasing risks for filter-feeding in key habitats like the Pelagos Sanctuary (Fossi et al., 2015).

The highest microplastic occurrences in the Ligurian Sea are near Genoa harbour and the Tuscan Archipelago, particularly around Capraia Island (Fossi et al., 2017).

Mediterranean fin whales accidentally ingest plastics directly during feeding and indirectly through contaminated zooplankton, such as *Meganyctiphanes norvegica*. Plankton sampling conducted with nets in the Iberian area frequently reveals microplastics in the samples (Tort et al., 2023).

Microplastics, concentrated in the sea-surface microlayer of the prey, act as carriers for harmful substances that bioaccumulate, potentially disrupting physiological processes like lipid metabolism. Additionally, microplastics release additives, such as phthalates, which are metabolized in whales and may cause endocrine disruption, impacting the viability of the populations (Fossi et al., 2012). The high plastic to plankton ratio reduces nutritional benefits, as fin whales feed on similar quantities of particulate matter but gain less energy, potentially ingesting thousands of microplastic pieces daily, impacting foraging efficiency and habitat suitability in key feeding grounds (Germanov et al., 2018; Fossi et al., 2015).

Model simulations show that areas with cyclonic circulation and upwelling, where food availability for fin whales is high, often have lower microplastic concentrations. In contrast, areas with anticyclonic circulation and downwelling, such as the Capraia gyre, have higher microplastic concentrations but are less favourable for feeding due to lower food availability. However, fin whale feeding habitats may overlap with high microplastic concentrations at the edges of both cyclonic and anticyclonic structures. In cyclonic areas, the high ingestion risk is driven by proximity to nutrient-rich upwelling zones, increasing feeding activity. In anticyclonic areas, elevated microplastic concentrations pose a greater ingestion risk, even in less nutrient-rich conditions, threatening fin whale health in key habitats like the Pelagos Sanctuary (Fossi et al., 2017).

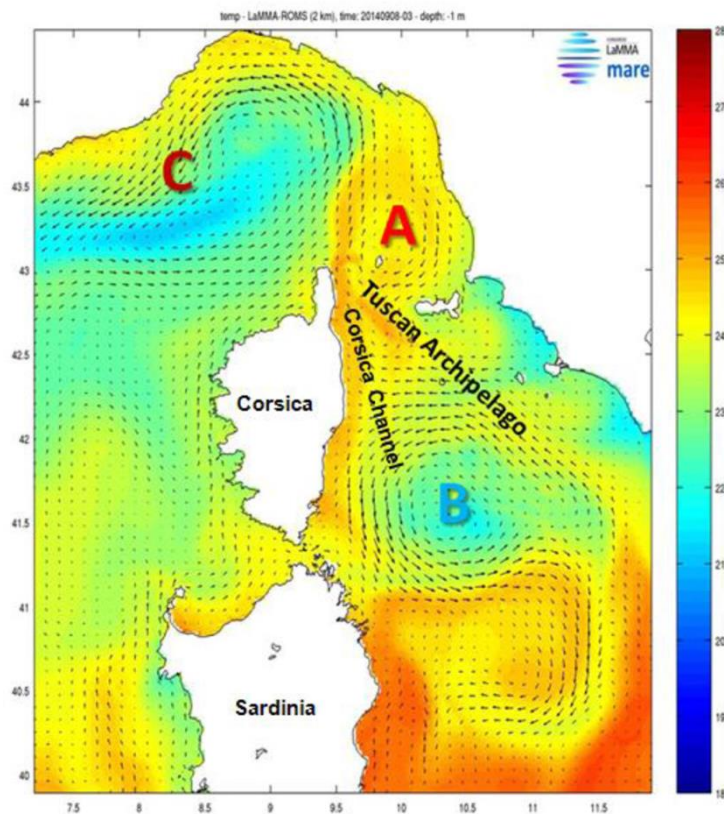


Figure 9. Overlap between microplastic accumulation zones and fin whale feeding habitats in the north-western Mediterranean Sea. (A) Anticyclonic circulation of the Capraia Gyre; (B) Northern Tyrrhenian cyclone; (C) Ligurian Current. Adapted from Fossi et al.; 2017.

1.2.5 Other disturbance

Increased whale-watching activities also affect fin whales, with unregulated operators approaching too closely or interacting disruptively, altering whale behaviour. Fin whales are less vulnerable to fishery entanglement compared to other cetaceans, such as dolphins, but some cases of gear entrapment occur. Although there is no direct competition between fin whales and fisheries in the Mediterranean, where fin whales are predominantly planktophagous, entanglement in lost or abandoned fishing gear or illegal driftnets, banned since 2002, remains a risk (Notarbartolo di Sciara et al., 2003; Panigada et al., 2021). Fin whales often show avoidance behaviour toward vessels, increasing speed and zigzagging while reducing surfacing frequency (Espada et al., 2024).

Although individual impacting factors may not constitute major threats alone, the cumulative effects in a semi-enclosed basin heavily affected by human presence, such as the Mediterranean Sea, should be interpreted cautiously, as they may lead to significant impacts on birth and death rates, potentially explaining the inferred population decline (Panigada et al., 2021). Some or all threats may interact temporally and spatially. Cumulative effects, defined as changes in reproduction

or survivorship negatively affecting population dynamics due to repeated exposure to single or multiple stressors, are complex to evaluate.

1.3 The Mediterranean sea: oceanographic characteristics and habitat features

The Mediterranean Sea, a semi-enclosed mid-latitude basin, features a predominantly narrow continental shelf, with exceptions in the Gulf of Lion, Gulf of Syrte, northern Adriatic Sea, and northern Aegean Sea, alongside extensive deep zones (Cañadas et al., 2023). The Mediterranean Sea operates as a miniature ocean with its own overturning circulation and deep water formation sites (Aracri, S. 2019). Complex morpho-bathymetry and water circulation create strong regional and local oceanographic patterns, with gradients in depth, longitude, and latitude driving primary and biological productivity (Cañadas et al., 2023). Higher evaporation, particularly in the eastern sector, exceeds precipitation and river runoff, resulting in elevated salinity and lower sea levels that promote Atlantic water inflow (Cañadas et al., 2023; Millot et al., 2005). Sea surface temperature (SST) displays two seasonal regimes: cooler winters (December–March) and warmer summers (June–September), with spring and autumn as transitional periods. In summer, the highest SSTs occur along the Libyan coast and occasionally in the southern Tyrrhenian Sea, while the coolest waters are found in the Alboran Sea, near the Strait of Gibraltar, and in the Gulf of Lion (Cañadas et al., 2023; Millot et al., 2005).

The Mediterranean hosts diverse geomorphological features, including submarine canyons, seamounts, mud volcanoes, deep trenches, and marine caves, which support high biodiversity and create unique feeding and reproductive zones (Pace et al., 2015). These ecosystems sustain human populations through marine services but face increasing anthropogenic impacts. As top predators, cetaceans like fin whales maintain marine trophic chains. Shelf edges with deep waters and nutrient upwelling foster high phytoplankton and zooplankton levels, creating favourable habitats for fin whales (Pace et al., 2015).

Submarine canyons enhance primary productivity by channelling currents that induce vertical water motions, creating upwelling zones that deliver nutrients to the euphotic zone. These processes transport sediments to deeper environments, supporting biodiversity hotspots that sustain species like fin whales (Pace et al., 2015).

Riverine inputs and coastal productivity introduce organic matter, which undergoes deposition and resuspension cycles on the continental shelf (Fernandez et al., 2017). Canyons accelerate the transfer of organic particles from coastal to deep-sea environments, enhancing nutrient fluxes and supporting complex pelagic food webs (Fernandez et al., 2017). This sustains high concentrations of euphausiids, such as *Meganyctiphanes norvegica* in productive Mediterranean habitats. The Coriolis effect directs riverine inputs to the right of river mouths, reinforced by onshore winds and the anticyclonic circulation of Atlantic Water. In large coastal indentations (gulfs spanning tens of kilometres), the Coriolis force aligns flow with topography, while in smaller embayment, flow bypasses with limited recirculation (Millot et al., 2005).

The Coriolis effect causes Atlantic Water and Mediterranean Water (MW) to follow isobaths, forming large cyclonic gyres in both western and eastern

Mediterranean basins (Millot et al., 2005). In southern sectors, Atlantic Water inflows like the Algerian and Libyo-Egyptian Currents (100–200 m deep) generate anticyclonic eddies, sometimes exceeding 200 km in diameter, which propagate eastward and may persist for years. These mesoscale structures transport Atlantic Water and Mediterranean Water from peripheral to central basin areas. In northern sectors, Atlantic Water subduction forms the Northern Current, prominent in the western basin. Shallow inter-basin sills require vertical mixing, dense water formation, and episodic cascading/upwelling to facilitate Mediterranean Water outflow (Millot et al., 2005).

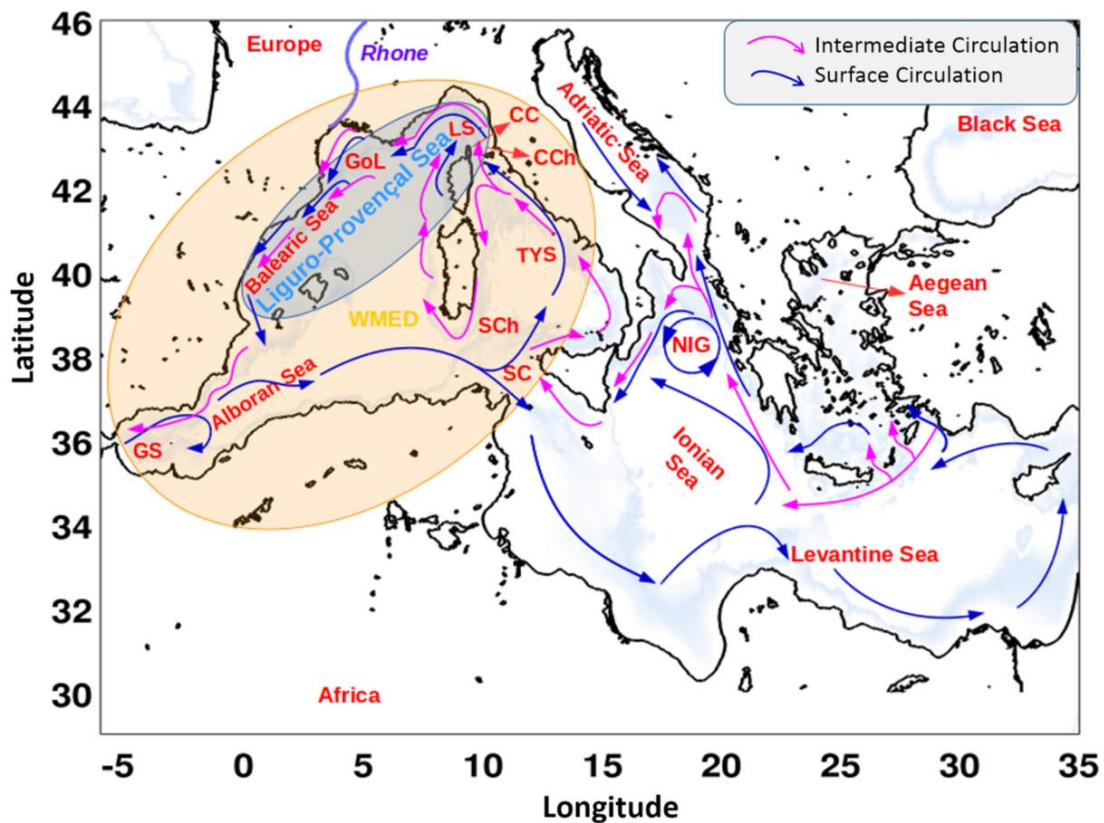


Figure 10. Schematic representation of Mediterranean Sea circulation patterns. Key features include the Western Mediterranean Sea (WMED), Strait of Gibraltar (GS), Corsica Channel (CC), Capraia Channel (CCh), Gulf of Lion (GoL), Ligurian Sea (LS), Tyrrhenian Sea (TYS), Sardinia Channel (SCh), Sicily Channel (SC), and North Ionian Gyre (NIG). Blue lines indicate surface circulation dominated by Atlantic Water (AW); magenta arrows show intermediate circulation driven by Levantine Intermediate Water (LIW). Adapted from Aracri, 2019.

1.3.1 Western Mediterranean

The Western Mediterranean, spanning areas between Spain, Morocco, and Algeria, comprises Atlantic Water, Levantine Intermediate Water (LIW), and both new and older Western Mediterranean Deep Water (Aracri, S. 2019). Fin whale sightings occur at an average depth of 2360 m, reflecting their preference for

pelagic habitats where upwelling and frontal structures boost primary productivity, supporting abundant *Meganyctiphanes norvegica* populations (Aïssi et al., 2007). Fin whales undertake deep foraging dives, often exceeding 470 m during daylight, tracking the diurnal vertical migration of euphausiids (Aïssi et al., 2007). The Liguro-Provençal Current drives a permanent cyclonic gyre, channelling Atlantic-origin waters along the continental slopes of Italy, France, and the Gulf of Lion, enhancing productivity and creating favourable feeding grounds for fin whales (Laran et al., 2016).

1.3.2 Catalano-Balearic Sea

The Catalano-Balearic Sea, between the northeastern Spanish coast (Catalan coast) and the northern Balearic Islands, features submarine canyons across a shallow continental shelf (approximately 400 m) and deeper pelagic waters (around 1500 m) (Panigada et al., 2024). The region's geomorphology and current patterns drive primary production, supporting high densities of *Meganyctiphanes norvegica* along the shelf edge in spring, coinciding with frequent fin whale sightings (Panigada et al., 2024). The Garraf coast, with a narrow continental shelf (~5 nautical miles) and the Foix and Cunit-Cubelles canyons, benefits from nutrient inputs from the Llobregat River and Garraf streams, combined with canyon-driven upwelling, creating a productive habitat for fin whales and other cetaceans (Tort et al., 2023).

1.3.3 Gulf of Lion

The Gulf of Lion, in the northwestern Mediterranean, features a broad continental shelf, numerous submarine canyons, significant Rhône River runoff, and intense frontal and eddy activity, creating a highly productive environment with elevated zooplankton biomass, particularly *Meganyctiphanes norvegica*. This attracts fin whales during summer months (Bauer et al., 2015). The Northern Current flows along the upper continental slope, with a secondary branch occasionally circulating over the shelf under favourable wind conditions (as reduced Mistral influence), converging at the gulf's western exit. The Coriolis effect modifies the Rhône River outflow along the gulf's perimeter, while canyons act as sediment traps, facilitating downslope transport of dense shelf waters (Millot et al., 2005). Deep water formation, driven by winter Mistral and Tramontane winds, cools and evaporates surface waters, causing them to sink. High-salinity LIW facilitates deep convection, even in milder winters, while shelf cascading, influenced by Rhône runoff, produces cooler, less saline deep water, enhancing productivity and supporting fin whale feeding grounds (Aracri, S. 2019).

1.3.4 Ligurian Sea

The Ligurian Sea's circulation, driven by the Liguro-Provençal Current (Northern Current), maintains a year-round cyclonic pattern with seasonal variations, influenced by the Tyrrhenian Sea's Eastern Corsica Current, with higher transport in winter and lower in summer (McGehee et al., 2004). Two main currents enter the southern sector: the West Corsica Current, carrying modified Atlantic Water from the Algerian Basin, and the Tyrrhenian Current, transporting water northward through the Corsica Channel. These waters follow a counterclockwise

path along the Italian and French coasts, exiting as the Ligurian Current toward the Gulf of Lion and Catalan Sea (McGehee et al., 2004). The Ligurian Sea, one of the coldest parts of the Western Mediterranean, supports high productivity, attracting fin whales, particularly in summer, due to abundant *Meganyctiphanes norvegica* (Aïssi et al., 2007).

The Pelagos Sanctuary, covering 15,920 km² in the northwestern Mediterranean (0.88°E to 9.852°E, up to 43.81°N), features varied topography, including canyons and seamounts, and a permanent cyclonic circulation driven by Atlantic and Tyrrhenian waters. This enhances primary productivity, supporting large *Meganyctiphanes norvegica* populations, making it a primary feeding ground for fin whales (Aïssi et al., 2007).

1.3.6 Central Mediterranean: Strait of Messina and Gulf of Catania

The Strait of Messina, spanning 1,220 km² (15.83°E to 15.84°E, 38°N to 38.3°N), is a narrow, 32-km-long channel connecting the Tyrrhenian and Ionian Seas, with an average depth of 80 m, increasing to 800 m south of the sill and 400 m north. Its funnel-shaped geography and steep bathymetric gradient drive complex hydrodynamics, including tidal currents and upwelling, sustaining high biomass of 11 out of 13 Mediterranean euphausiid species, including *Meganyctiphanes norvegica*. Alternating tidal currents, northward during Ionian high tide and Tyrrhenian low tide, and southward during the reverse, create turbulent mixing, forming horizontal sea steps and vertical eddies. This supports dense krill aggregations, attracting fin whales year-round, with peak feeding in spring and summer (Aïssi et al., 2007; Brancato et al., 2001).

The Gulf of Catania, with steep coastal slopes reaching 200 m within 2 km from shore, features nutrient-rich waters from river inputs, notably the Simeto River, driving seasonal productivity peaks in spring and autumn. Currents linked to the Strait of Messina's tidal upwelling sustain year-round euphausiids (*Meganyctiphanes norvegica* and *Nyctiphanes couchii*), making the gulf a key feeding ground for fin whales, with peak presence from late winter to summer (Sciacca et al., 2015).

1.3.7 Tyrrhenian Sea: Caprera and Cuma Canyons

The Tyrrhenian Sea, the deepest and most isolated Western Mediterranean basin, connects to the Algerian Basin in the southwest and the Ligurian Sea in the north via the Corsica Channel. A cyclonic wind pattern, driven by cold Rhône Valley winds between Corsica and Sardinia, enhances nutrient upwelling, supporting high productivity and attracting fin whales in spring and autumn (Aracri, S. 2019). The Caprera Canyon area, east of the Bonifacio Strait (central-western Tyrrhenian Sea), features a complex seabed with a broad continental shelf (~20 km off northeastern Sardinia), a continental slope (17–26 km wide, ~120 m deep, steeper in the south), and depths up to 1500 m. The Olbia Basin plain extends to 1650 m, bordered by the Etruschi seamounts. The northeastern Sardinian slope includes turbidite canyons (Caprera, Mortorio, Tavolara), with the Caprera Canyon comprising two 16-km-long tributary canyons merging into a 2.5-km-wide canyon at 1000 m depth, extending 9 km toward the continental rise. The Tyrrhenian Gyre and wind-driven currents from the Bonifacio Strait form a persistent cyclonic “Bonifacio Cyclone” and an anticyclonic eddy off Sardinia, driving

upwelling and supporting *Meganyctiphanes norvegica* populations, making this a critical fin whale feeding ground in spring and autumn (Bittau et al., 2025).

The Cuma Canyon, a deep submarine valley in the Tyrrhenian Sea, extends from coastal areas near Cuma and Ischia Island to 800 m depth between Ischia and Ventotene. It channels sediments from the Volturno and Garigliano rivers (Gulf of Gaeta), enhances upwelling, and facilitates water exchange between the coastal shelf and deeper basin, boosting primary productivity.

1.3.8 Southern and Eastern Mediterranean

The Lampedusa area (7,550 km²), located south of Sicily on the African continental plate, features depths up to 250 m (Aïssi et al., 2007). In the Turkish Levantine Sea (between Iskenderun to Adana) and coastal Israel (near Haifa), fin whale sightings suggest potential habitats, with sub-adult presence possibly indicating calving grounds, though targeted surveys are needed for confirmation (Stephens et al., 2021).

1.4 Climate change

Over the past several decades, Earth has entered a new phase of rapid and potentially irreversible warming driven by positive radiative imbalances. In recent decades, our planet has begun a period of rapid and possibly permanent heating caused by an excess of incoming radiation over outgoing energy (Albouy et al., 2020). Greenhouse gas releases are the cause of worldwide temperature rise, causing global warming. Carbon dioxide outputs total 7 giga tons of carbon annually and trigger severe environmental disruptions. Yearly, oceans take in 2 giga tons of carbon via natural mechanisms of oceans, but this absorption system might reach higher capacity speeding up the heating of the planet (Gambaiani et al., 2007). Methane stored in hydrate forms within ocean floor layers on continental margins and in permafrost areas might exceed atmospheric methane by 3000 times. Methane traps infrared radiation 20 times better than carbon dioxide, potentially causing devastating weather shifts. Raising air temperatures by 4 to 8 degrees while cutting oxygen could have 80% extinction of sea life previously. Carbon dioxide from the air dissolves into oceans, causing acidification in upper layers. Upcoming rises in air carbon dioxide from burning fossil fuels will deeply alter sea chemistry and ocean organisms (Gambaiani et al., 2007).

Planetary heating changes in rain, heat, carbon dioxide levels, and air movement will cause a chain of shifts in sea systems (Gambaiani et al., 2007):

- physical aspects: vertical water layer steadiness, water body creation and movement, flow directions and upwelling regimes
- impact chemical aspects such as sea pH, salinity levels, and nutrient balances
- biological characteristics: species timing, growth, locations, numbers, variety, and recruitment

1.4.1 Climate change in the Mediterranean Sea

The Mediterranean Sea represents 0.82% of the world's ocean surface, has a quick renewal cycle of 40 to 50 years, holds 8% to 9% of worldwide ocean variety in life forms and many unique types. It probably reacts quickly to outside pressures such as climate change. By changing weather aspects like air temperature, rain amounts, and extreme meteorological events, planetary heating impacts the characteristics of Mediterranean Sea water (Gambaiani et al., 2007). This sea is warming at a rate exceeding global averages, despite relatively low greenhouse gas emissions from regional countries. Mean annual temperatures across the basin have risen by approximately 1.5°C since the late 19th century, about 0.4°C above the global mean, with sub-regional increases ranging from 1.5°C to 4°C (Lange et al., 2020). Sea surface temperatures (SSTs) have increased by roughly 0.35–0.4°C per decade since 2000, with mean annual SSTs exceeding 20°C in the eastern and southeastern Mediterranean (Lange et al., 2020). In recent decades, research shows links between weather trends and sea water shifts, with overall rises in heat and salt throughout the Mediterranean. Western Mediterranean deep water has grown warmer and more saline due to human-caused heat-trapping gases and freshwater balance changes. Between 1900 and 2000, summer rain in the Mediterranean dropped by 10% (Gambaiani et al., 2007). It is thought that marine heat waves become more frequent, more longer and more intense; exacerbating ocean warming and thermal stratification (Hassoun et al., 2025). This stratification reduces vertical mixing, limiting nutrient supply to surface waters and oxygen replenishment at depth, potentially leading to eutrophication and oxygen depletion (Hassoun et al., 2025). These patterns should continue and worsen, making extreme weather like dry spells and floods more common altering the biochemical and physical characteristics of the sea (Gambaiani et al., 2007).

Weather changes by human impacts affect broad air flows like the North Atlantic Oscillation and El Niño Southern Oscillation. Global warming supports the active stage of the North Atlantic Oscillation, linked to milder European winters in the past 10 to 20 years, and El Niño events might happen more often. Mediterranean weather depends on big air circulation setups, including long-term North Atlantic Oscillation and El Niño Southern Oscillation. Sea water heat and salt changes in the Mediterranean are connected to the North Atlantic Oscillation. This oscillation affects rain and river flows into the Mediterranean, usually lower in active phases. Connections exist between El Niño Southern Oscillation and unusual fall rain in the Mediterranean and changes in the sea level (Gambaiani et al., 2007).

Key surroundings controls for Mediterranean species' development, numbers, locations, variety, and new member success include local heat differences, river inputs and wind mixing, affecting surface heat and salt. Water traits like sea boundaries, layer steadiness, upwelling zone, and wave conditions and upwelling movements can also impact the higher-level trophic species.

The Mediterranean counts as oligotrophic due to limited river nutrients and low-nutrient Atlantic entry via Gibraltar Strait. Nutrient inputs for the Mediterranean sea euphotic zones are: winter vertical mixing, coastal nutrient rises, and river flows. Sea physical actions like upwelling phenomena strongly shape primary

output spread via upward nutrient-rich deep-water movement reducing nutrient access (Gambaiani et al., 2007).

Extreme meteorological events as floods, will push lots of land solids and toxins into seas, harming shore life groups. Weather shifts should bring active North Atlantic Oscillation with reduced rain and run off (Gambaiani et al., 2007). Rising atmospheric CO₂ drives ocean acidification through chemical reactions that increase H⁺ ions, lowering seawater pH. Mediterranean surface waters (upper 80 m) are experiencing pH declines of 0.001–0.009 units per year, with more pronounced rates in the Western Basin compared to the Eastern (Hassoun et al., 2025; Pace et al., 2015). By 2100, pH is projected to drop by 0.28–0.46 units below pre-industrial levels, a rate approximately 1.5 times higher than the global ocean average (Hassoun et al., 2025).

Climate change has driven a sea level rise of approximately 3 cm per decade in the Mediterranean, threatening low-lying coastal regions (Lange et al., 2020). Unlike historical changes that unfolded over millennia, current shifts are occurring within 100–150 years, largely due to anthropogenic greenhouse gas emissions (Lange et al., 2020).

Increased evaporation and reduced rainfall, particularly in the Western Mediterranean, alter the water cycle, intensifying risks like wildfires and forest pests, and reducing river runoff, which limits nutrient inputs to coastal waters (Lange et al., 2020). Climate-driven droughts, linked to positive North Atlantic Oscillation phases, reduce river runoff, limiting nutrient inputs to the euphotic zone, particularly in the Gulf of Lion (Gambaiani et al., 2007).

1.4.2 Effects of climate change on plankton

In certain areas, some organisms survive within narrow temperature ranges and cannot adapt or migrate when environmental conditions change, as planetary heating impacts their physiological processes, potentially harming the performance and survival of those living near their thermal limits or at the northern or southern edges of their distribution (Gambaiani et al., 2007). Climate shifts also alter phytoplankton composition through changes in nutrient concentrations and ratios, and over the past twenty years in the northwest Mediterranean, meteorological anomalies such as warmer water, decreased salinity, longer periods of sunshine, and lower wind stress have affected water column stability and reduced nutrient replenishment into the euphotic zone (Gambaiani et al., 2007). By modifying phytoplankton communities, climate change could seriously disrupt nutrient cycling, food web dynamics, and the temporal match between plankton and higher trophic levels (Gambaiani et al., 2007). These changes further disrupt primary production, favouring smaller plankton groups like pico- and nanophytoplankton and bacteria, while larger phytoplankton (e.g., diatoms like *Cyclotella* and *Thalassiosira*) decline, reducing energy transfer to higher trophic levels (Hassoun et al., 2025). Variations in nutrient load and seawater properties, such as temperature increases, can lead to coastal eutrophication and algal blooms, particularly affecting shallow northern Adriatic waters, where increased seawater stratification from meteorological anomalies regularly causes bottom water anoxia and red tide events, provoking mass mortality episodes of fish and benthic organisms (Gambaiani et al., 2007).

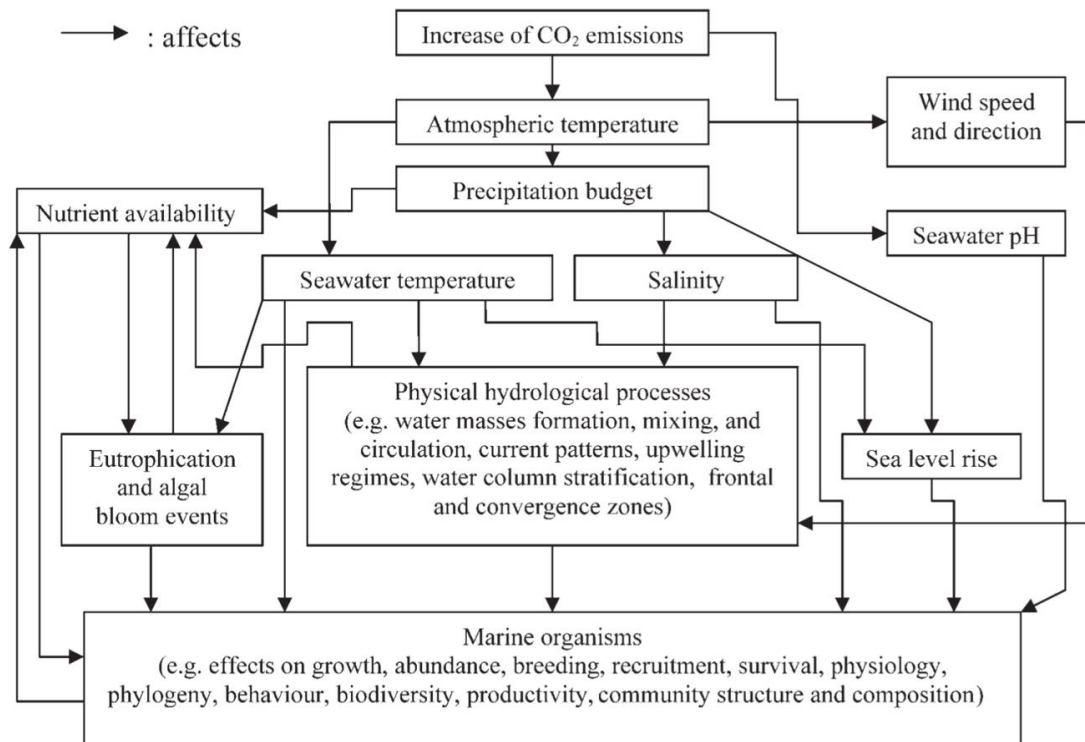


Figure 11. Primary greenhouse gas-related factors influencing marine organisms, including CO₂-driven ocean acidification, temperature rise, and altered stratification. Adapted from Gambaiani et al. (2007).

These alterations also disrupt ocean circulation and vertical mixing, diminishing nutrient-rich upwelling zones critical for phytoplankton and zooplankton production (Pace et al., 2015). In the Western Mediterranean, climate change warms and salinizes Western Mediterranean Deep Water (WMDW), increasing water column stability and thermal stratification, which reduces upwelling of nutrient-rich deep waters (Gambaiani et al., 2007). Zooplankton are critical grazers in marine food webs, transferring energy from phytoplankton to higher trophic levels, including fin whales, fish, and sea turtles; they contribute to the biological pump by consuming phytoplankton that fixes CO₂ and facilitating carbon transfer to the seabed for sequestration, removing it from the carbon cycle, with daily vertical migrations to deeper waters evading predators enhancing this transport (Richardson et al., 2008). Without zooplankton, marine ecosystems would lack the large mammals and fish of significant ecological and economic value (Richardson et al., 2008). As poikilothermic organisms, zooplankton are highly sensitive to temperature, with feeding, respiration, and reproduction rates accelerating with warming; their short lifespans (typically <1 year) enable rapid population responses, making them sensitive indicators of climate change that amplify subtle environmental shifts, and their dispersal relies on ocean currents, simplifying predictions of distribution changes under warming conditions (Richardson et al., 2008).

These euphausiid, sensitive to temperatures above 18°C and salinity changes (20–24 ppm), faces disrupted larval transport and recruitment due to altered ocean

circulation, potentially causing mismatches with phytoplankton blooms and reducing prey availability (Gambaiani et al., 2007; Richardson et al., 2008). Shifts in environmental cues may also alter migratory behaviours, challenging fin whale populations, while rising temperatures directly stress fin whales, increasing pathogen prevalence and transmission as species ranges shift, further threatening this genetically isolated population (Panigada et al., 2021; Albouy et al., 2020; Gambaiani et al., 2007).

1.5 Protected areas and conservation frameworks in the Mediterranean Sea

1.5.1 IUCN red list and other protecting organization

The fin whale in the Mediterranean Sea is safeguarded by multiple international agreements and conventions due to its vulnerable status and ecological importance. It is listed in Appendices I and II of the Convention on the Conservation of Migratory Species of Wild Animals (CMS), also known as the Bonn Convention, which aims to protect migratory species across their range. Appendix I includes species threatened with extinction, requiring strict protection measures, while Appendix II covers species with unfavourable conservation status and benefit from international cooperation for conservation. The Mediterranean fin whale's inclusion reflects its migratory behaviour and the need for coordinated protection across countries bordering key habitats like the Pelagos Sanctuary, Gulf of Lion, and Tyrrhenian Sea. The fin whale is also included in Appendix I of the Convention on International Trade in Endangered Species of Wild Fauna and Flora (CITES), which prohibits international trade in specimens of this species to prevent exploitation, ensuring that activities like illegal hunting do not threaten Mediterranean populations. Under the Barcelona Convention, specifically Annex 2 of the Protocol on Specially Protected Areas and Biological Diversity in the Mediterranean, fin whales are recognized as a priority species requiring special protection measures to preserve biodiversity in critical habitats such as the Pelagos Sanctuary, a marine protected area established to safeguard cetaceans in the Ligurian Sea (Panigada et al., 2021; Gauffier et al., 2020; Zanardelli et al., 2022).

Further protection is provided by the Agreement on the Conservation of Cetaceans of the Black Sea, Mediterranean Sea, and Contiguous Atlantic Area (ACCOBAMS), which coordinates conservation efforts for cetaceans, including fin whales, through measures like habitat protection, research, and mitigation of threats like climate change and pollution in the Mediterranean. Additionally, the International Whaling Commission (International Whaling Commission et al., 2020) officially banned commercial whaling in 1986, prohibiting commercial hunting of fin whales globally, including in the Mediterranean, to prevent population declines. These combined international frameworks underscore the critical need to protect the genetically isolated Mediterranean fin whale population, particularly in productive feeding grounds like the Gulf of Lion and Tyrrhenian Sea, where climate-driven changes and pollutants threaten prey availability and habitat suitability (Panigada et al., 2021).

Surveys conducted in summer 2018 using line transect distance sampling in the Mediterranean Sea estimated a fin whale population of approximately 3,282 individuals, with a coefficient of variation of 30.85%. For this subpopulation to exceed the threshold of 2,500 mature individuals, assuming 48% of the total population is mature, a total abundance of at least 5,200 individuals would be required. As the estimated population falls below this threshold, the Mediterranean fin whale likely meets the criteria for classification as Endangered under Criterion C2, which identifies species with small populations vulnerable to decline; meanwhile globally the fin whale is classified as Vulnerable. This status underscores the conservation challenges faced by this genetically isolated population, particularly in key Western Mediterranean habitats like the Pelagos Sanctuary, Gulf of Lion, and Tyrrhenian Sea, where threats such as reduced prey availability and vessel collisions exacerbate risks to their survival (Panigada et al., 2021; Zanardelli et al., 2022).

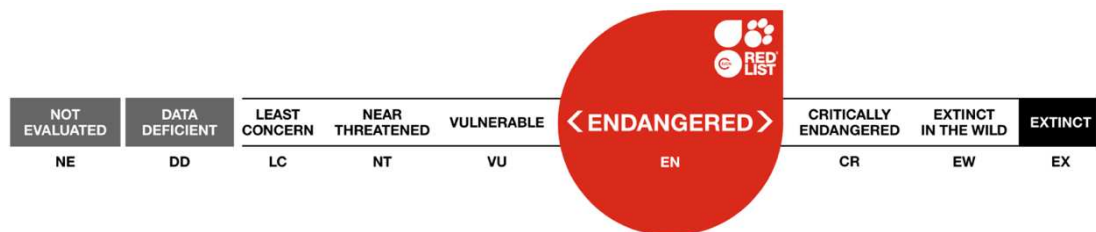


Figure 12. IUCN Red List conservation status of the fin whale (*Balaenoptera physalus*) classified as Endangered (EN) in the Mediterranean sea. Source Panigada et al., 2021 IUCN.

The Mediterranean fin whale, the only baleen whale species in the Mediterranean Sea, is a key focus of conservation efforts under the Marine Strategy Framework Directive (MSFD, 2008/56/EC) and the Habitats Directive (HD, 92/43/EEC), which mandate regular systematic surveys to assess its density and abundance. The MSFD, aimed at achieving Good Environmental Status (GES) in EU marine waters, ensuring the long-term viability of marine biodiversity and supporting economic and social activities dependent on marine resources (European Commission, 2023; Tepsich et al., 2020). Under the MSFD’s Descriptor 1 (Marine biodiversity), fin whale abundance is a primary criterion (D1C2) for evaluating GES, with trends in population abundance serving as a critical indicator to establish threshold values and measure progress toward environmental health; fin whales is also related to Descriptors 8 for contaminants and Descriptor 10 for marine litter (Tepsich et al., 2020 ; European Commission, 2023). The Habitats Directive similarly requires monitoring to support conservation objectives, including assessments for the IUCN Red List, the Pelagos Sanctuary, the ACCOBAMS agreement, and the Barcelona Convention. Despite these requirements, comprehensive long-term, basin-wide data on fin whale populations remain limited, hindering robust conservation planning. To address this, monitoring networks are expanding, particularly in Spain, with new survey routes covering the “Corredor de Migración de Cetáceos del Mediterráneo”, a Specially Protected Area of Mediterranean Importance (SPAMI) established in 2018 in the Balearic Sea, and the Strait of Gibraltar, a critical migratory corridor. These efforts also extend to southern Mediterranean areas, such as Lampedusa and Malta, recognized as important habitats for fin whales.

Enhanced monitoring in these regions supports the assessment of population trends and threats, such as reduced prey availability and vessel collisions, critical for the conservation of this genetically isolated population in the Western Mediterranean (Panigada et al., 2017; Tepsich et al., 2020 ; European Commission, 2023)

The International Whaling Commission (International Whaling Commission et al., 2020) and the Agreement on the Conservation of Cetaceans of the Black Sea, Mediterranean Sea and Contiguous Atlantic Area (ACCOBAMS) are developing a Conservation and Management Plan (CMP) to ensure the favourable conservation status of the Mediterranean fin whale across its historical range. The primary objective of the CMP is to regulate human activities impacting fin whales, such as vessel collisions and habitat degradation, using the best available scientific evidence to promote population recovery and sustainability. A key component of this plan involves establishing and maintaining a centralized photo-identification catalogue, integrated with a genetic-ID catalogue, to enhance understanding of population structure, migratory movements, abundance, trends, demographic parameters, and threats like scarring from human activities. This initiative supports conservation efforts in critical Western Mediterranean habitats, including the Pelagos Sanctuary, Gulf of Lion, and Strait of Gibraltar, where fin whales face challenges from reduced prey availability and anthropogenic pressures (Panigada et al., 2021; Zanardelli et al., 2022).

The establishment of marine protected areas (MPAs) is a cornerstone of biodiversity conservation and a critical tool for the protection of cetacean populations, including the Mediterranean fin whale (*Balaenoptera physalus*), a genetically isolated and Endangered subpopulation (Panigada et al., 2021; Bianchi et al., 2012). Scientific evidence demonstrates that well-managed MPAs enhance biological characteristics, resulting in higher population densities and increased body condition compared to adjacent non-protected areas (Grau et al., 2022). This ecological benefit arises from reduced anthropogenic pressures such as vessel traffic, noise pollution, and habitat degradation allowing species like the fin whale to feed, rest, and migrate with lower disturbance. In the Mediterranean context, where human activities are intense and overlapping with cetacean critical habitats, MPAs serve not only as refugia but also as living laboratories for monitoring long-term population trends and evaluating conservation efficacy.

1.5.2 Protected Areas and Conservation Projects for Cetaceans in the Mediterranean Sea

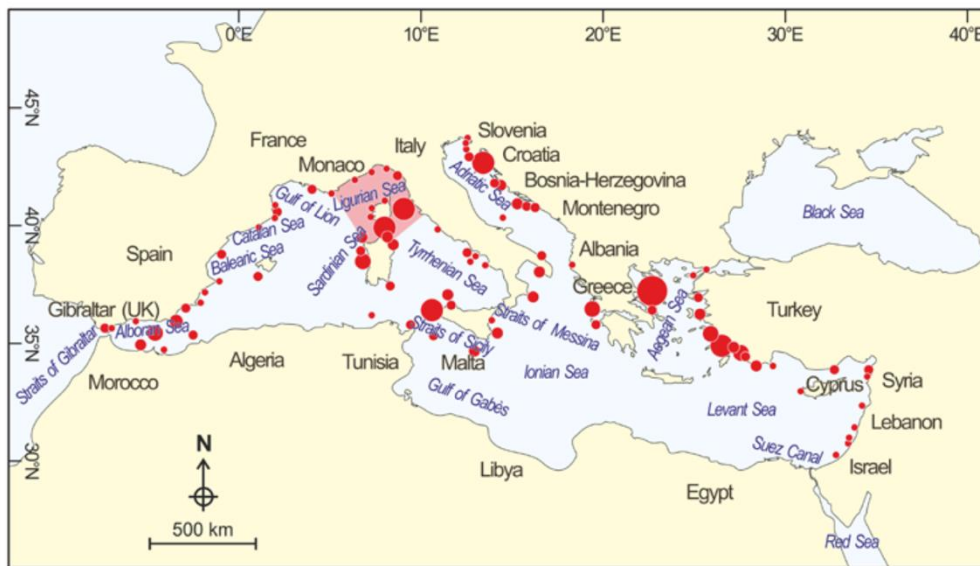


Figure 13. Geographical distribution of Marine Protected Areas (MPAs) in the Mediterranean Sea. Red circles indicate coastal MPAs, with circle diameter roughly proportional to protected surface area. The pink triangle highlights the international Pelagos Sanctuary for Mediterranean marine mammals. Adapted from Bianchi et al., 2012.

Among the most emblematic and ambitious initiatives there is the Pelagos Sanctuary for Mediterranean Marine Mammals, formally established in 1999 through a tripartite agreement between Italy, France, and the Principality of Monaco. Covering approximately 90,000 km², this transboundary MPA encompasses a vast pelagic region within the Corso-Ligurian-Provençal Basin, extending across the Provençal, Corsican, Ligurian, northern Tyrrhenian, and northern Sardinian Seas (Zanardelli et al., 2022). In 2001, it was designated a Specially Protected Area of Mediterranean Importance (SPAMI) under the Protocol Concerning Specially Protected Areas and Biological Diversity in the Mediterranean (Barcelona Convention), marking it as one of the first MPAs to include significant portions of high seas areas beyond national jurisdiction (Panigada et al., 2011). The area's exceptional productivity is driven by the permanent Ligurian-Provençal Front, intense upwelling, and recurrent blooms of the euphausiid *Meganctiphanes norvegica*, the fin whale's primary prey (Zanardelli et al., 2022). By preserving these dynamic foraging hotspots, the sanctuary plays an irreplaceable role in sustaining the reproductive output and survival of fin whale, while simultaneously mitigating chronic threats such as vessel collisions, underwater noise, and climate-induced reductions in prey availability.

Complementing the Pelagos Sanctuary, the Cetacean Migration Corridor (“Corredor de Migración de Cetáceos del Mediterráneo”), located between the Spanish mainland and the Balearic Islands, was designated a Spanish Marine Protected Area and elevated to SPAMI status under the Barcelona Convention

(Espada et al., 2024; Sèbe et al., 2023). The corridor serves as a critical migratory highway for fin whales traveling between northern feeding grounds and potential southern breeding or wintering areas, possibly extending into the Atlantic. Its protection enhances the connectivity of the Mediterranean cetacean habitat network, but the protection measures are voluntary (Panigada et al., 2021; Espada et al., 2024).

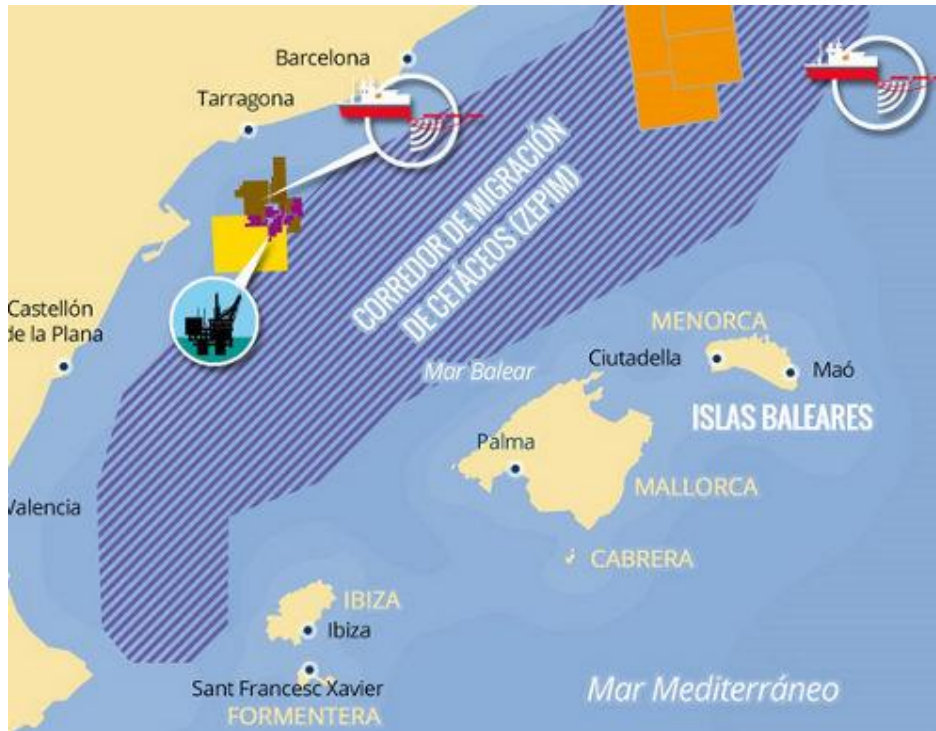


Figure 14. In this image, the migration corridor of cetaceans between the Iberian Peninsula and the Balearic Islands is highlighted with blue lines. This is a key area for the passage of fin whales (and other cetaceans) during migration. Imagine by: Bravo Villa, C . “Llamamiento internacional al gobierno español para proteger el corredor de migración de cetáceos del mediterráneo.” EFeverde. <https://efeverde.com/migracion-cetaceos/>

In the Strait of Gibraltar, a globally significant key point for marine megafauna, conservation efforts focus on mitigating one of the most lethal threats to fin whales: vessel collisions. In 2007, the Instituto Hidrográfico de la Marina, under Spain’s Ministry of Defense, implemented a Traffic Separation Scheme (TSS) specifically designed to reduce ship-strike mortality for fin and sperm whales. This maritime routing measure establishes a designated security zone where vessels are advised to reduce speed and maintain heightened navigational caution, particularly during the peak cetacean transit period from April to August. Despite its scientific foundation, the TSS suffers from significant limitations: there is no robust evidence of consistent compliance by commercial or recreational mariners, and the measure is seasonal, leaving fin whales unprotected during their winter migrations through the strait as they move between Mediterranean feeding areas and putative Atlantic breeding grounds (Panigada et al., 2021; Gauffier et al., 2018).

Further north, the Caprera Canyon a prominent submarine canyon in the north-western Mediterranean, is recognized within the North-western Mediterranean Pelagic Ecosystems Ecologically or Biologically Significant Area (EBSA), identified for its outstanding biodiversity value. Since 2012, the canyon has been incorporated into Italy's Ecological Protection Zone (EPZ), a jurisdictional extension beyond territorial waters. However, this designation prioritizes sovereign control rather than active conservation, lacking enforceable measures to protect marine mammals or their habitats. The canyon lies close to a mosaic of protected sites, including La Maddalena Archipelago National Park (Italy), the Bouches de Bonifacio Natural Reserve SPAMI (France), and several Special Areas of Conservation (SACs) under the EU Habitats Directive (92/43/EEC). In 2011, the International Maritime Organization (IMO) designated the Bonifacio Strait and its surrounding waters as the Mediterranean's first Particularly Sensitive Sea Area (PSSA), acknowledging its ecological uniqueness, high maritime traffic, and vulnerability to shipping-related impacts such as collisions, oil spills, and noise pollution. Despite this dense network of designations, the majority focus on continental shelf and coastal habitats, leaving the deep pelagic ecosystem of the Caprera Canyon largely unprotected. No targeted management actions currently address the needs of cetacean populations particularly fin whales that utilize this canyon for feeding on krill aggregations or as a migratory corridor linking the Pelagos Sanctuary to the Tyrrhenian Sea (Bittau et al., 2025; Panigada et al., 2021).

To address such gaps, Bittau et al. (2025) propose the formal designation of the Caprera Canyon as an Important Marine Mammal Area (IMMA), a non-regulatory but scientifically robust conservation tool developed by the IUCN Marine Mammal Protected Areas Task Force. Initially identified as an Area of Interest (AoI) in 2016 based on preliminary data, the canyon meets all IMMA candidacy criteria (Bittau et al., 2025):

1. High species diversity and abundance, including cetaceans and the Vulnerable Mediterranean monk seal (*Monachus monachus*);
2. Critical life-cycle functions, serving as a feeding and potential breeding habitat with suitable conditions for mating, calving, and foraging on *Meganyctiphanes norvegica*;
3. Connectivity, forming part of documented fin whale migratory routes linking northern and central Mediterranean basins.

Despite these advances, the overall effectiveness of Mediterranean MPAs remains severely constrained. Although approximately 6% of the basin is technically designated as protected only 0.23% benefits from full or high-level protection the management intensity required to deliver measurable ecological gains. Moreover, in 95% of nominally protected areas there is no regulatory differentiation between activities inside and outside the MPA, rendering the designation largely symbolic (Panigada et al., 2024).

The Mediterranean fin whale faces significant threats from vessel interactions, including collisions with ships and disturbances from recreational boats that often disregard regulations protecting cetaceans by approaching too closely, driven by

irresponsible or uninformed behaviour. These interactions are particularly concerning in high-density areas like the Pelagos Sanctuary, Gulf of Lion, and Strait of Gibraltar, where fin whales feed or migrate. Various technological solutions have been explored to reduce ship strikes, such as onboard whale detection systems (e.g., sonar, night vision devices), acoustic alerts to warn whales of approaching vessels, bottom-anchored passive sonar to track whale locations, and trained observers on ferries. However, these methods have limitations, including interference with whale communication, high costs, or effectiveness only in specific conditions (e.g., daytime, nighttime, short distances, or when whales vocalize) (Pace et al., 2015).

1.6 Aim and structure of this study

The main objective of this study is to investigate the species distribution model of the fin whale (*Balaenoptera physalus*) in the Mediterranean Sea and to assess how climate change may affect its spatial distribution in the future.

The study focuses on the western and central Mediterranean basins, where most sightings of the Mediterranean fin whale population have been reported, particularly within the Gulf of Lion, the Strait of Messina and Balearic sea.

To achieve this objective, presence data of fin whales collected between 2006 and 2022 were used to build ecological models that describe the relationship between species occurrence and key environmental variables. These variables include sea surface temperature (SST), phytoplankton biomass, zooplankton biomass, and phosphate concentration.

Two complementary modelling approaches were applied:

- Generalized Additive Models (GAMs), to explore non-linear relationships between fin whale presence and environmental factors.
- Random Forest (RF), a machine-learning algorithm capable of handling complex interactions among variables and providing accurate habitat suitability predictions.

The performance of both models was evaluated to determine which better explains the observed fin whale distribution. The best-performing model was then projected under two future climate scenarios (RCP 4.5 and RCP 8.5), allowing the estimation of how suitable habitat for fin whales may shift under moderate and severe global warming conditions.

These results contribute to a better understanding of the ecological requirements of the Mediterranean fin whale population and provide a predictive framework for assessing the potential impacts of climate change on its distribution.

2. MATERIAL AND METHODS

2.1 Ecological modelling for species distribution

2.1.1 Species Distribution Models (SDMs)

Species Distribution Models (SDMs) represent one of the most widely adopted approaches for predicting and assessing the impacts of climate-driven environmental changes on natural systems (D'Amen et al., 2024). By integrating a suite of environmental, oceanographic, and physiographic covariates, SDMs characterize habitat conditions suitable for a given species and map their spatial and temporal distribution (Elith et al., 2009). In marine ecosystems, SDMs have been successfully applied to predict various climate change effects over the coming decades, including shifts in species ranges and biological invasions (Robinson et al., 2017). These ecological components operate across diverse spatial and temporal scales and are subject to both natural oscillations and anthropogenic influences (D'Amen et al., 2024).

SDMs serve as a critical tool for informing conservation and management strategies, particularly for highly mobile marine species such as cetaceans (Grossi et al., 2025). In cases where ecological knowledge of a species remains limited, SDMs provide a valuable framework for exploring empirical relationships between cetacean occurrence and physical, biological, and human-induced factors (Grossi et al., 2025). Understanding species distributions is fundamental to effective environmental management (Robinson et al., 2017). However, tracking the location of individuals across all species at any given time is impractical, except in rare cases involving intensively studied for highly endangered megafauna (Robinson et al., 2017). Consequently, SDMs are used to estimate a species' geographic and environmental range, explicitly incorporating both seasonal and temporal variability (Robinson et al., 2017).

At global or regional scales, SDMs relate species occurrence records to environmental predictors, offering substantial potential in conservation biology and spatial planning. They provide insights into species–environment interactions and enable testing of ecological and biogeographic hypotheses regarding distribution patterns and range dynamics. Published studies demonstrate that SDMs perform robustly in characterizing natural species distributions within current ranges, especially when based on well-designed survey data, functionally relevant predictors, and appropriately specified modelling algorithms. In this context, SDMs deliver both ecological understanding and strong predictive performance. An SDM is defined as a statistical model that links species distribution data whether occurrence or abundance at known locations with environmental and/or spatial characteristics of those sites, enabling both explanatory analysis and predictive mapping across landscapes (Elith et al., 2009).

The ecological origins of SDMs trace back to early studies that linked biological patterns to geographic and environmental gradients. Advances in remote sensing and environmental data layers have since enabled comprehensive characterization of conditions across entire landscapes, including at historically surveyed sites. Concurrently, the advent of Geographic Information Systems (GIS) has provided

essential infrastructure for managing and analysing both species and environmental datasets (Elith et al., 2009).

Regression-based approaches outperform environmental envelope models (also known as bioclimatic envelopes) and similarity-based methods by explicitly modelling gradients in species occurrence or abundance within the realized environmental niche, rather than defining rigid presence boundaries based solely on observed ranges of predictor variables. Generalized Linear Models (GLMs) dominated early investigations of presence–absence and count data through simple additive structures of linear predictors. With growing recognition of pervasive non-linear species and environment dynamics, an increasing number of studies integrated higher-order parametric terms, such as quadratic or cubic transformations. Generalized Additive Models (GAMs) retain the foundational framework of GLMs but substitute rigid parametric coefficients with data-adaptive smoothing functions to characterize nonlinear responses. This capability has delivered essential flexibility for constructing biologically plausible relationships within species distribution models (SDMs) (Elith et al., 2009).

Species Distribution Models (SDMs) have emerged as a cornerstone in ecology, biogeography, evolutionary biology, and, increasingly, conservation science. A critical challenge in SDM application and in spatial ecology more broadly, lies in reliably extrapolating species distributions across vast, poorly surveyed regions using limited occurrence records (Mi et al., 2016).

2.1.2 Generalized Additive Models

Regression models are frequently employed to capture the associations between a species' spatial distribution and its environmental drivers. These techniques span a spectrum of approaches that vary in their specifications of variable distributions and the mathematical structure of predictor response relationships.

Generalized Additive Models (GAMs), as semiparametric extensions of generalized linear models, rely on two core premises: predictor effects are additive, and each effect is represented by a smooth function. They are widely described as data-driven, since the observed data themselves shape the form of the relationships, free from any a priori constraints on functional specification (Mannocci et al., 2013).

Generalized Additive Models (GAMs) were employed to evaluate the influence of interannual trends on fin whale presence across all spatial scales examined (Tepsich et al., 2020). Although linear regression is frequently applied to detect distributional shifts, GAMs were preferred due to their superior ability to model highly non-linear and non-monotonic relationships, making them particularly well-suited to capturing the complex, dynamic presence patterns in the Mediterranean region (Tepsich et al., 2020).

The application of Generalized Additive Models (GAMs) in cetacean distribution modelling is particularly effective due to their capacity to accommodate non-linear species–habitat relationships (Grossi et al., 2025; Tepsich et al., 2020).

Generalized Additive Models (GAMs) allow for the inclusion of simplistic user-specified interaction terms within a flexible smoothing framework (Grossi et al., 2025; Tepsich et al., 2020).

2.1.3 Random Forest

As the primary goal of Species Distribution Models (SDMs) shifted from understanding ecological processes to accurate spatial prediction, researchers increasingly turned to predictive algorithms specifically designed for high forecasting performance, particularly those developed within the machine learning (Elith et al., 2009).

In an analysis evaluating multiple machine learning algorithms under low-sample conditions, Random Forest consistently outperformed other methods across most evaluation metrics, delivering superior fit to validation datasets and generating more robust and biologically plausible range predictions for each focal species in data-scarce environments. Random Forest, introduced over two decades ago, has long been recognized for its outstanding predictive accuracy in ecological modelling. Despite its growing adoption, the technique remains markedly underutilized in conservation practice, spatial ecology, and inferential studies. By streamlining model selection and reducing analytical effort, Random Forest enables rapid, reliable assessments that support timely and effective conservation decision-making (Mi et al., 2016). Emerging research indicates that machine learning (ML) techniques consistently outperform conventional regression-based approaches in such data-limited scenarios. Among the leading ML algorithms, TreeNet, Random Forest, CART, and MaxEnt are widely regarded as the most robust and versatile tools for routine ecological modelling applications (Mi et al., 2016).

In the context of cetacean SDM, Random Forest has been successfully applied to leverage detections of unidentified baleen whales using a random forest classifier using R package (Derville et al., 2022). This approach is particularly valuable in the Mediterranean Sea, where fin whale sightings are opportunistic and spatially clustered, and environmental gradients are highly non-linear. Random Forest's ability to handle multicollinearity, interactions, and imbalanced datasets makes it ideal to model mobile marine megafauna in under sampled regions such as the Northwestern Mediterranean Sea (Mi et al., 2016).

To complement the Generalized Additive Models (GAMs) and capture potential non-linear and high-order interactions among environmental predictors, a Random Forest (RF) model was implemented using the randomForest package in R.

Random Forests are ensemble learning methods that build multiple decision trees and combine their predictions to boost classification accuracy. This algorithm fits well with ecological data, where predictors often show complex, non-linear, and non-parametric links to species presence. Each partition creates exclusive groups of variances as uniform as possible for the response variable. The algorithm picks

the best split at the parent node to lower the average impurity of the two child nodes. When no gain is possible in a partition, a terminal node is set, ending that branch. Splitting stops when all cases in a node have the same independent variable values, blocking further splits. Together, the nodes form rules that run down the tree to produce a prediction (Evans et al., 2011; Mi et al 2016).

2.2 Study area

Based on sightings collected across various regions, the study area focuses primarily on the northwestern Mediterranean, a key hotspot for fin whales due to its high primary productivity and abundant populations of their primary prey, *Meganyctiphanes norvegica* (Notarbartolo di Sciara et al., 2003; Aïssi et al., 2007). The dataset also includes scattered observations from the central/southern Mediterranean, providing a comprehensive view of the species' distribution in relation to oceanographic features.



Figure 15. Creation of a visual map with observation from 2006 to 2022 using QGIS program: initially the whole of the Mediterranean Sea was considered, but as can be seen visually, the presences are focus on the western part of the Mediterranean Sea reducing the study area only in the western basin.

The distribution of fin whale sightings across the Mediterranean Sea from 2006 to 2022, illustrated in Figure 13 (generated using QGIS), reveals a marked concentration in the northwestern sector, with the highest densities between the Ligurian sea and the Gulf of Lions.

Secondary area with presence of data occurs along the Catalan coasts, Tyrrhenian Sea and Balearic sea. In contrast, sightings are scattered in the southern basins, with isolated records near the Strait of Sicily, Strait of Messina and Sardinia Channel

No observations were recorded in the Adriatic Sea, Libyan Sea, Levantine Sea, Aegean Sea and Black Sea.

The absence of data near the African peninsula is likely due to data deficiency, as no public databases are available for cetacean sightings in this area.

Since the various data of presence focus on the western region of the Mediterranean Sea, and there are no presences detected in the central and eastern parts, the areas of the Adriatic Sea, Libyan Sea, Levantine Sea, Aegean Sea or Black Sea have been removed from the study area. Considering the areas of where the data used for this study are found, the study area was delimited using these coordinate:

xmin = -6.07°	xmax = 16°
ymin = 35°	ymax = 44.5°

Table 1. Minimum and maximum of the latitude (Y) and longitude (X) of the study area.

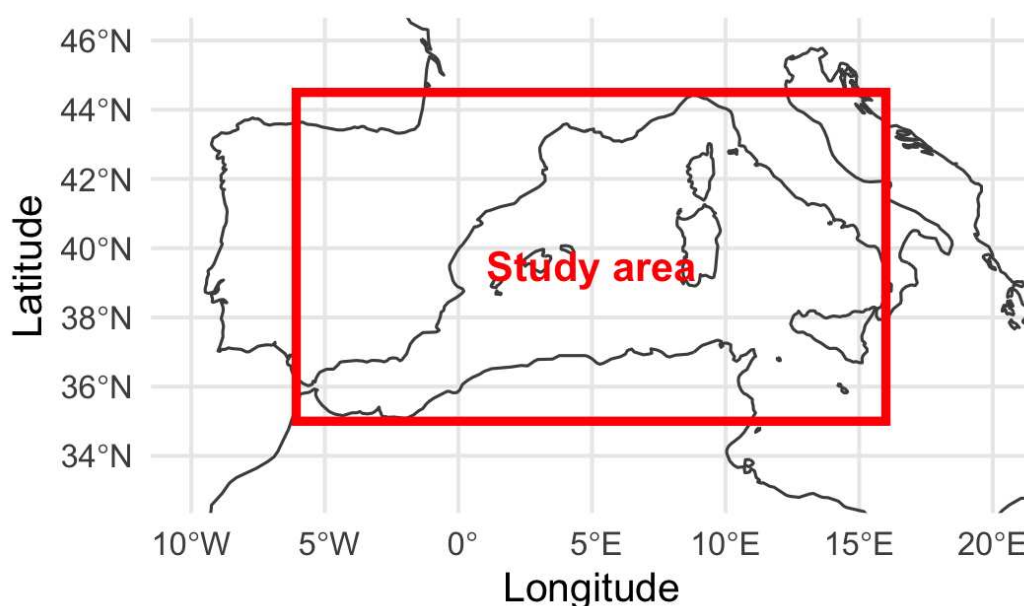


Figure 16. Visualisation with R studio with the coordinate delimiting the study area in Table 1.

This area includes:

- Western Mediterranean: The Alboran Sea, Balearic Sea (between Spain and the Balearic Islands), Ligurian Sea (including the Pelagos Sanctuary), Gulf of Lion, and parts of the Algerian Basin.
- Central Mediterranean: The Tyrrhenian Sea, Strait of Sicily, western Ionian Sea (Strait of Messina, Gulf of Catania), and areas around Sardinia and Corsica.

This area aligns with the North-western Mediterranean Sea Slope and Canyon System, designated as an Important Marine Mammal Area (IMMA).

The occurrence and distribution of species are shaped by a complex interplay of physical, biological, and environmental factors that vary across multiple spatial and temporal scales, as well as by natural fluctuations and human-driven changes in these drivers. In the Mediterranean Sea, a pronounced west-to-east decline in primary productivity mirrors similar gradients in the abundance and diversity of both benthic and pelagic organisms.

At the Strait of Gibraltar, surface inflow of nutrient-rich Atlantic waters contrasts with deep outflow of denser Mediterranean waters, generating a dominant eastward surface current that spawns numerous eddies and cyclonic gyres under the influence of the Coriolis effect. There is no direct surface return flow; instead, intermediate waters from the Levantine Basin move westward along large-scale cyclonic circuits (Millot et al., 2005).

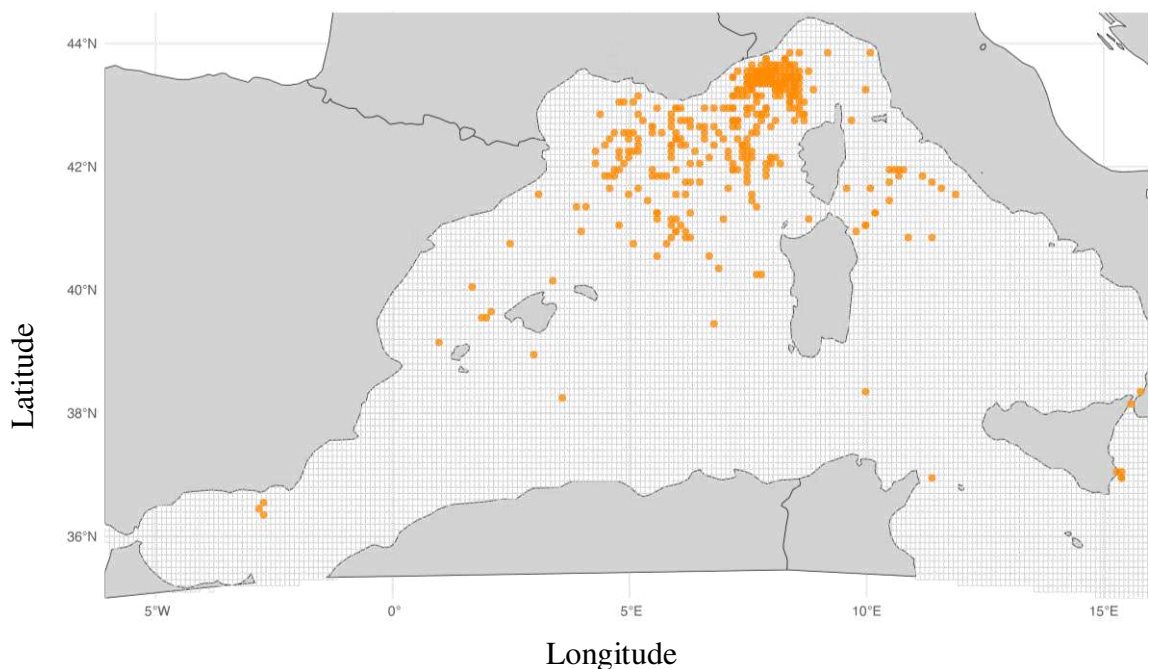


Figure 17. Plot of fin whale observations during summer (June- September) from 2000 to 2022 obtain with R studio. The study area was limited to: $x_{min} = -6.07^\circ$, $x_{max} = 16^\circ$, $y_{min} = 35^\circ$, $y_{max} = 44.5^\circ$

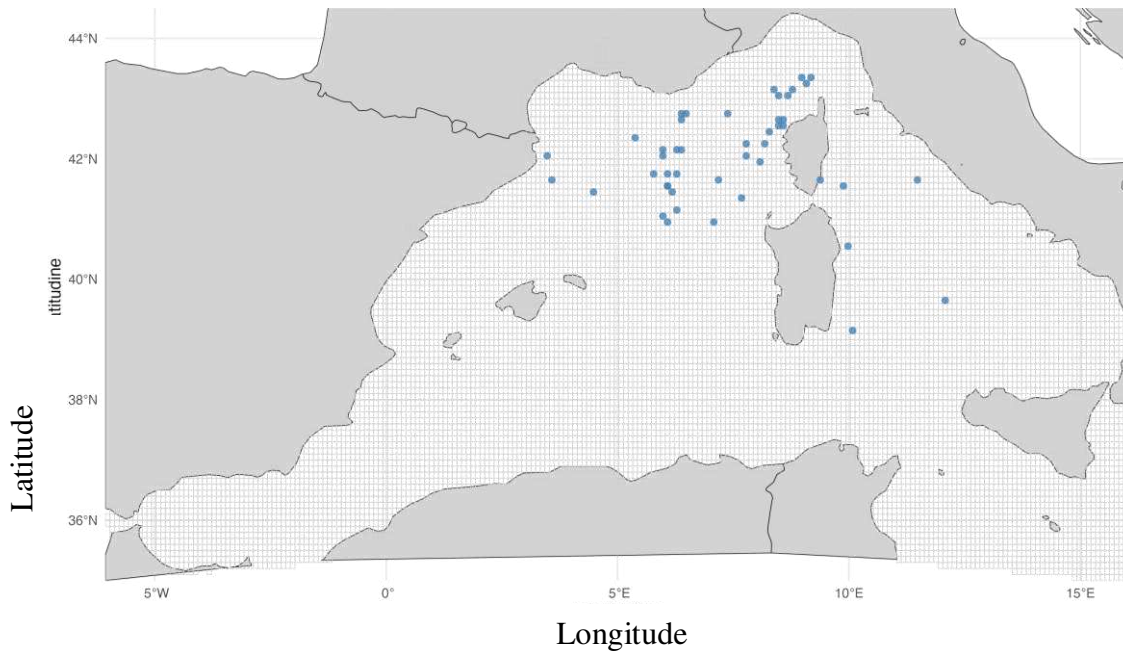


Figure 18. Plot of fin whale observations during winter (December- February) from 2000 to 2022 in the study area obtain with R studio.

2.3 Environmental variables selected

Numerous studies have characterized cetacean occurrence patterns and ecological requirements by establishing links between animal sightings and a suite of environmental predictors. These investigations have traditionally emphasized connections with sea surface temperature, seabed morphology, hydrodynamic features such as currents and frontal zones, seasonal pulses in primary productivity, and the spatial distribution of prey resources. Fin whale distribution in the Mediterranean feeding grounds is primarily driven by prey availability, particularly dense aggregations of the euphausiid *Meganyctiphanes norvegica* (Panigada et al., 2006).

To model distribution habitat in the northwestern and central Mediterranean from 2006 to 2022, dynamic oceanographic and biogeochemical variables were retrieved from the Copernicus Climate Data Store (CDS; Copernicus Climate Change Service, 2020) with a spatial resolution of $0.1^\circ \times 0.1^\circ$ and monthly temporal resolution (D'Amen et al., 2024). In the Copernicus Climate Data Store was used the Dataset: "Marine biogeochemistry data for the Northwest European Shelf and Mediterranean Sea from 2006 up to 2100 derived from climate projections". The data were downloaded using the Polcoms-Ersem origin with an $0.1^\circ \times 0.1^\circ$ spatial resolution (Copernicus Climate Change Service, 2020).

Although I originally wanted to use daily data to get a more detailed view of the changes on a small scale, I had to change to using monthly data because chlorophyll-a, phytoplankton carbon, zooplankton, and phosphate are provided at monthly temporal resolution in the reanalysis product. Although sea surface temperature (SST) is (the only) available daily, it was averaged to monthly means

to maintain coherence with the other biogeochemical variables and to minimize short-term meteorological variability unrelated to fin whale habitat selection.

The selected variables included sea surface temperature (SST, 0.5 m), phosphate (PO_4^{3-}), phytoplankton biomass (Phyc), and zooplankton biomass (Zooc), each extracted at 10 m and 100 m depth layers to capture vertical gradients in productivity and nutrient availability: these depth was selected to capture both surface-layer productivity and potential subsurface chlorophyll maxima that develop during water column stratification. The conceptual model that links the relationship between the variables is as follows: a bottom-up trophic linkage from phosphate availability \rightarrow phytoplankton biomass \rightarrow zooplankton abundance \rightarrow fin whale presence. These variables were chosen because SST represents the direct physical effect of climate warming, phosphate reflects riverine nutrient input and eutrophication, and phytoplankton and zooplankton indicate primary and secondary productivity, respectively, which influence prey availability for fin whales.

Values were sampled at $0.1^\circ \times 0.1^\circ$ grid cell centroids using nearest-neighbour matching after rounding longitude and latitude to one decimal place (D'Amen et al., 2024).

Variable	Depth	Unit	CMEMS Product
Sea Surface Temperature (SST)	0.5 m	C° Celsius	thetao
Phosphate concentration (PO_4)	10 m and 100 m	mol m^{-3}	Po4
Phytoplankton carbon concentration	10 m and 100 m	mol m^{-3}	phyc
Zooplankton carbon concentration	10 m and 100 m	mol m^{-3}	Zooc
Nitrate concentration (NO_3)	10 m and 100 m	mol m^{-3}	No3

Table 2. Environmental variables used in the models with its depth used, unit of measurement, and name of the variable in the Copernicus Climate Data Store.

The variables were chosen based on two criteria:

1. Direct or indirect influence on fin whale presence, particularly via effects on prey distribution, aggregation, and productivity
2. Susceptibility to climate change, enabling future projections of habitat shifts under warming and altered circulation scenarios

All predictors were standardized (z-score normalization) using the mean and standard deviation from the training dataset to ensure comparability across variables and to prevent scale-dependent bias in the Random Forest model.

2.3.1 Sea Surface Temperature (SST)

Although fin whales are endothermic and capable of thriving across a broad spectrum of sea surface temperatures, temperature does not constitute a direct physiological barrier. Instead, SST exerts a powerful indirect influence on habitat suitability by:

- shaping the vertical migration and aggregation patterns of krill in the upper water column
- influence the mixed layer depth (MLD) and thermocline dynamics, which in turn control nutrient upwelling and water column stratification
- acting as a robust predictor for chlorophyll-a concentration and phytoplankton biomass, especially in areas exhibiting pronounced seasonal thermal gradients (Arcangeli et al., 2012).

Sea surface temperature was extracted at 0.5 m depth on a 0.1° grid, using as unit of measurement degrees Celsius (°C).

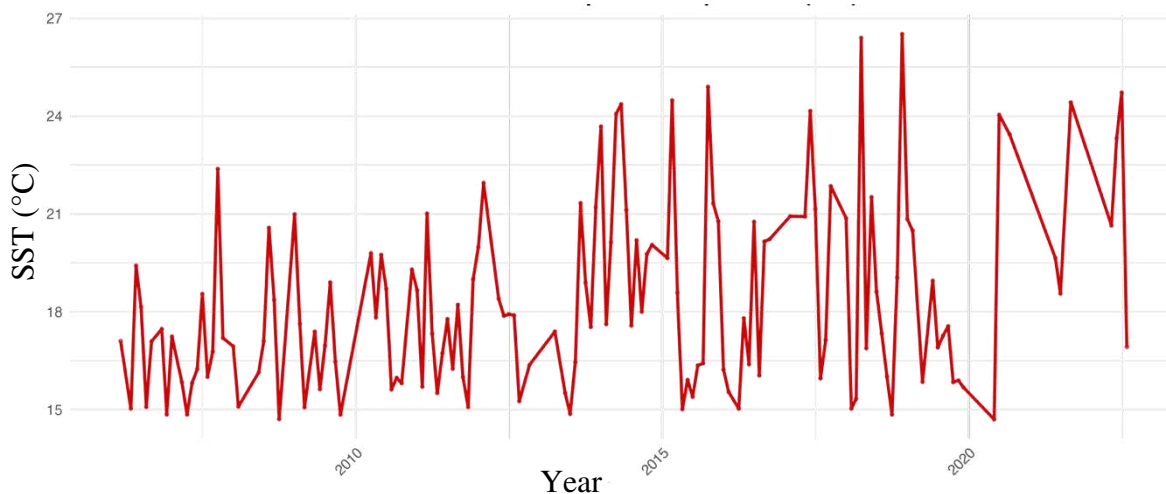


Figure 19. Interannual variability of mean Sea Surface Temperature (SST °C) across the study area in the Mediterranean Sea between 2006 and 2022.

From the Figure 19, we can observe that SST values range approximately between 15°C and 26°C, showing a clear seasonal cycle imposed on interannual fluctuations. Warmer peaks correspond to summer months, while minima reflect winter conditions. Despite the high short-term variability, a general warming tendency can be observed after 2013, with more frequent and intense summer temperature maxima exceeding 24°C–26°C in 2017-2018 meanwhile from the 2020 there is an increase of minima temperature. The observed increase in Sea Surface Temperature (SST) across the Mediterranean Sea represents a clear manifestation of the direct effects of global climate change on marine systems. The Mediterranean basin, being a semi-enclosed and relatively shallow sea, responds rapidly to atmospheric warming and has been identified as one of the world's climate change hotspots. This warming trend is largely attributed to the enhanced greenhouse effect, caused by elevated atmospheric concentrations of carbon dioxide (CO₂) and other heat-trapping gases, which reduce longwave radiation loss from the ocean surface. The persistence of positive heat anomalies has altered the seasonal thermal cycle, producing earlier and longer-

lasting summer peaks and delayed autumn cooling. Prolonged warming periods and the intensification of marine heatwaves may lead to shifts in prey distribution and the displacement of key feeding habitats.

2.3.2 Phytoplankton

Phytoplankton carbon concentration (with unit of measurement mol m^{-3}) were extracted at 10 m and 100 m depths to capture both surface productivity and subsurface chlorophyll maxima during stratification.

Chlorophyll-a is a direct proxy for phytoplankton biomass and primary production (Grossi et al., 2025).

Chlorophyll-a fronts are critical mesoscale foraging hotspots: persistent for some weeks, they enable energy transfer to zooplankton and higher trophic levels, including krill and fin whales (Panigada et al., 2017).

Druon et al. (2012) demonstrated that 80% of Mediterranean fin whale sighting occurred within 10 km of predicted chl-a fronts, confirming their role as primary feeding habitat indicators (Druon et al., 2012).

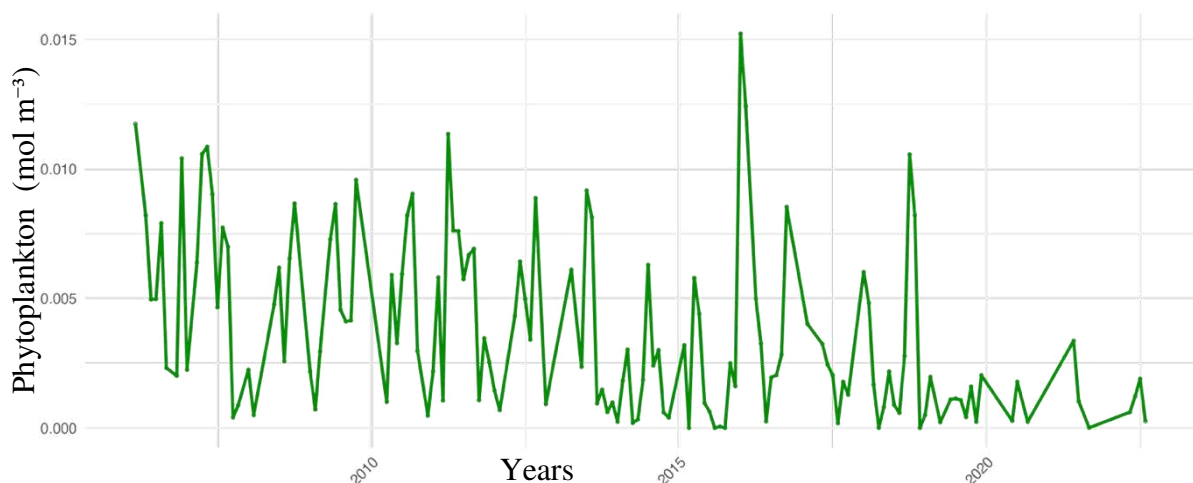


Figure 20. Interannual variability of mean Phytoplankton carbon (mol m^{-3}) at 10m depth across the study area in the Mediterranean Sea between 2006 and 2022.

Generally, looking the Figure 20. we can see a decreasing trend of phytoplankton concentration during the years, maybe linked at the rising temperature that enhance stratification reducing the nutrient supply to surface water.

In 2006 we can see phytoplankton carbon values with higher values and more variable, with several strong peaks (around 0,01- 0,015 mol m^{-3}). From 2010 we can see a decline in mean and the variability of the concentration.

After 2015, excluding for some peaks, the values drop significantly, and by 2020-2022 they remain very low and stable close to 0.001 mol m^{-3} .

2.3.3 Zooplankton

Total zooplankton concentration (mol m^{-3}) at 10 m and 100 was included as a direct proxy for secondary production. While *Meganyctiphanes norvegica* is not resolved in global biogeochemical models, total zooplankton biomass reflects

krill-supporting food webs. Zooplankton blooms lag phytoplankton by 2–4 weeks, concentrating in productive fronts and upwelling zones (Panigada et al., 2017).

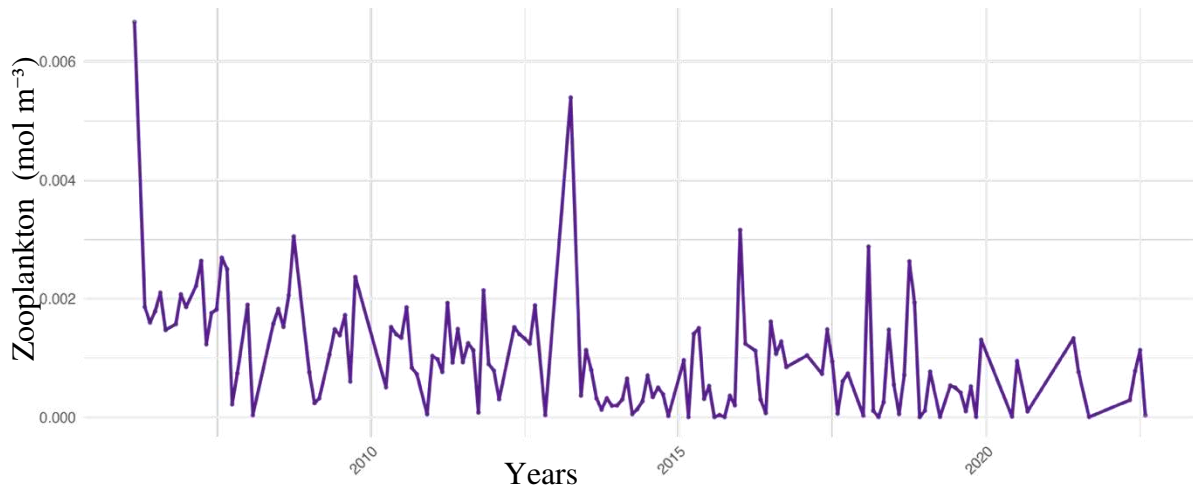


Figure 21. Interannual variability of mean Zooplankton at 10m depth carbon (mol m^{-3}) across the study area in the Mediterranean Sea between 2006 and 2022.

Looking at the Figure 21. at the beginning in 2006 there is a very high peak, reaching higher value than 0.006 mol m^{-3} , followed by a rapid decline. After the peak, values of concentration fluctuate between 0.005 and 0.002 until 2012, with a peak in 2013. From 2015 we can see fluctuations reaching 0.003 mol m^{-3} ; but generally a slight decline. Generally there is a decline of the zooplankton biomass, it's linked to the reduction of the phytoplankton biomass, since zooplankton use phytoplankton as prey so there is a reduction of food availability.

2.3.4 Phosphate

Phosphate concentration (mol m^{-3}) at 10 m and 100 m was selected to capture nutrient limitation and terrestrial inputs for the rivers: Rhône, Ebro, Simeto, Turia. Although both nitrate and phosphate were initially considered, high collinearity led to the exclusion of nitrate to prevent model overfitting.

Phosphate is a key limiting nutrient in the oligotrophic Mediterranean, particularly in the western basin.

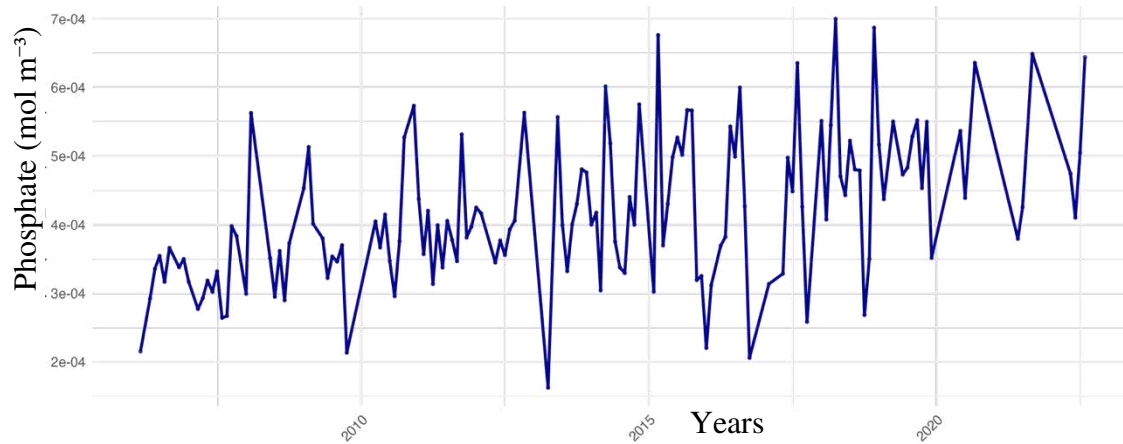


Figure 22. Interannual variability of mean Phosphate at 10m depth (mol m^{-3}) across the study area in the Mediterranean Sea between 2006 and 2022.

In the early years phosphate levels fluctuate around $2\text{e-}04$ and $6\text{e-}04$ (mol m^{-3}), after 2015 value tend to be higher and more variable reaching $7\text{e-}04$ (mol m^{-3}); after the 2020 the level increase with the minimum of level staying up to $3.5\text{e-}04$ (mol m^{-3}). The observed increase in phosphate concentration in the Mediterranean Sea is primarily associated with riverine inputs of nutrients originating from anthropogenic sources. Rivers act as the main conduits transferring dissolved and particulate phosphorus from land to the marine environment.

This enrichment is largely driven by intensive agricultural activities, particularly the widespread use of phosphate-based fertilizers, which enhance soil nutrient leaching into river system. In addition, urban and industrial wastewater discharges contribute significant loads of organic phosphorus and detergents, further elevating phosphate levels in coastal waters, especially near densely populated regions. Episodes of extreme weather events, such as floods and heavy rainfall, have also intensified in recent decades due to climate variability, leading to increased runoff and erosion of agricultural soils. These events accelerate the transport of nutrient-rich sediments and pollutants toward river mouths and the sea, resulting in short-term but substantial spikes in phosphate concentration.

2.4 Data collection

Fin whale occurrence data were compiled from multiple datasets covering the period from 2006 to 2022. Coordinates were rounded to a spatial resolution of 0.1° (~ 11 km) to reduce positional uncertainty, and duplicate records were merged by giving priority to confirmed presences (D'Amen et al., 2024). Temporal duplicates were removed by retaining a single record per location per month. Data were gathered from the following sources:

1. OBIS SEAMAP (Ocean Biogeographic Information System Spatial Ecological Analysis of Megavertebrate Populations): data were obtained

through R Studio using the `OBIS.R` package (OBIS SEAMAP 2025)(<https://seamap.env.duke.edu/species/180403>)).

2. Torreblanca et al. (2019): supplemental material providing additional opportunistic fin whale sightings
3. ACCOBAMS Survey Initiative (ASI): data exchanged through the [ACCOBAMS platform] (<https://accobams.org/main-activites/accobams-survey-initiative-2/asi-preliminary-results/>).
4. Balears data: fin whale sightings provided by the Asociación Tursiops (Palma de Mallorca, 2025)

The spatial occurrence data for the fin whale were retrieved from the OBIS-SEAMAP repository (OBIS, 2025) using the R programming environment (R Studio, 2025) through the following workflow:

1. Clean the R environment
2. Check and set a working directory in the computer
3. Install and load R packages: devtools, robis, leaflet
4. Explore the documentation of robis to understand how it works
5. Specify the area where you want to download sightings, using occurrence (function from robis)
6. Write down the species in the scientific name and download the data with occurrence
7. Save the downloaded data to a CSV file

To ensure the dataset reflected genuinely opportunistic sightings rather than structured survey effort, records exhibiting a strictly linear spatial arrangement (indicative of systematic ferry-based or dedicated transect surveys) were excluded. This filtering step was applied to avoid over-representation of high-effort sampling routes, which could bias habitat suitability models toward areas of frequent monitoring rather than true environmental preference. The retained observations are spatially dispersed and irregular, consistent with heterogeneous, non-systematic reporting from platforms of opportunity (whale-watching vessels, fishing boats, and citizen science contributions). This approach aligns with best practices in species distribution modelling when using presence-only data from heterogeneous sources. The OBIS database provides open access to over 40 million marine species records across 115,000 species, contributed by nearly 500 institutions worldwide. Data are stored in a PostGIS relational database, integrating information from scientific surveys, monitoring programs, and research projects. The OBIS system ensures data quality through expert validation of species identification and spatial accuracy (OBIS, 2025). Access to OBIS data is managed through the D4Science e-Infrastructure, which connects users to the PostGIS database via authenticated read-only access (OBIS, 2025). All data were standardized and merged into a unified geospatial database. The combined dataset comprised 1,451 distinct fin whale sightings across the Mediterranean Sea, primarily recorded between May and September. For spatial visualization, the data were imported into QGIS, using the ESRI Satellite Basemap (EPSG:3857) projection to display the distribution of fin whale sightings across the study area (Figure 23).

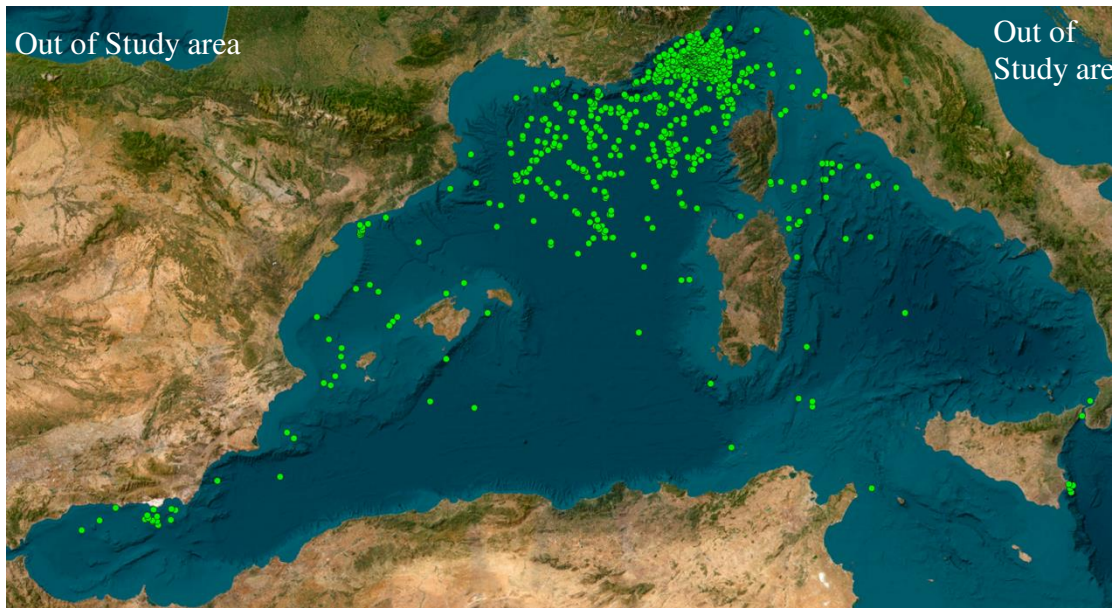


Figure 23. Opportunistic data of presence of fin whale in the study area from 2006 to 2022; figure obtain with QGIS.

To minimize bias associated with transient individuals, records within 10 km of the coastline or near the Strait of Gibraltar were excluded during the temporal period of migration in the Atlantic sea (June-July). These areas are typically associated with migratory movements between the Atlantic and Mediterranean populations. The filtering process ensured that the models focused on the resident Mediterranean population, which occupies pelagic habitats during feeding periods. Fin whale observations were aggregated as daily presence records, while environmental variables were averaged at monthly temporal resolution to match the scale of the climatic and biogeochemical data. Each whale sighting was associated with the corresponding mean monthly value of environmental predictors (SST, chlorophyll, phosphate, zooplankton biomass).

2.4.1 Opportunistic data

Given the high cost and logistical constraints of marine surveys, opportunistic sightings (OS) provide valuable information on cetacean distribution at relatively low cost. These data originate from non-systematic observation platforms such as recreational vessels, research cruises, or citizen-science initiatives where search effort is not standardized (Torreblanca et al., 2019).

In the case of fin whales, OS data are considered highly reliable for presence detection due to the species' large size, distinctive blow, and characteristic body shape. However, OS datasets are subject to detection biases, including availability bias, when animals are submerged and not visible to observers and perception bias, when visible animals are missed by observers. Moreover, the absence of sightings in OS datasets may result from a lack of observation rather than a true absence, leading to spatial sampling bias (Torreblanca et al., 2019).

Despite these limitations, OS data remain useful for habitat modelling, allowing comparison between regions with similar observation effort and ecological conditions.

2.4.2 Pseudo-Absence Generation

In this study, a pseudo-absence approach adapted from Torreblanca et al. (2019) was employed, assumes equal sampling effort across both subsets (fin whale and striped dolphins), thereby mitigating biases inherent in opportunistic sighting (OS) data. Unlike true absence which requires systematic surveys and are not available in OS datasets this method uses real observations of another ecologically relevant species to define background conditions.

Pseudo-absences were generated following a target-group approach, using Striped dolphins (*Stenella coeruleoalba*) occurrences as a proxy for sampling effort. This method assumes that areas with observations of Striped dolphins were surveyed but fin whales were not detected, thereby reducing sampling bias. However, potential ecological overlap between the two species should be acknowledged as a source of uncertainty. The resulting model does not predict absolute habitat suitability, but rather the differential spatio-temporal distribution of fin whale relative to *Stenella coeruleoalba*, reflecting potential niche partitioning or resource competition in pelagic environments (Torreblanca et al., 2019). Fin whale (*Balaenoptera physalus*) presence was defined as ≥ 1 opportunistic sighting within a $0.1^\circ \times 0.1^\circ$ grid cell on a given day (2006–2022). Pseudo-absences were defined as ≥ 1 sighting of the striped dolphin (*Stenella coeruleoalba*) with no co-occurring fin whale in the same grid cell and day.

The choice of use striped dolphins' data was based on a preliminary analysis of occurrence records retrieved from the Ocean Biodiversity Information System (OBIS, 2025), which revealed that the striped dolphin is the most frequently reported cetacean across the Mediterranean Sea. Its high observation density provides the largest available sample of opportunistic sightings, thereby maximizing the robustness and statistical power of the pseudo-absence layer while minimizing sampling bias associated with less commonly reported species.

The modelling dataset was structured as binomial presence/pseudo-absence data:

- A grid cell on a given day was assigned a value of 1 (presence) if at least one fin whale (*Balaenoptera physalus*) was recorded.
- A value of 0 (pseudo-absence of fin whale) was assigned when at least one striped dolphin (*Stenella coeruleoalba*) was observed in the same cell and day, with no co-occurring fin whale sighting.

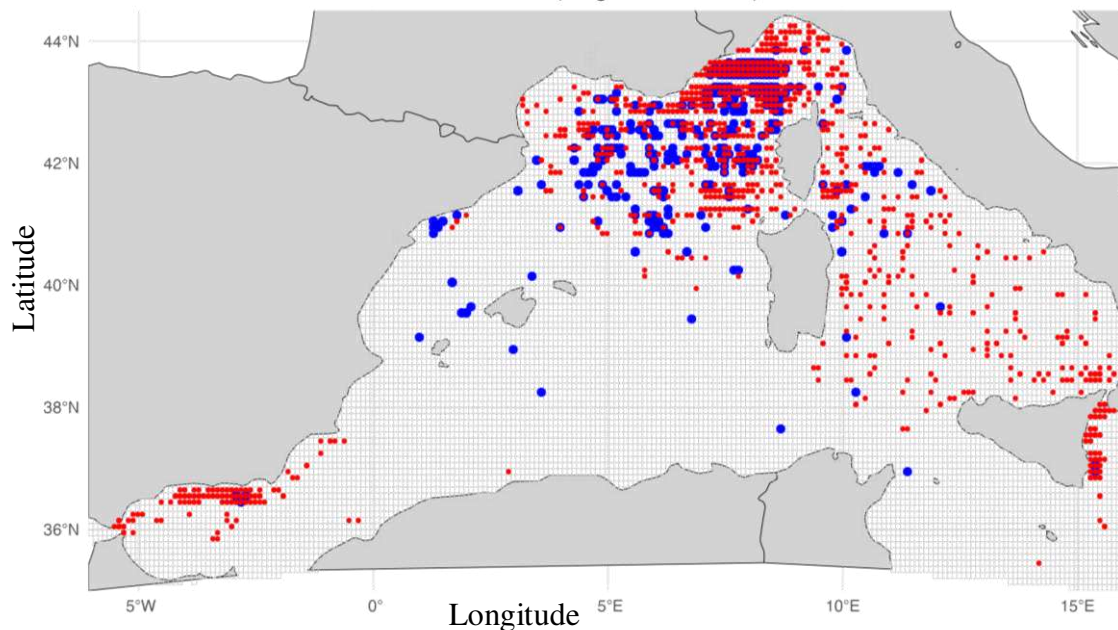


Figure 24. Distribution map in the study area of the fin whale (with a grid $0,1^{\circ} \times 0,1^{\circ}$) obtain with R Studio. Red point indicates Pseudo-absence of fin whale meanwhile blue point indicate presence of fin whale

2.5 Workflow of ecological models

The ecological modelling process was conducted in “R Studio (version 4.3.2)” and followed a structured multi-step workflow designed to integrate environmental predictors with fin whale (*Balaenoptera physalus*) presence and pseudoabsence data.

The objectives were to

- identify the main environmental drivers of the species’ spatial-temporal distribution in the northwestern Mediterranean Sea (2006–2022)
- select the model with the highest predictive performance

2.5.1 Workflow of presence and pseudo absence data

The following workflow was implemented in R to construct a spatially and temporally explicit binomial dataset of fin whale (*Balaenoptera physalus*) presence and pseudo-absence records, using striped dolphin (*Stenella coeruleoalba*) observations as a proxy for sampling effort.

Step 1. Data Ingestion and Preprocessing

Two raw datasets were imported as Excel file, one for fin whale and the other for striped dolphins (to see how they were obtained, refer to the Data collection section). Relevant columns (lat, lon, date) were selected and standardized. A species identifier was added: "fin_whale" for presence data and "stenella" for pseudo-absence candidates. Date fields were parsed using “as.Date()”, with robust

handling of multiple input formats (ISO 8601 with time, or YYYY-MM-DD). Invalid or missing dates were logged and removed.

Step 2. Spatial and Temporal Filtering

Observations were restricted to the study domain with longitude from -6.07° to 16° E and latitude from 35° to 44.5° . The temporal window has been selected from 2006 to 2022. This step aligned both datasets with the environmental covariate period and geographic extent of the Mediterranean modelling domain.

Step 3. Conversion to Spatial Objects

Both datasets were converted to “sf” objects using WGS84 (EPSG:4326) as the coordinate reference system, enabling spatial operations.

Step 4. Application of marine mask

A Mediterranean Sea polygon was loaded from the IHO shapefile (iho.shp). The shapefile was cropped to the study bounding box, transformed to EPSG:4326, validated (`st_make_valid()`), and filtered to exclude non-relevant basins (Adriatic and Cantabrian Seas). Polygons were united into a single mask (`med_sea_union`). Observations falling outside this mask were removed via spatial intersection (`st_intersects`), ensuring all records lie within valid marine areas.

Step 5. Construction of $0.1^{\circ} \times 0.1^{\circ}$ analysis grid

A regular grid was generated over the study domain using “`st_make_grid()`” with a cell size of 0.1° in both dimensions. Grid cells were masked to retain only those intersecting the Mediterranean marine area. Each cell was assigned a unique `grid_id`, and centroid coordinates (lon, lat) were computed for spatial referencing.

Step 6. Spatial Assignment of observation to grid cells

Point in polygon intersection (`st_intersects`) was used to assign each observation to its corresponding grid cell. Observations not intersecting any valid cell were excluded. Rigorous validation ensured all retained `grid_id` values were present in the reference grid.

Step 7. Daily Aggregation and Binomial Labeling (Presence/Pseudo-Absence Logic)

All unique observation dates from both species were extracted to define the temporal scope. For each date and each grid cell containing at least one observation:

- Presence (1): Assigned if ≥ 1 fin whale was recorded in the cell on that day (priority rule).
- Pseudo-absence (0): Assigned if ≥ 1 striped dolphin was recorded, and no fin whale was present in the same cell and day.

This hierarchical rule prevents co-occurrence conflicts and ensures pseudo-absences reflect confirmed sampling effort without target species detection.

Step 8. Data assembly and quality control

Daily records were compiled into a master data frame (`model_data`). Rounded coordinates (`lon_round`, `lat_round`) were added to facilitate environmental data joining. Comprehensive checks were performed: 1) No duplicate records per date + `grid_id`, 2) All `grid_id` values valid, 3) No missing values in core fields. Summary statistics (number of presences, pseudo-absences) were logged.

Step 9. Data Export

The final binomial dataset was saved csv file; this table serves as the foundation for subsequent species distribution modelling.

2.5.1 Workflow of GAM

A Generalized Additive Model (GAM) was selected as the initial modelling approach due to its ability to capture non-linear relationships between environmental predictors and species occurrence.

The model was implemented in R Studio using the following structured workflow:

Step 1: Spatial Domain Definition and Grid System Construction.

The modelling domain was explicitly defined to cover the western and central Mediterranean Sea, spanning longitude from -6.07° to 16° E and latitude from 35° to 44.5° N. A regular rectangular grid was generated using `sf::st_make_grid()` with a cell resolution of $0.1^{\circ} \times 0.1^{\circ}$. This produced an initial lattice of 6,139 candidate grid cells. To ensure ecological relevance, the grid was masked to valid marine areas by overlaying a topologically cleaned version of the International Hydrographic Organization (IHO) seas vector layer (`iho.shp`). The shapefile was cropped to the study bounding box, reprojected to EPSG:4326 (WGS84), validated using `st_make_valid()`, and filtered to exclude non-target marine regions (specifically the Adriatic Sea and Cantabrian Sea). The remaining polygons were dissolved into a single multipart feature using `st_union()` to create `med_sea_union`. Only grid cells whose centroids intersected this marine mask were retained, resulting in a final set of 5,842 valid analysis cells. Each cell was assigned precise geographic centroid coordinates (`lon`, `lat`) via `st_centroid()` and `st_coordinates()` to facilitate subsequent spatial joins with environmental data.

Step 2. Preprocessing of the Binomial Response Dataset

The core response dataset: “`model_data_grid_presence_pseudoabsence.csv`” was imported using `read.csv()`. This file contains daily records where each 0.1° grid cell on a given date is labelled as presence (1) if at least one fin whale was observed, or pseudo-absence (0) if at least one striped dolphin was observed with no co-occurring fin whale. Dates were parsed and converted to Date class using `as.Date(..., format = "%d-%m-%Y")` to ensure consistent temporal alignment. A derived field, `year_month`, was created in YYYY-MM format using `format(date, "%Y-%m")` to enable matching with monthly environmental averages. Spatial coordinates were rounded to one decimal place (`lon_round`, `lat_round`) using `round(..., 1)` to guarantee exact alignment with the gridded environmental layers, avoiding floating-point mismatches during joins.

Step 3. Preprocessing of Environmental Covariate Layers with a Dedicated Function

A reusable custom function, `prepare_env()`, was developed to standardize the processing of all oceanographic predictor variables. This function accepts a CSV file path, target variable name, optional depth level (10 m or 100 m), and optional month filter. For each input table:

- Dates are parsed and a `year_month` field is generated.
- Longitude and latitude are rounded to one decimal place.
- If a specific month or depth is provided, records are filtered accordingly.
- Duplicates are removed using `dplyr::distinct(year_month, lon_round, lat_round, .keep_all = TRUE)` to retain a single mean value per cell and month.
- The target variable is renamed for clarity (e.g. `thetao` → `sst`; `phosphate` at 10 m → `phosphate_10m`). This function was applied to produce seven clean, grid-aligned predictor layers: Sea Surface Temperature (SST), phosphate at 10 m and 100 m, phytoplankton biomass at 10 m and 100 m, and zooplankton biomass at 10 m and 100 m.

Step 4. Integration of Response and Predictor Data with Quality Control

The response dataset was sequentially merged with all seven environmental layers using `dplyr::left_join()` on the composite key (`year_month`, `lon_round`, `lat_round`). This ensured that each observation retained its full suite of predictors. Records with any missing values across the seven core variables were removed using `complete.cases()`, resulting in a final analytical dataset of 1,523 complete observations. A reproducible 70/30 train/test split was performed using `set.seed(123)` to fix the random partition. Class distribution was explicitly logged: the full dataset contained 132 presences and 1,391 pseudo-absences (~8.7% presence rate), with the training set preserving a similar imbalance (~8.7% presences) and the test set slightly lower (~8.5%).

Step 5. Model Calibration Using 5-Fold Spatial Block Cross-Validation

To mitigate the risk of spatial overfitting and ensure robust generalization, a spatial block cross-validation scheme was implemented. Training observations were assigned to $2^\circ \times 2^\circ$ spatial blocks by applying `floor(lon / 2) * 2` and `floor(lat / 2) * 2`, and combining these into a unique `block_id`. This created a set of spatially coherent units. The `caret::createFolds()` function was then applied to the list of unique block IDs (not individual points) to generate five spatially independent folds, preventing information leakage across geographically proximate areas. A systematic grid search was conducted over the smoothing basis dimension parameter with $k \in \{3, 4, 6, 8, 10\}$. For each candidate k and each fold:

- A GAM was fitted on the four training folds using `gam()` with binomial family, logit link, REML smoothness selection, and class-weighted penalties (presence weight = 1.0, pseudo-absence weight = 0.1) to address imbalance.
- Predictions were generated on the held-out fold using `predict(..., type = "response")`.

- Discriminatory performance was quantified via the under the-curve area (AUC) from the receiver operating characteristics (ROC); using `pROC::auc()`. Mean and standard deviation of AUC across the five folds were computed for each `kkk`. The value `k=4` was selected as optimal, achieving the best mean AUC.

Step 6. Fitting the Final GAM and Extracting Comprehensive Diagnostics

The final model was refit on the entire training dataset using the calibrated `k=4`:

```
Presence ~ s(SST,k=4) + s(phosphate 10m, k=4) + s(phosphate 100m,
k=4) + s(phytoplankton 10m ,k=4) + s(phytoplankton 100m ,k=4) +
s(zooplankton 10m ,k=4) + s(zooplankton 100m ,k=4)
```

A custom diagnostic function, `fit_gam_diagnostics()`, was used to extract:

- Effective Degrees of Freedom (EDF) and significance (p-values) for each smooth term, derived from `summary.gam()$edf` and `anova.gam(..., test = "Chisq")`.
- Global performance metrics on the independent test set: accuracy (threshold = 0.5), AUC, adjusted R^2 , percentage deviance explained, and Generalized Cross-Validation (GCV) score. Residual spatial autocorrelation was assessed using Moran's I on Spearman residuals. A neighborhood matrix was constructed with a maximum distance of 0.3° using `spdep::dnearneigh(..., longlat = TRUE)`, and row-standardized weights were applied via `nb2listw(..., style = "W", zero.policy = TRUE)` to accommodate isolated cells. The test yielded $I = 0.018$, $p = 0.412$, indicating no significant residual clustering.

Step 7. Construction of the July 2018 Prediction Grid and Probability Inference

A complete prediction surface was built by joining all valid grid centroids to the July 2018 monthly means of the seven environmental predictors using the same `left_join()` logic. After removing cells with incomplete data via `drop_na()`, 5,842 cells remained for prediction. Presence probability was computed for each cell using `predict(final_model, newdata = pred_grid, type = "response")`. These probabilities were transferred to a `SpatRaster` object (resolution 0.1° , CRS EPSG:4326) via `terra::rast()` and `cellFromXY()`. Minor gaps in coverage were filled using a 3×3 focal mean filter (`focal(..., w = matrix(1,3,3), fun = mean, na.rm = TRUE, pad = TRUE)`), and the final raster was masked to the Mediterranean marine area using `terra::mask()` with `med_sea_union`.

Step 8. Visualization, Sensitivity Analysis, and Deliverable Generation

The probabilistic habitat suitability map was rendered using `ggplot2::geom_tile()` with the viridis "plasma" color ramp, scaled from 0 to 1, and overlaid with medium-scale coastlines from `rnaturalearth::ne_coastline()`. Map annotations included model performance metrics in the subtitle. Partial dependence plots for all seven smooth terms were arranged in a 2×4 grid using base R `plot.gam()`, with EDF and p-values displayed in each panel title for immediate interpretability. A sensitivity analysis was conducted by fitting a secondary model with `k = 10`, and results were compared side-by-side. All outputs performance tables, smooth term summaries, comparison CSVs, high-resolution maps, and effect plots were exported with descriptive, versioned filenames.

2.5.2 Workflow of Random Forest

Since we obtained low performance values for the GAM, we proceed to create a model development of a Random Forest (RF) model, a non-parametric ensemble method known for superior predictive performance in ecological presence-only/pseudo-absence datasets with moderate sample sizes and multicollinearity among covariates.

The model was implemented in R Studio using the following structured workflow for a Random Forest calibrated with 500 trees.

Step 1. Grid and Response Data Preparation

The $0.1^\circ \times 0.1^\circ$ analysis grid was constructed using `st_make_grid()` and masked to the Mediterranean marine area (`med_sea_union`) as previously described. The binomial dataset (`model_data_grid_presence_pseudoabsence.csv`) was loaded, dates parsed (`%d-%m-%Y`), and coordinates rounded (`lon_round`, `lat_round`). Duplicates per date + `grid_id` were identified and resolved using priority aggregation: presence (1) takes precedence over pseudo-absence (0). A `year_month` field was added for environmental joining.

Step 2. Environmental Covariate Preprocessing and Integration

All seven predictor layers (SST, phosphate/phytoplankton/zooplankton at 10 m and 100 m) were loaded from CSV tables. For each: Dates were converted to Date class and formatted to `year_month`, coordinates were rounded to 0.1° , depth-specific layers were split (10 m vs. 100 m) and renamed (e.g., `phosphate_10m`); monthly duplicates per cell were removed using `distinct()`. The response data were left-joined to all predictors on `year_month`, `lon_round`, `lat_round`. Records with any missing predictor were dropped via `complete.cases()`, yielding 1,523 complete observations.

Step 3. Exploratory Data Analysis and Visualization

Summary statistics (mean per predictor by presence class) were computed and logged. For each predictor, three diagnostic plots were generated and saved:

- Univariate response of fin whale presence to each predictor was explored using boxplots of raw environmental values stratified by presence/absence records.
- The shape of the response and marginal effect of individual predictors on presence probability were further assessed through partial dependence plots (PDPs) generated with the `pdp` package

Step 4. Training–Test Split
A 70/30 stratified random split was applied using `set.seed(123)`. The response variable was converted to a factor ("Absent", "Present") for compatibility with `randomForest`.

Step 5. Random Forest Model Fitting

The RF was trained on the full training set using the formula: `presence ~ sst + phosphate_10m + phosphate_100m + phytoplankton_10m + phytoplankton_100m + zooplankton_10m + zooplankton_100m`. Hyperparameters: `n tree = 500`, `m try = 3` ($\approx \sqrt{7}$), `importance = TRUE`. Class weighting: Implicit via balanced sampling in OOB; no explicit weights needed due to RF robustness. Model convergence was monitored via OOB error rate stabilization.

Step 6. Performance Evaluation on Test Set In this step I used as predictions Probability (type = "prob") and class (type = "response"), metrics: Accuracy (threshold = 0.5) and AUC via `pROC::roc()`

The OOB error rate extracted from `rf_model$serr.rate`. All values were logged and compared to GAM benchmarks.

Step 7. Internal Cross-Validation with `caret`

A 5-fold CV was performed using `trainControl()` with `classProbs = TRUE` and `twoClassSummary`. The same `mtry = 3` was used. Mean AUC and accuracy across folds were computed from saved predictions, confirming model stability.

Step 8. Variable Importance and Partial Dependence

Importance was assessed using Mean Decrease in Gini and % Increase in MSE, extracted via `importance()`. A bar plot of Gini importance was generated and saved, Univariate PDPs were created for all seven predictors using `pdp::partial()` (100-grid resolution), showing marginal effect on presence probability. A 2-way PDP (SST × phosphate_10m) was generated to explore interactions.

Step 9. Residual Spatial Autocorrelation

Training predictions were generated on the full training set, residuals computed as: observed (1/0) – predicted probability. Moran's I was calculated on residuals using a 0.3° neighborhood (`dnearneigh`, `nb2listw`, `zero.policy = TRUE`).

Step 10. Model Stability Assessment

The RF was retrained 10 times with different 70/30 splits (`set.seed(999)`). AUC was computed on each held-out test set. Mean ± SD reported to quantify robustness

Step 11. July 2018 Habitat Suitability Prediction

July 2018 environmental layers were filtered, rounded, and joined to all valid grid centroids (`pred_grid_rf`). After `drop_na()`, ~5,800 cells remained, presence probability predicted using `predict(..., type = "prob")[, "Present"]`. Values were rasterized using `terra::rast()` and `cellFromXY()` and the gaps filled with 3×3 focal mean, then masked to `med_sea_union`.

Step 12. Final Map and Deliverables

The probability surface was plotted with `ggplot2::geom_tile()` using the same `viridis` "plasma" scale and layout as the GAM map. Subtitle included AUC and OOB error (%) for direct comparison.

Step 13. Diagnostics Summary Table

A comprehensive table (`RF_Diagnostics_FINAL.csv`) was generated including: OOB error (%), Test AUC, Moran's I and p-value, AUC stability (SD) and 2-way PDP confirmation

2.5.3 Workflow of future prediction

To explore how climate change might reshape fin whale habitat in the Mediterranean, we used the Random Forest (RF) model already trained and validated on historical data (2006–2022) to generate future projections under the RCP 4.5 and RCP 8.5 scenario for two key time horizons: mid-century (2050) and end-of-century (2099).

- RCP4.5: Intermediate stabilization scenario, assumes an increase of global emissions and after the mid-century a decline with the use of technologies and strategies for control the emission (Copernicus, 2020; D’Amen et al., 2024).
- RCP8.5: Vey high-emission, business-as-usual scenario, assumes continued rise in emissions and significant climate change, pessimistic scenario (Copernicus, 2020; D’Amen et al., 2024).

So, to create future prediction, I used the four combinations of scenarios and years:

1. RCP 4.5 for year 2050
2. RCP 4.5 for year 2099
3. RCP 8.5 for year 2050
4. RCP 8.5 for year 2099

Workflow of the future prediction:

Step 1. Define spatial domain and grid preparation

The script started by defining the exact same study area used in the historical models with longitude: -6.07° to 16° E and latitude 35° to 44.5° N.

Using `terra::rast()`, it was built a $0.1^{\circ} \times 0.1^{\circ}$ raster template about 11 km per cell at 40° N with EPSG:4326 (WGS84) as the coordinate system. This gave a grid of $221 \times 95 = 20,995$ cells. To keep things ecologically meaningful, I applied the same marine mask as before. The IHO seas shapefile (`iho.shp`) was loaded, cropped to our bounding box, cleaned with `st_make_valid()`, and filtered to exclude non-target basins (like the Adriatic and Cantabrian). The remaining polygons were rasterized into a binary mask (`mask_raster`) using `terra::rasterize()`. This mask was used later to clip all outputs to valid Mediterranean waters.

Step 2. Preparation future environmental data

The future environmental data downloaded on Copernicus Climate Data Store (Copernicus, 2020), came in four large CSV files, each containing monthly, 0.1° -resolution projections for 2050–2099 under RCP4.5 and RCP 8.5 scenario. It has been maintaining the same depth for the environmental variable that I used for the past models: sea surface temperature at a 0.5m depth; while phosphate, phytoplankton and zooplankton values were downloaded at depths of 10m and 100m.

Each file included columns for date (YYYY-MM-DD), lon, lat, depth, rcp, and the target variable (`thetao`, `po4`, `phyc`, `zooc`). These datasets were statistically downscaled and bias-corrected to match historical patterns while reflecting projected climate shifts.

Step 3. Building the Annual Environmental Layers

It has been implemented two near-identical versions of the “unisci_dati(target_year)” function one for each RCP. The only difference was the filtering criterion: `rcp == "RCP4.5"` versus `rcp == "RCP8.5"`. For each scenario and target year (2050 and 2099), the function began by parsing the date column to extract the year using `format(as.Date(...), "%Y")`. Then data have been filtered the data to the specified `rcp` and `target_year`. Next, data were separated by depth and renamed variables to match the RF model’s expectations: `thetao` became `sst`, `po4` was split into `phosphate_10m` and `phosphate_100m`, and similarly for phytoplankton and zooplankton. Each data point was mapped to its corresponding raster cell using `cellFromXY()`, and values were assigned to seven individual blank rasters, one per predictor. To address isolated missing cells, a 9×9 focal mean filter was applied using `focal(..., fun = mean, na.rm = TRUE)`, providing smooth, spatially coherent interpolation. Each layer was then masked to the marine domain. Finally, the seven rasters were assembled into a `SpatRaster` stack and saved as a NetCDF file. This process was executed four times, producing four fully aligned environmental stacks.

Step 4. Applying the predictive model

The pre-trained RF model (`rf_model.rds`) fitted with `ntree = 500`, `mtry = 3`, and calibrated on 1,523 presence and pseudo-absence records was loaded once using `readRDS()`. This model was then applied without modification to all four future environmental stacks, ensuring that any differences in predicted suitability arise solely from changes in environmental conditions, not from model variation.

Step 5. Generating habitat suitability predictions

A single, reusable function: `predict_fin_whale(stack, model, year, rcp)`, produced all predictions. The only input variation was the `rcp` label (“`rcp45`” or “`rcp85`”), which controlled output naming. The function converted the stack into a full data frame with coordinates, imputed any remaining missing predictor values using column-wise means, a robust and unbiased approach and computed presence probability via `predict(model, newdata = ..., type = "prob")`. These probabilities were written back to a new raster using the first layer as a template, masked to the marine domain, and saved as NetCDF files.

Step 6. Creating maps visualization

It has been used a shared `plot_predictions()` function, we generated four habitat suitability maps. Each used the `viridis` “`plasma`” color scale from 0 to 1, overlaid with medium-scale coastlines from `rnaturalearth`, featured bold and included a right-aligned legend with 10 labeled probability breaks.

Step 7. Habitat change quantification

To reveal where and by how much habitat suitability might shift, we computed delta rasters using the formula: $\Delta P = P_{\text{July 2018}} - P_{\text{future}}$
The July 2018 baseline was subtracted from each future prediction, yielding four change maps. These employed a diverging red–white–blue palette, centered at zero, with ±60% change as limits and labeled breaks at ±30% and ±60%. A consistent caption clarified: “Red = habitat loss | Blue = habitat gain”.

2.6 Software and Computational Details

All analyses were performed in R 4.3.2 (R Studio, 2025) under macOS, using the following main packages:

Category	R Packages
Geospatial processing	`sf`, `terra`, `rnaturalearth`, `rnaturalearthdata`
Data manipulation	`dplyr`, `data.table`, `lubridate`, `tidyr` `readxl`
Modelling	`mgcv`, `pROC`, `caret`, `randomForest` `pdp`
Visualization	`ggplot2`, `corrplot`, `reshape2`, `viridis`, `ggpubr`, `gridExtra`
Parallel computation	`future`, `furrr`

Table 3. Packages used in R studio for the various models (R Studio, 2025)

3. RESULTS

	Total sightings	Train set (70%)	Test set (30%)
Presence (1)	361	263	98
Pseudo-absence (0)	2238	1556	682
Percentage absence	13.89%	14.46%	12.56%

Table 4. Number of total sightings which includes presence and pseudo- absence of the fin whale in the dataset used for all the models inside the study area; the corresponding number of presence (1) and pseudo-absence(0) used for the test set (30% of total sightings) and train set (70%).

3.1 GAM

To understand which k (k= number of knots) is better for our Gam model, we compare 5 model with different k, with results of model performance in Table 5.

K	Mean AUC	Sd AUC
3	0.570	0.060
4	0.569	0.060
6	0.572	0.028
8	0.546	0.080
10	0.571	0.031

Table 5. Model performance with Five-Fold cross validation: comparison of the efficiency of GAM models by comparing the various k values using AUC values; Sd refers to Standard deviation.

To establish an optimal level of model complexity while preserving interpretability, the Generalized Additive Model (GAM) was fitted iteratively across a range of basis dimension values with $k \in \{3,4,6,8,10\}$ for each environmental predictor. Model performance was rigorously evaluated using five-fold cross-validation, with Area Under the Receiver Operating Characteristic Curve (AUC) as the primary diagnostic metric. Cross-validated AUC estimates were computed for each k , along with their standard deviations, to assess both predictive accuracy and stability. From the Table 5. It can be notice that the higher value of mean AUC has been reached by the model with $k= 6$ with mean AUC of 0.572; follow by the model with $k=10$ with mean AUC of 0.571.

Variables	k	EDF	p-value
SST	4	3.01	0.593
SST	10	3.17	0.614
Phosphate_10m	4	2.72	0.23
Phosphate_10m	10	2.71	0.297
Phosphate_100m	4	1.00	0.245
Phosphate_100m	10	1.00	0.252
Phytoplankton_10m	4	1.00	0.35
Phytoplankton_10m	10	1.00	0.343
Phytoplankton_100m	4	1.00	0.278
Phytoplankton_100m	10	1.00	0.285
Zooplankton_10m	4	1.00	0.5
Zooplankton_10m	10	1.00	0.496
Zooplankton_100m	4	0.00	0.981
Zooplankton_100m	10	0.00	1

Table 6. Summary of Generalized Additive Model (GAM) results for environmental predictors using basis dimension $k=4$ and $k=10$ showing effective degrees of freedom (EDF) and significance of smooth terms (p-value).

The Generalized Additive Model (GAM) with $k = 4$ yielded the following effective degrees of freedom (EDF) and p-values for each environmental predictor (Table 6): SST exhibit EDF = 3.01 and p- value = 0.593, phosphate_10m exhibit EDF = 2.72 , p-value = 0.23, phosphate_100m exhibit EDF = 1.00 and p-value 0.245, phytoplankton_10m exhibit EDF = 1.00, p-value = 0.35, phytoplankton_100m exhibit EDF = 1.00, p-value = 0.278, zooplankton_10m exhibit EDF = 1.00, p-value = 0.5, zooplankton_100m exhibit EDF = 0.00, p-value = 0.981. None of the predictors were statistically significant; variable is considered statistically significant when p-value: < 0.05 (Derville et al., 2022).

Increasing the number of knots to $k = 10$ resulted in the following EDF and p-values (Table 6): SST exhibit EDF = 3.17 and p- value = 0.614, phosphate_10m exhibit EDF = 2.71 , p-value = 0.297, phosphate_100m exhibit EDF = 1.00 and p-value 0.252, phytoplankton_10m exhibit EDF = 1.00, p-value = 0.343, phytoplankton_100m exhibit EDF = 1.00, p-value = 0.285, zooplankton_10m exhibit EDF = 1.00, p-value = 0.496, zooplankton_100m exhibit EDF = 0.00, p-value = 1.

Again, no predictors reached statistical significance (all p-value > 0.05). Zooplankton at depths 100m exhibited EDF = 0 in both models, indicating exclusion from the fitted smooths.

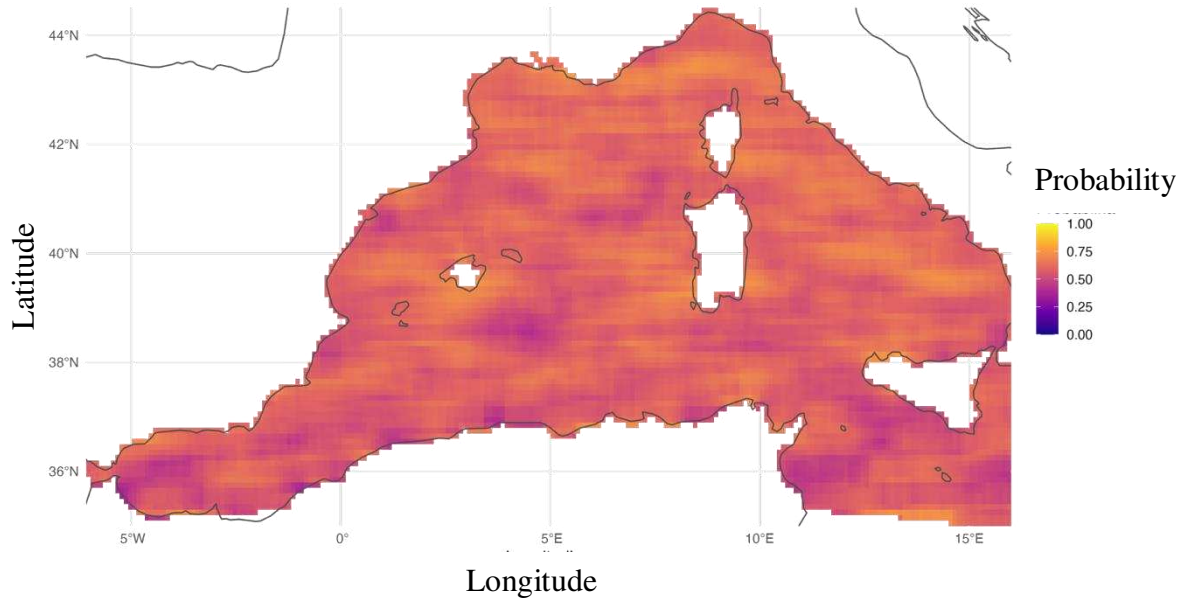


Figure 25. Habitat prediction of the fin whale in July 2018 with GAM using k=4. On the right side of the image, there is the colour scale showing the probability of occurrence, with 1 (100% of probability of occurrence) represented by the colour yellow and 0 (0% probability of occurrence) represented by the colour purple. The July 2018 habitat suitability map covered 7,613 marine grid cells, with predicted probabilities ranging from 0 to 0.70 (Figure 25).

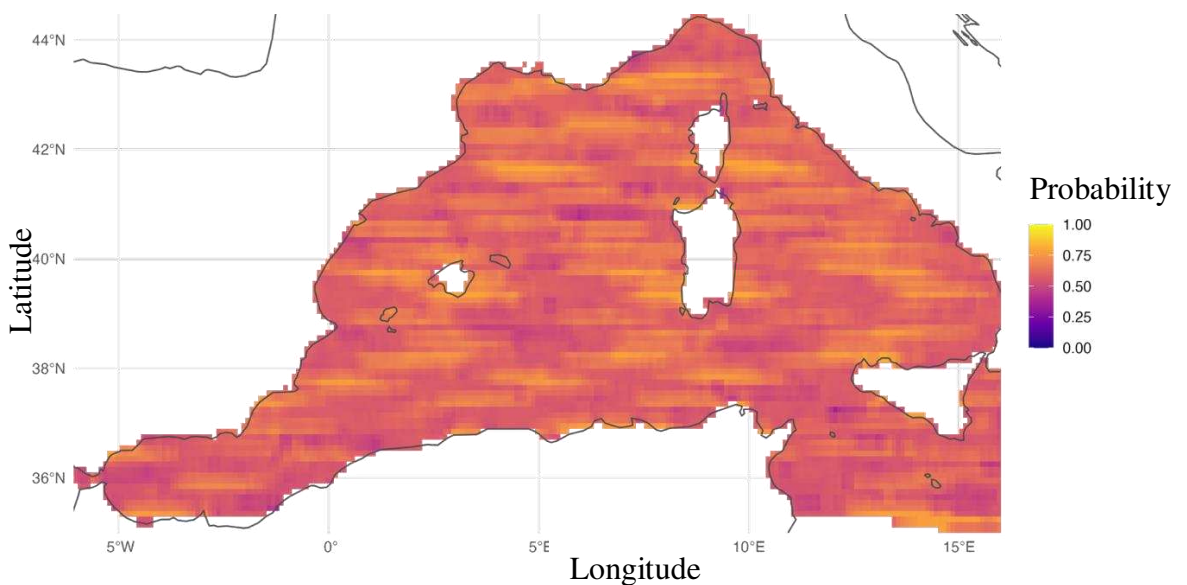


Figure 26. Habitat prediction of the fin whale in July 2018 with GAM using k=10. On the right side of the image, there is the colour scale showing the probability of occurrence from yellow (1) to purple (0).

3.2 Random Forest

Below there are the results of random forest, a type of machine learning model that should best explain the presence of whales in our study area.

Metric	Value
Accuracy	95.87%
AUC	0.9888
Sensitivity	80.11%
Specificity	98.18%
Precision	86.56%
OOB Error rate	4.27%
P- value	2.2 e-16
Mcnemar's test p-value	4.734 e-08

Table 7. Results of random forest model performance.

The Random Forest model achieved an AUC of 0.9888, accuracy of 95.87%, sensitivity of 80.11%, and specificity of 98.18% on the test set. The OOB error rate was 4.27% (Table 7).

Variable	Mean Decrease Accuracy	Mean Decrease Gini
SST	202.964	1657.694
phosphate_10m	72.283	961.568
phosphate_100m	70.508	741.933
phytoplankton_10m	69.749	730.479
phytoplankton_100m	67.615	803.593
zooplankton_10m	47.785	786.518
zooplankton_100m	68.699	915.640

Table 8. Results using the Random Forest of the environmental variable importance using Mean Decrease Accuracy and Mean Decrease Gini

Sea Surface Temperature (SST) had the highest importance with Mean Decrease Accuracy = 202.964, Mean Decrease Gini = 1657.694, followed by phosphate at 10 m (Mean Decrease Accuracy of 72.283) and phosphate at 100 m (Mean Decrease Accuracy of 70.508) (Table 8).

Statistic	Value (°C)
Min	12.35
1st Quartile	15.47
Median	16.42
Mean	18.21
3rd Quartile	20.87
Max	27.59

Table 9. Sea surface temperature (SST) distribution summary with presence observations. Sea Surface Temperature (SST) across presence observations ranged from 12.35°C to 27.59°C, with a median of 16.42°C and mean of 18.21°C

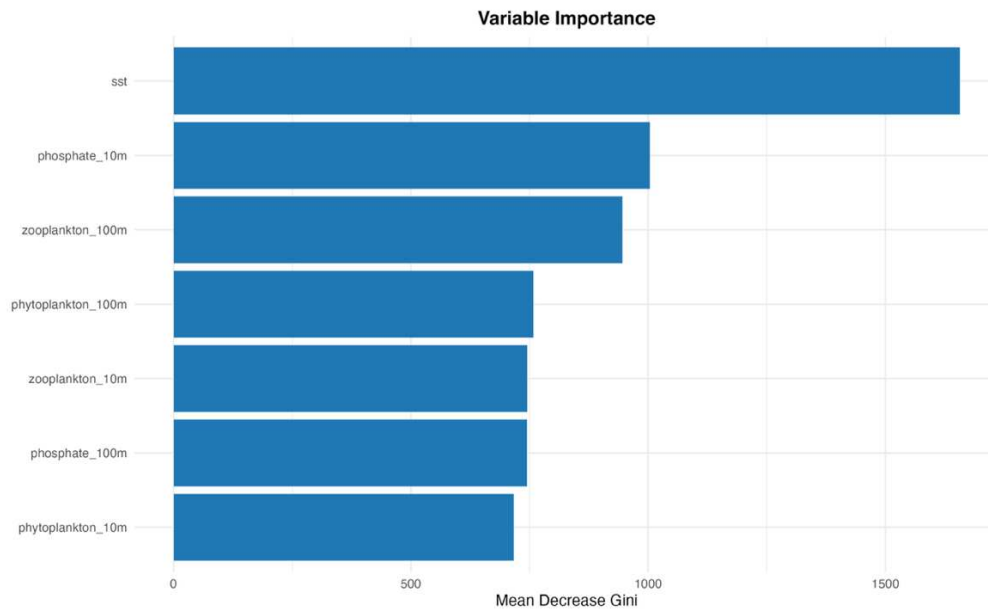


Figure 27. Variable importance of environmental variable using the Mean Decreasing Gini (coordinate y) for rank the most important variable in the random forest model.

Spearman Correlation Heatmap of Environmental Predictors and Fin Whale Presence

Spearman's rank correlation coefficient (monotonic relationships)

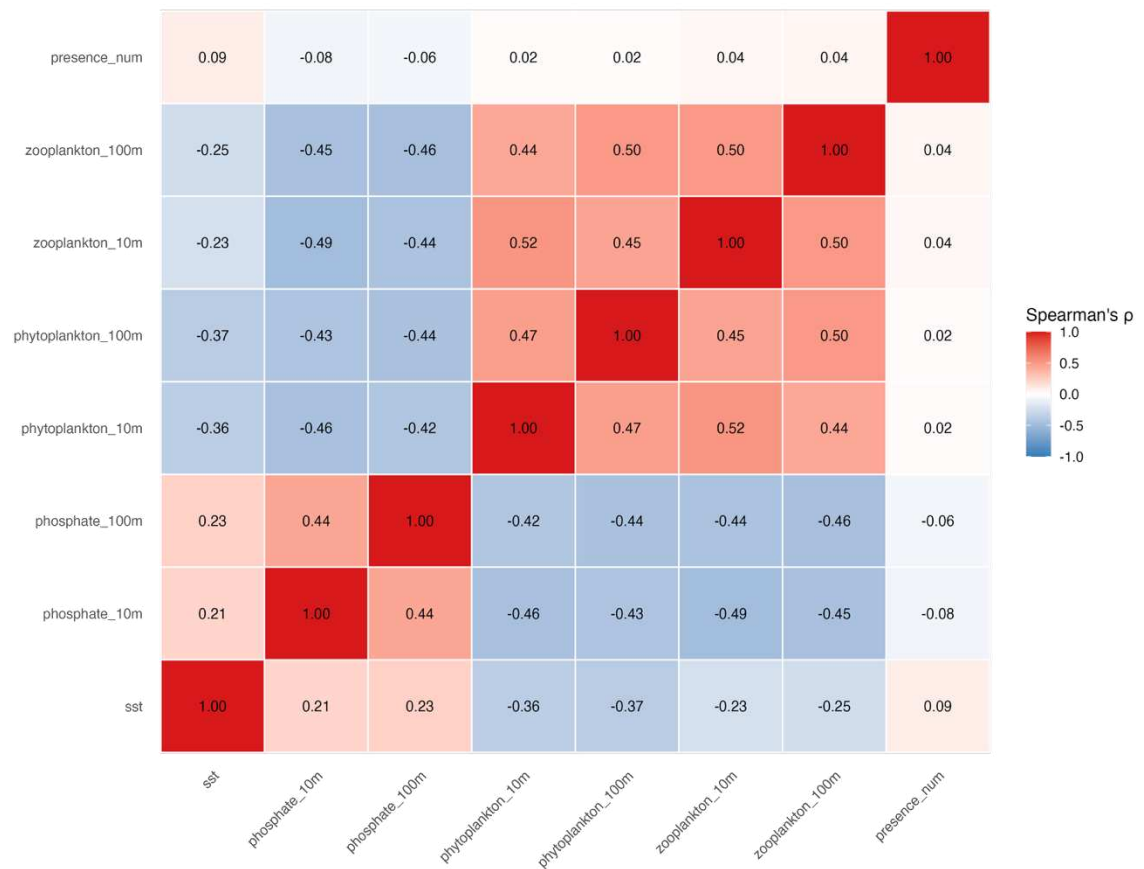


Figure 28. Spearman’s rank correlation heatmap showing monotonic relationships among environmental predictors and fin whale presence used in the Random Forest model. Values represent Spearman’s ρ correlation coefficients; stronger colours indicate stronger monotonic associations (positive in red +1, negative in blue -1).

The top row and the associated column of the correlation heatmap (Figure 28) display these relationships between each environmental variable and fin whale presence (presence_num, coded as 0/1). Spearman correlations between fin whale presence and the environmental predictors were generally weak (Figure 28). Specifically, the correlation coefficients were: SST ($\rho = 0.09$), phosphate_10m ($\rho = -0.08$), phosphate_100m ($\rho = -0.06$), phytoplankton_10m ($\rho = 0.02$), phytoplankton_100m ($\rho = 0.02$), zooplankton_10m ($\rho = 0.04$) and zooplankton_100m ($\rho = 0.04$), (Figure 28).

3.2.1 Phosphate

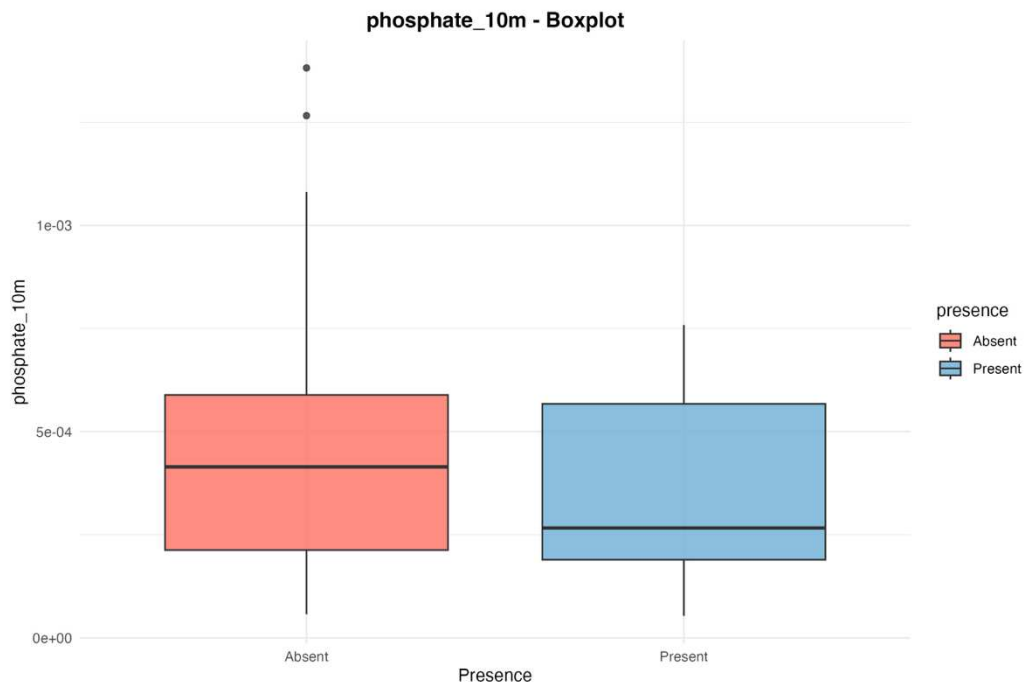


Figure 29. Boxplot of phosphate at 10m depth, in the Y axis there is phosphate with its concentration (mol m^{-3}) meanwhile in the X axis there is the presence (red) and absence (blue). Median phosphate concentration is lower in presence cells, and variability is smaller than in absence cells.

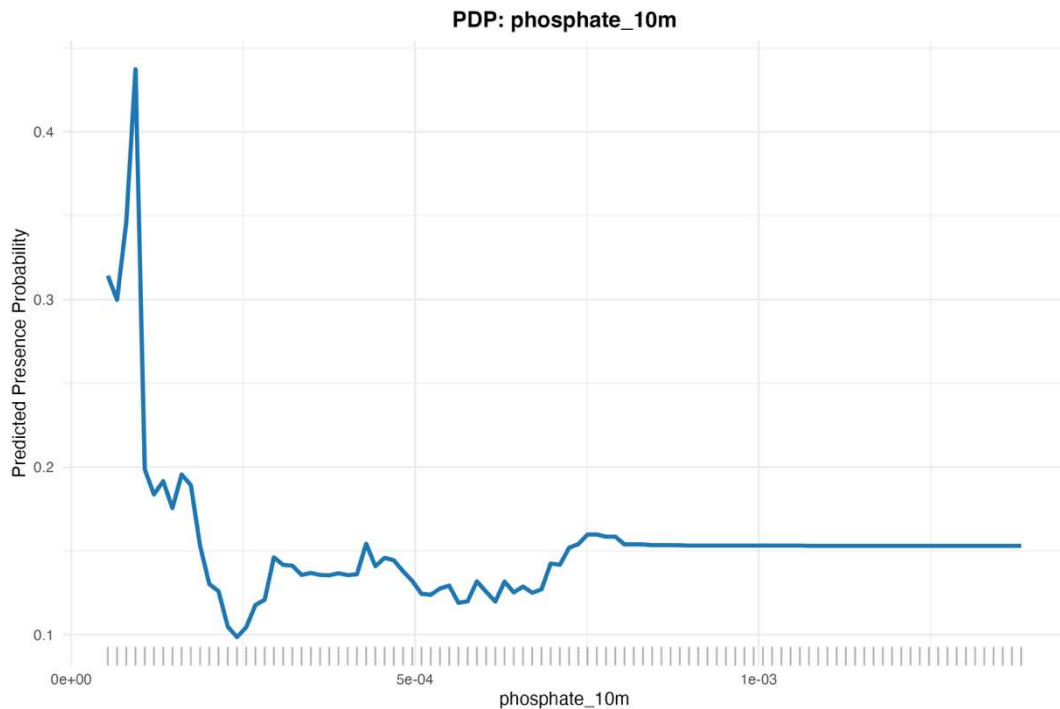


Figure 30. Partial Dependence Plot of the fin whale with phosphate at 10m. the Y axis show the probability of the presence meanwhile the X axis there is the concentration of the phosphate (mol m^{-3}) of fin whale. The curve shows a sharp decrease in presence probability as phosphate increases from 0.0000 (mol m^{-3}) to

around 0.0004 (mol m^{-3}), after which the probability stabilizes around a low constant value.

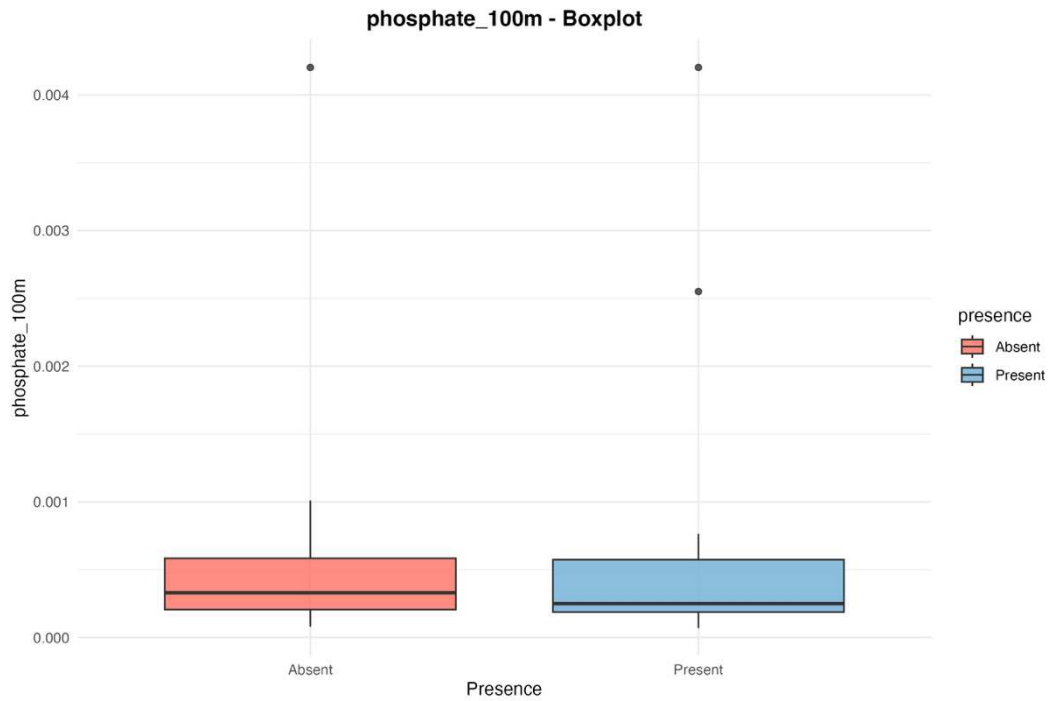


Figure 31. Boxplot of phosphate at 100m depth (mol m^{-3}) obtain with random forest model. The presence distribution of present and absent boxes are very similar, but the median for presence is slightly shifted toward higher phosphate values for the absent box.

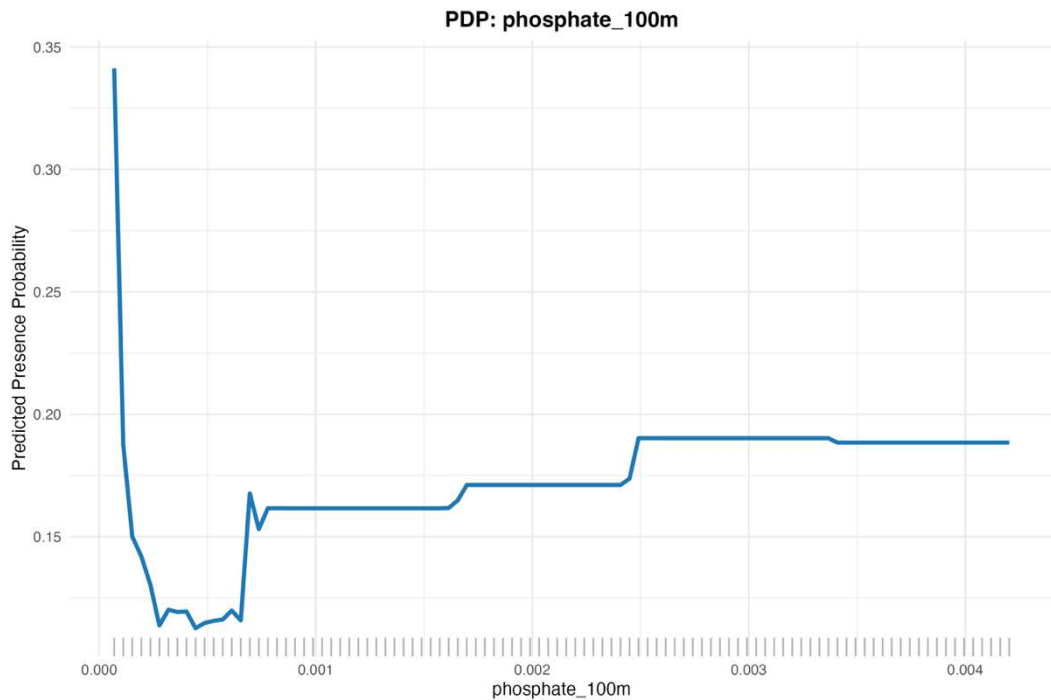


Figure 32. Partial Dependence Plot of the fin whale with phosphate at 100m

The PDP (Figure 32.) shows a U-shaped trend at very low values: a sharp decline from 0.000 to 0.001 mol m⁻³, followed by a gradual increase in presence probability beyond ~0.002 mol m⁻³.

3.2.2 Sea Surface Temperature

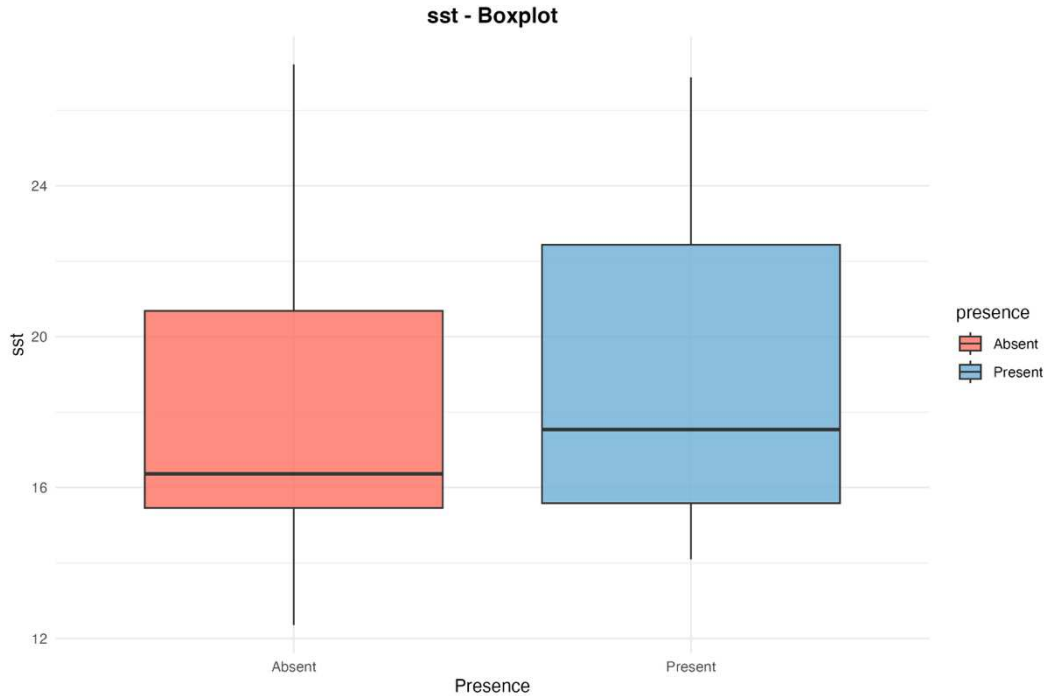


Figure 33. Boxplot of sea surface temperature obtain with random forest model comparing the presence (blue) and the absence (red) of in whale. The median SST (horizontal line inside the box) is higher for presence than for absence, also the box of present reach higher SST value.

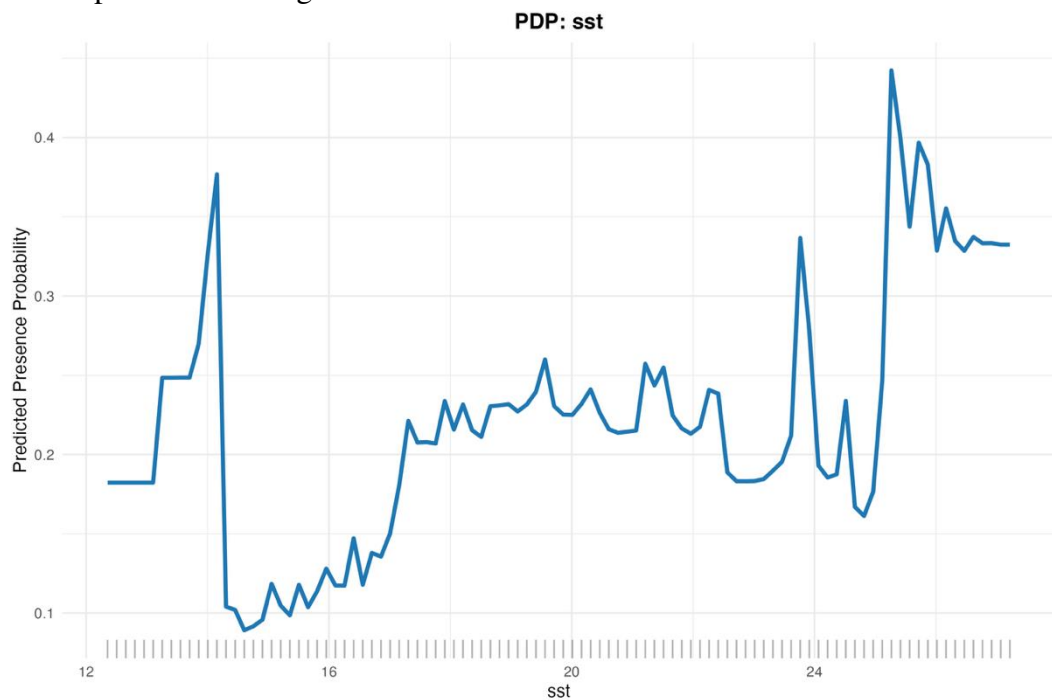


Figure 34. Partial Dependence Plot of the fin whale with sea surface temperature.

This plot (Figure 34.) isolates the marginal effect of SST on the predicted probability of fin whale presence, holding all other variables constant (averaged over the dataset).

The curve shows a non-linear relationship: the presence probability starts with an increasing trend until reach a peak at 14C°, then the probability drop immediately after the peak. From 15 C° we can see an increasing of probability, then the probability remains fairly constant around 0.2-0.25 until the 23C°; at 24C° and 25C° there are two peaks, the second one reaching the 0.45 probability of presence, then there is a decrease of probability.

3.2.3 Phytoplankton

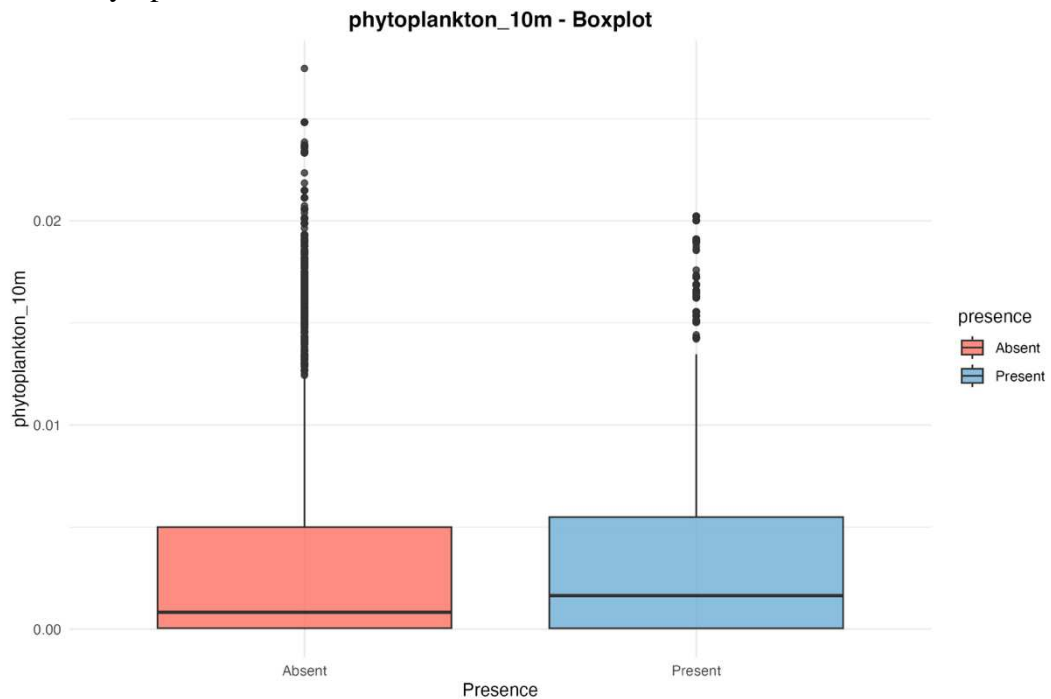


Figure 35. Boxplot of phytoplankton at 10 m depth (mol m^{-3}) obtain with random forest model comparing the presence (blue) and the pseudo absence (red) of in whale. The medians and interquartile ranges are very similar, with only a slight shift toward higher values in presence cells.

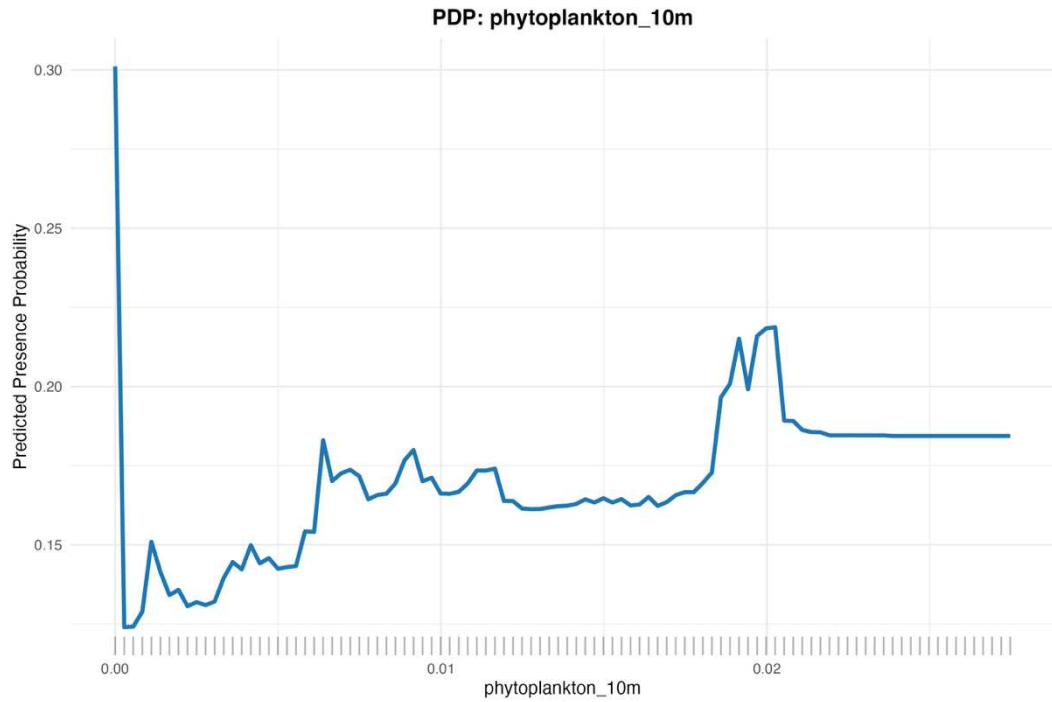


Figure 36. Partial Dependence Plot of the fin whale with phytoplankton at 10 m depth.

The PDP shows the marginal effect of phytoplankton 10m (mol m^{-3}) on the predicted probability of fin whale presence, while averaging over all other predictors.

The curve starts with a drop of probability presence at very low concentrations ($\sim 0.00 \text{ mol m}^{-3}$), followed by a gradual increase of probability between ~ 0.005 and 0.02 mol m^{-3} , then at 0.02 there is a small double peak reaching more than the 0.20 probability and then the probability stabilizes.

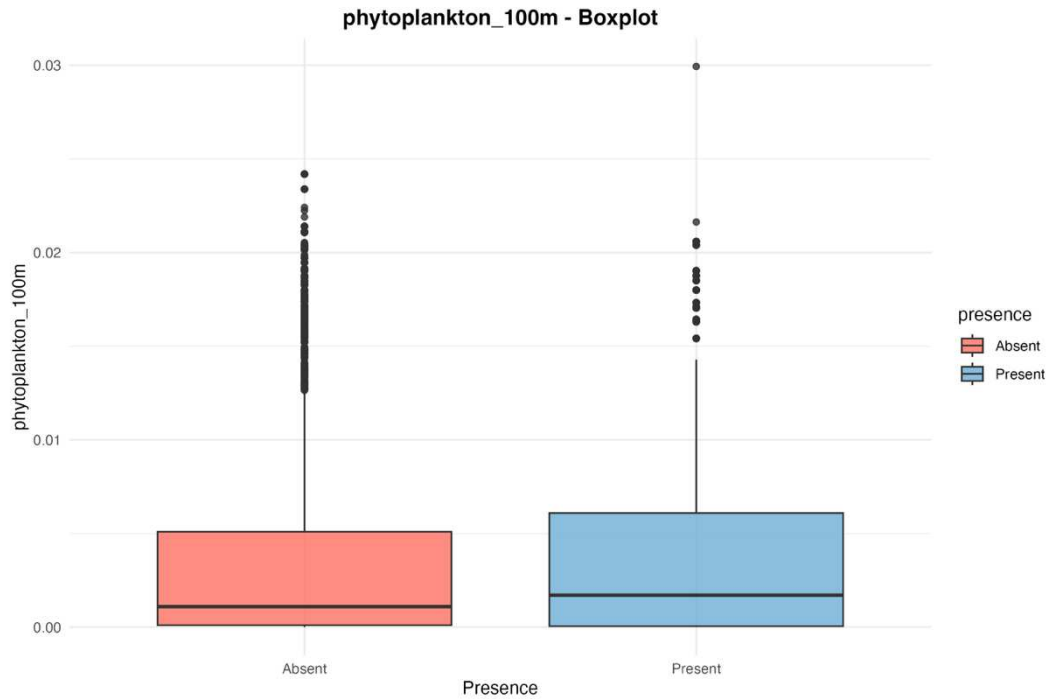


Figure 37. Boxplot of phytoplankton at 100 m depth obtain with random forest model comparing the presence (blue) and the pseudo absence (red) of in whale. The median phytoplankton at 100 m seems slightly higher when whales are present, but the difference is small.

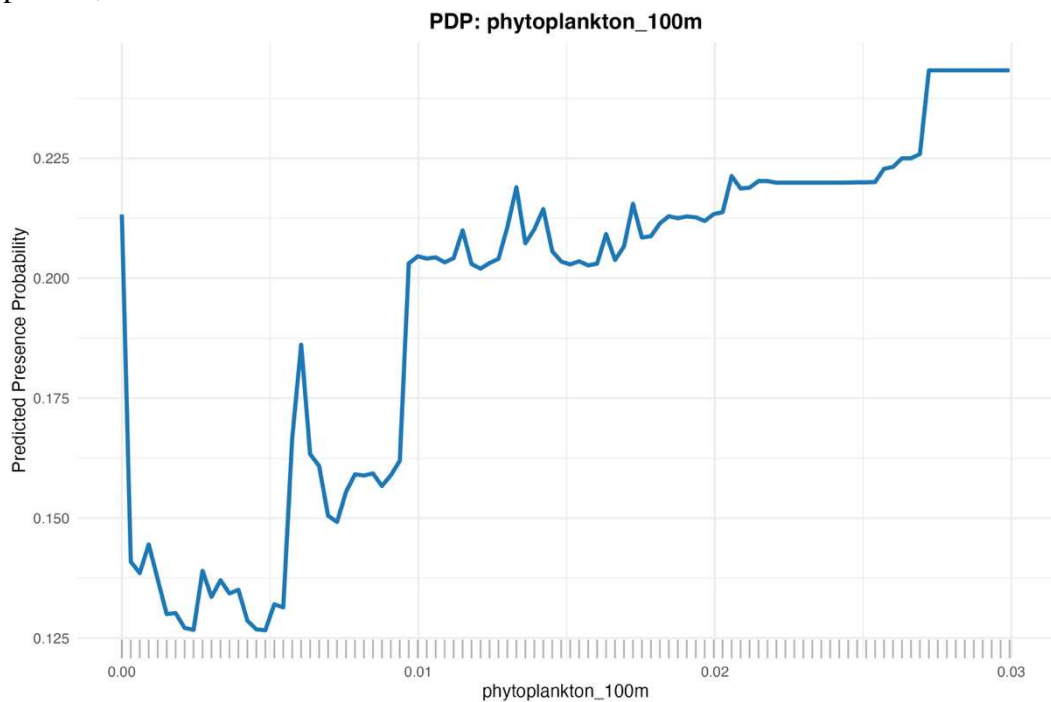


Figure 38. Partial Dependence Plot of the fin whale with phytoplankton at 100 m depth; with the isolation of the effect of phytoplankton alone. At very low phytoplankton ($\sim 0.00 \text{ mol m}^{-3}$) presence probability drops, but with an increase of the phytoplankton concentration also the presence increase; there is a big increase of the probability from 0.150 to more than 0.2 when the phytoplankton concentration exceeded approximately $0.01 \text{ (mol m}^{-3}\text{)}$ achieving high stability after 0.027

3.2.4 Zooplankton

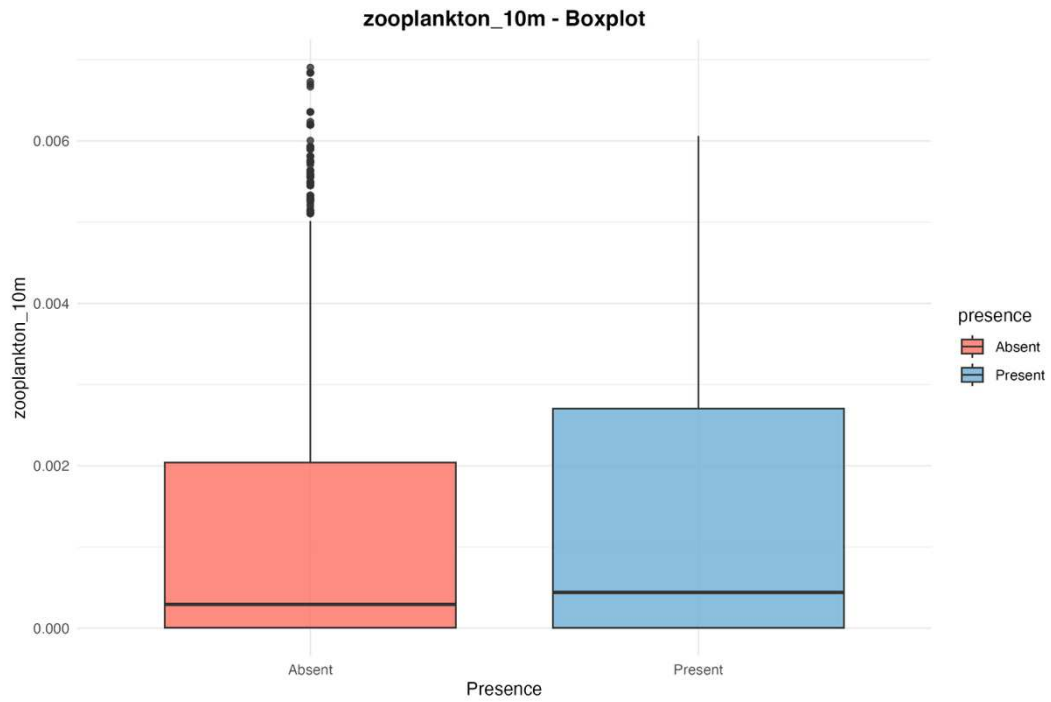


Figure 39. Boxplot of zooplankton at 10 m depth (mol m^{-3}) obtain with random forest model comparing the presence (blue) and the pseudo absence (red) of in whale. Median zooplankton is slightly higher when whales are present, and the distributions box of the presence reach higher level when fin whale is present.

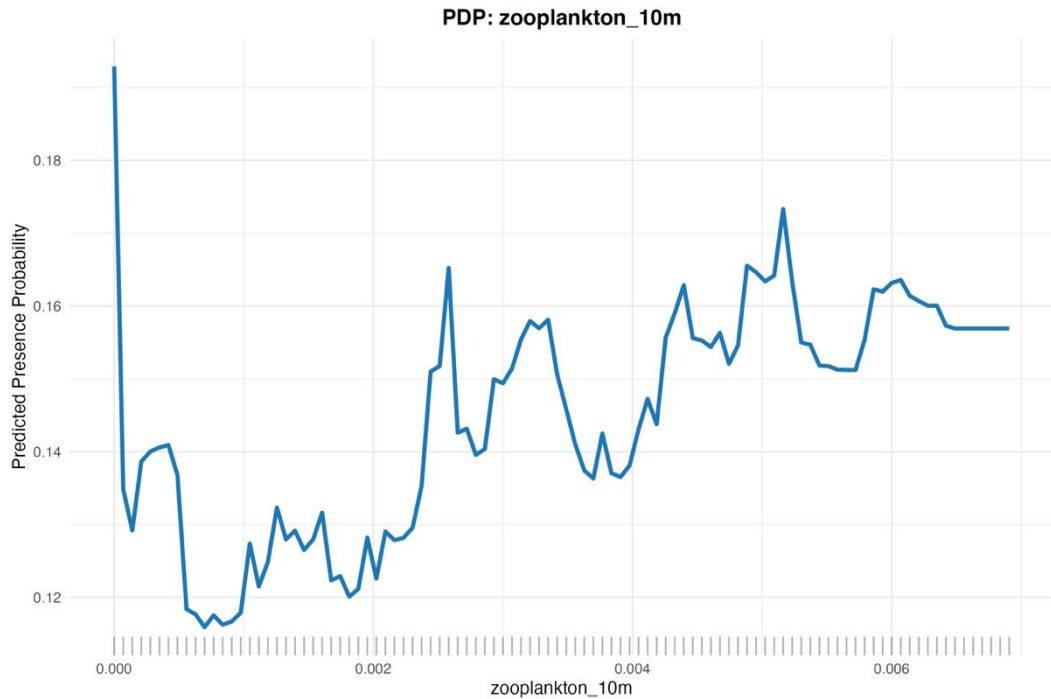


Figure 40. Partial Dependence Plot of the fin whale with zooplankton at 10 m depth (mol m^{-3})

The probability (Figure 40.) initially start with a drop, then when there are low zooplankton level ($\sim 0-0.001 \text{ mol m}^{-3}$) there are low probability of whale presence ($\sim 0.12-0.14$). Between $0.002-0.005$ presence probability increases creating some small peak, with the highest reaching the 0.17 probability of presence with 0.005 mol m^{-3} ; then after the 0.006 mol m^{-3} of zooplankton the probability seems to remain fairly constant below 0.16.

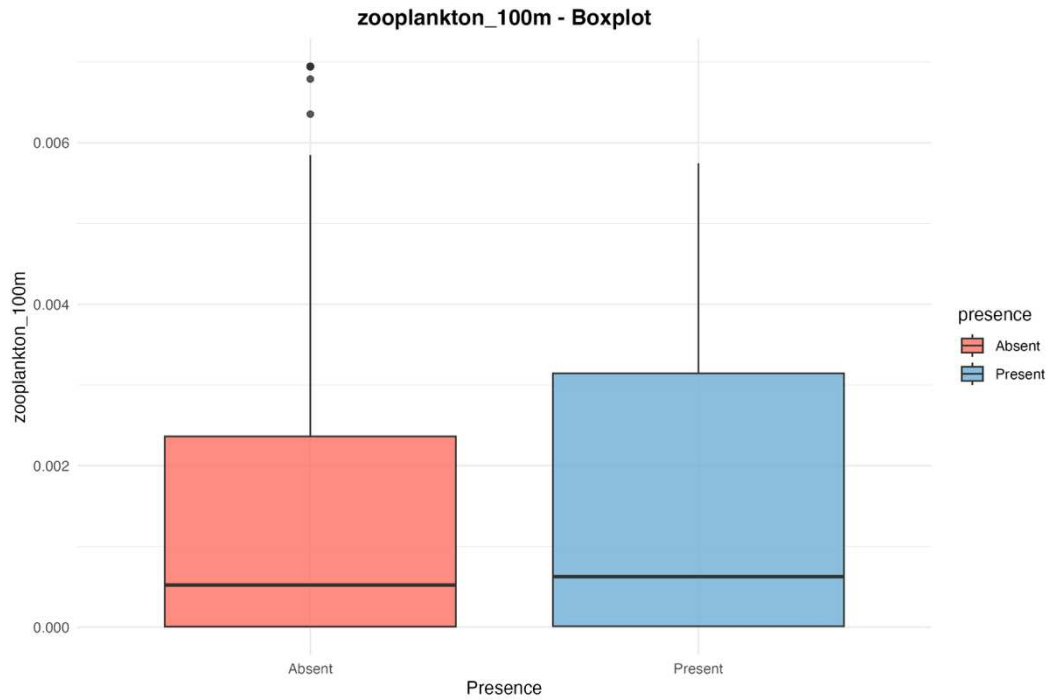


Figure 41. Boxplot of zooplankton at 100 m depth (mol m^{-3}) obtain with random forest model comparing the presence (blue) and the pseudo absence (red) of in whale.

The box when fin whale is present reaching an higher value of zooplankton concentration (mol m^{-3}) with the median zooplankton 100m is slightly higher when fin whales are present.

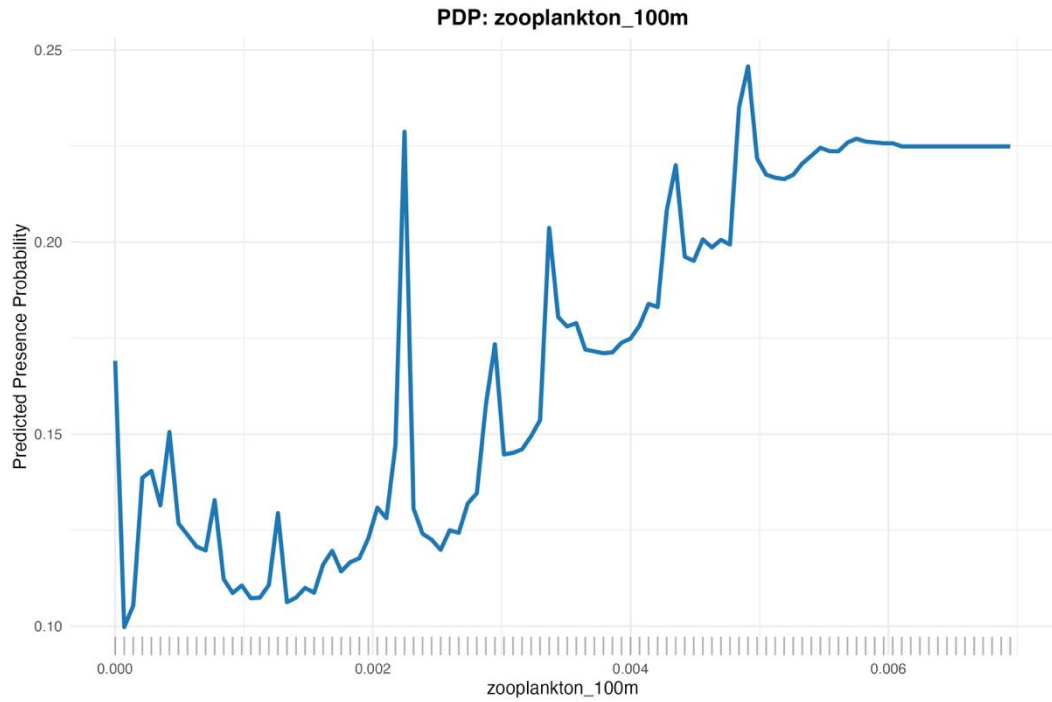


Figure 42. Partial Dependence Plot of the fin whale with zooplankton at 100 m depth (mol m^{-3}). With low value of zooplankton ($0.000\text{-}0.002 \text{ mol m}^{-3}$) the presence of fin whale shows a decreasing trend; at 0.002 the values of presence show a peak reaching $0,23$ of probability. After the drop we can see an increase of the presence linked with an increase of the zooplankton concentration; then after 0.005 (mol m^{-3}) concentration of the zooplankton the presence stabilize at 0.25 probability of presence.

3.3 Future prediction

3.3.1 RCP 4.5

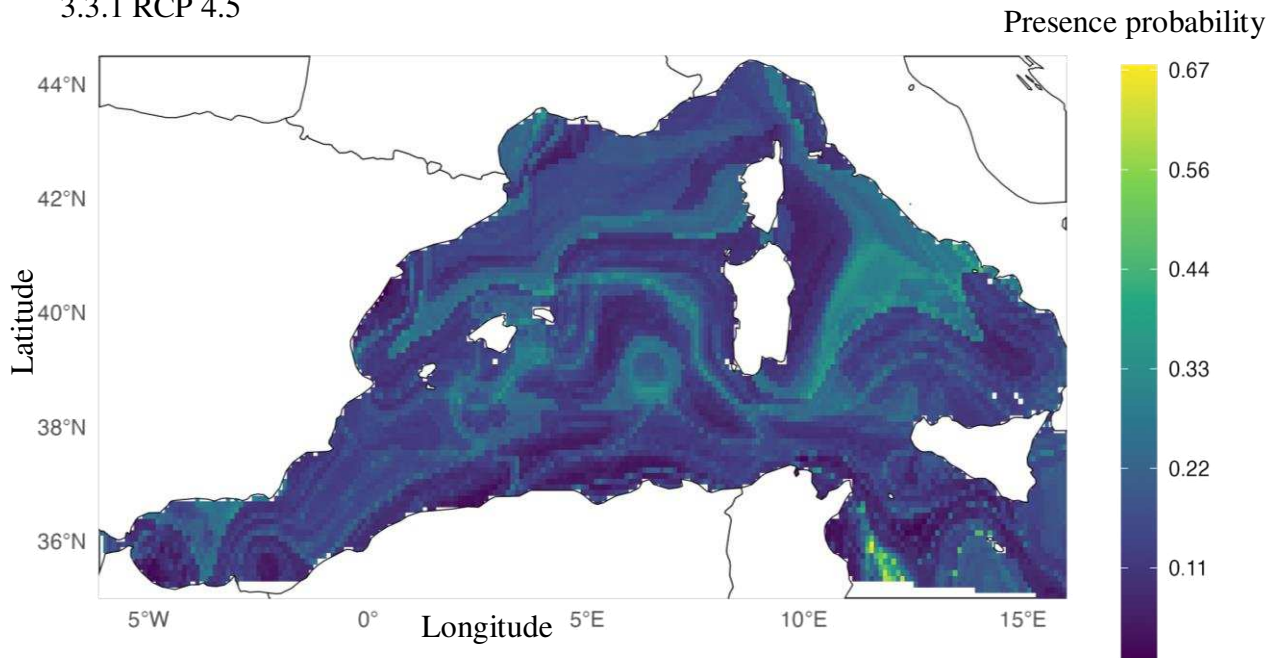


Figure 43. Projected probability of fin whale presence in the study area for the year 2050 under the RCP4.5 (intermediate) emissions scenario. Values represent absolute predicted probabilities (0–1), with yellow colours indicating higher likelihood of encountering fin whales (maximum of 0.67), and blue colour indicating lower probability (0.11).

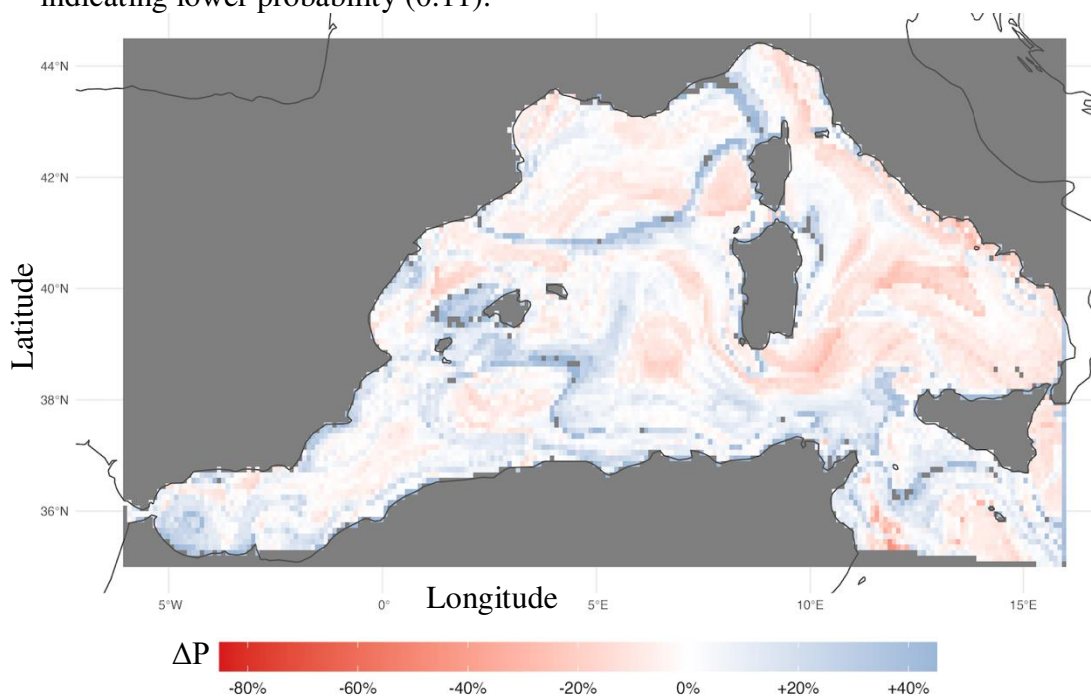


Figure 44. Habitat change obtained by comparing presence between 2018 and 2050 with RCP 4.5 ($\Delta P = P_{2050} - P_{2018}$) red areas represent habitat loss, while blue areas represent habitat gain

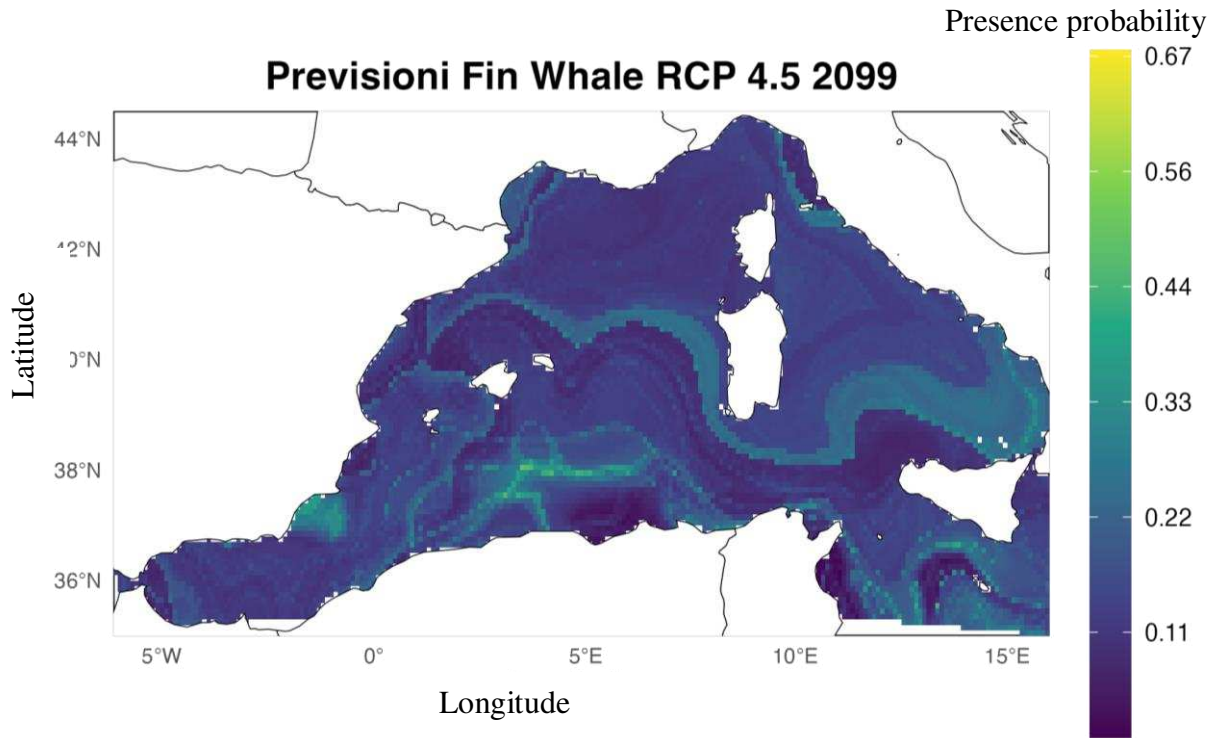


Figure 45. Projected probability of fin whale presence in the study area for the year 2099 under the RCP4.5 (intermediate) emissions scenario. Values represent absolute predicted probabilities (0–1), with yellow colours indicating higher likelihood of encountering fin whales (maximum of 0.67), and blue colour indicating lower probability (0.11).

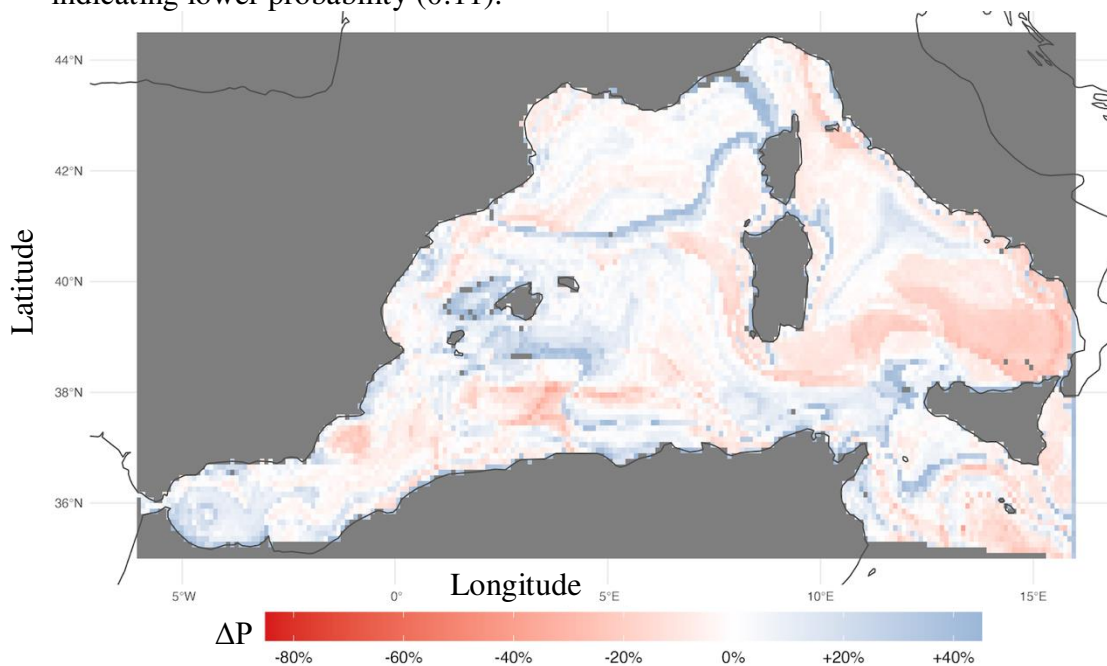


Figure 46. Habitat change obtained by comparing presence between 2018 and 2099 with RCP 4.5 ($\Delta P = P_{2099} - P_{2018}$) of the fin whale, red areas represent habitat loss, while blue areas represent habitat gain

3.3.2 RCP 8.5

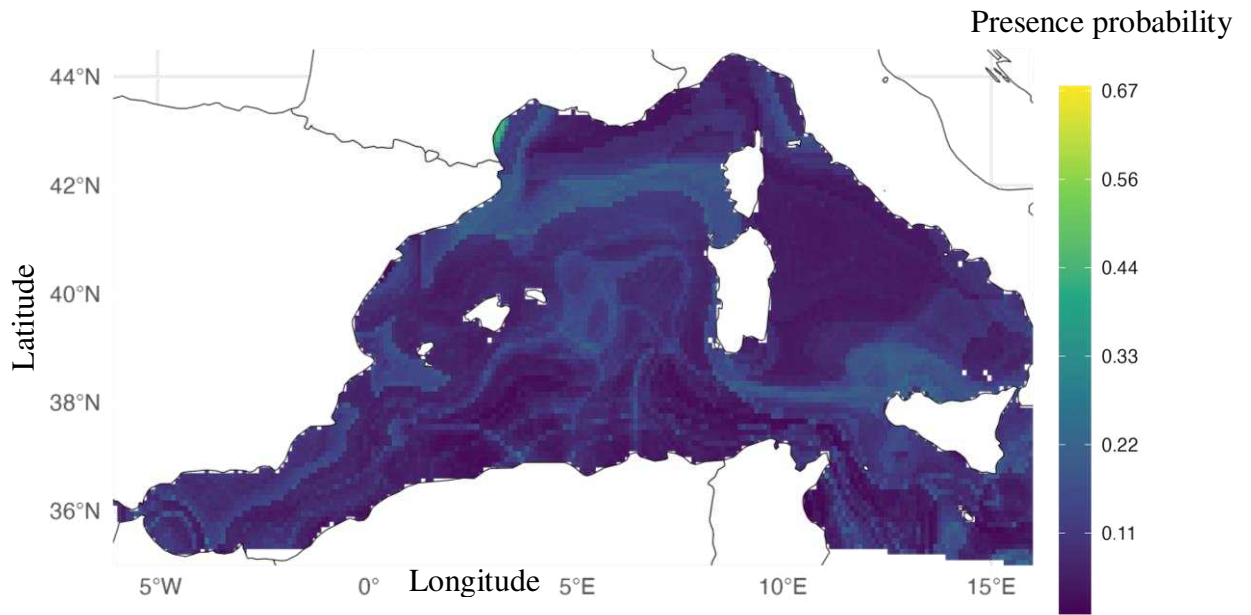


Figure 47. Projected probability of fin whale presence in the study area for the year 2050 under the RCP8.5 (business as usual) emissions scenario. Values represent absolute predicted probabilities (0–1), with yellow colours indicating higher likelihood of encountering fin whales (maximum of 0.67), and blue colour indicating lower probability (0.11)

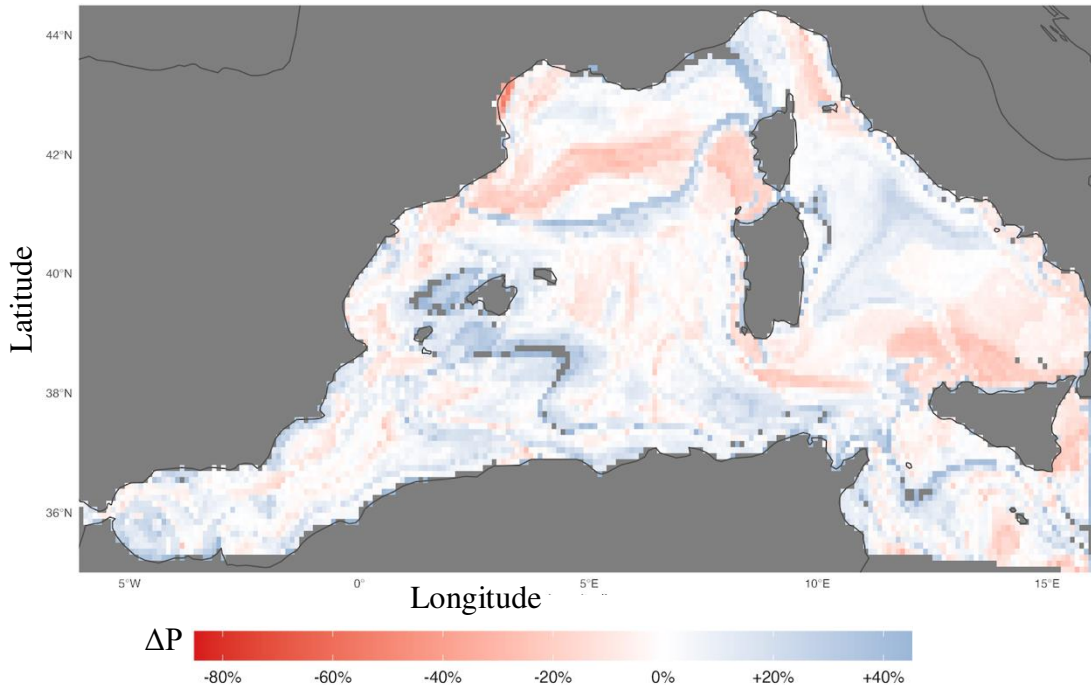


Figure 48. Habitat change obtained by comparing presence between 2018 and 2050 with RCP 8.5 ($\Delta P = P_{2050} - P_{2018}$)

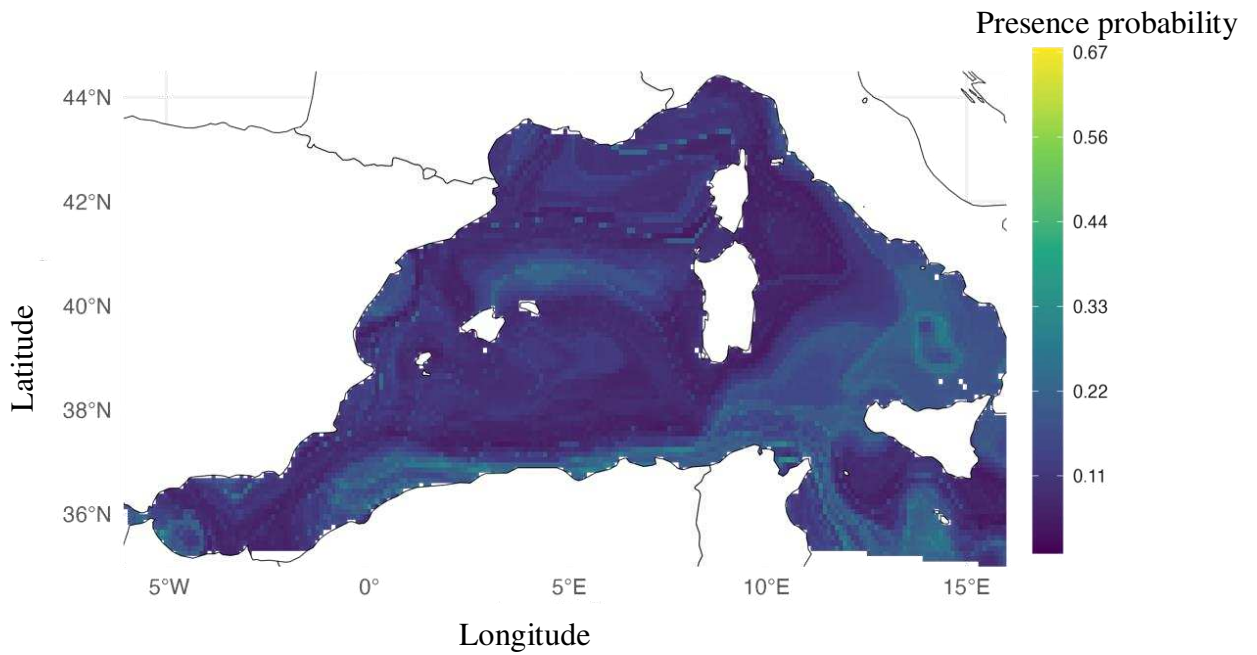


Figure 49. Projected probability of fin whale presence in the study area for the year 2099 under the RCP8.5 (business as usual) emissions scenario. Values represent absolute predicted probabilities (0–1), with yellow colours indicating higher likelihood of encountering fin whales (maximum of 0.67), and blue colour indicating lower probability (0.11)

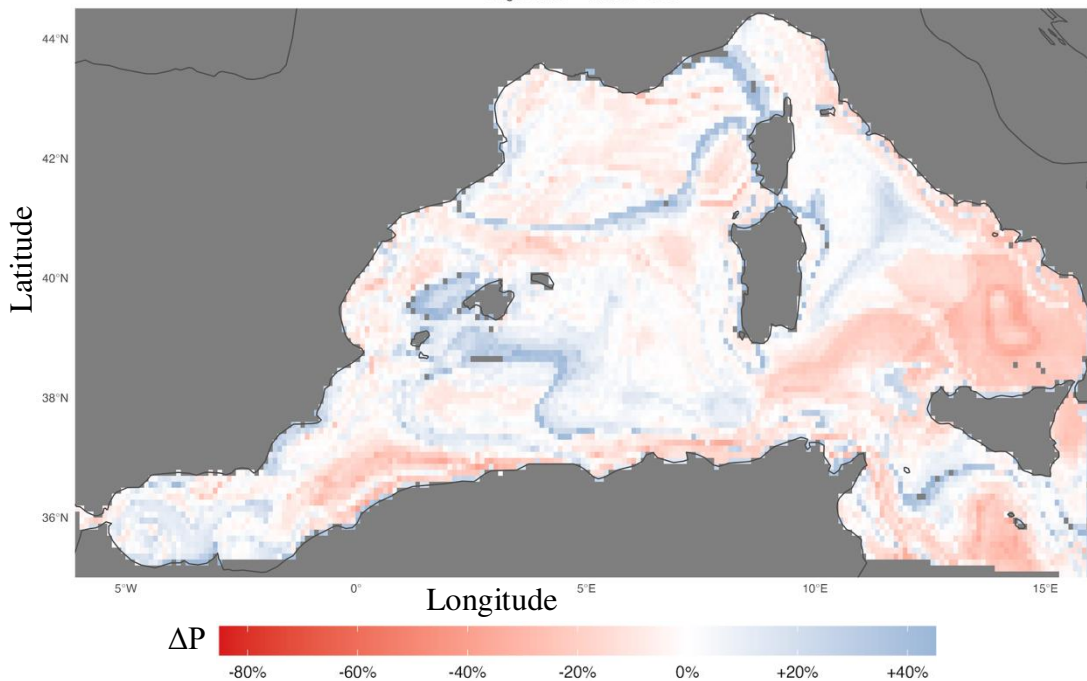


Figure 50. Habitat change obtained by comparing presence between 2018 and 2099 with RCP 8.5

4. DISCUSSION

4.1 GAM

Despite its theoretical ability to capture non-linear relationships between environmental variables and the presence of fin whales, the Generalised Additive Model (GAM) showed limited predictive performance and a lack of statistical significance for all environmental predictors analysed. Disappointing predictive performance exhibit AUC lower than 0.7, the 5-fold cross-validation analysis (Table 5) revealed that the best mean AUC value was obtained with $k = 6$ ($AUC = 0.572 \pm 0.028$), followed by $k = 10$ ($AUC = 0.571 \pm 0.031$). The AUC values ranging from 0 to 1, with 1 indicating very good performance; all AUC values are well below the threshold of 0.7, generally considered the minimum for an acceptable model in species ecology (Papale et al., 2025). This indicates poor discriminatory power between presence and pseudo-absence sites.

Although flexible, GAM failed to identify robust spatial or temporal patterns in the fin whale presence data. This can be attributed to several factors:

- Inadequate spatial scale: the resolution of 0.1° (~10 km) may be too coarse to capture the fine gradients of productivity that drive the species' movements.
- Temporal lag between predictors and response: Copernicus environmental variables represent instantaneous conditions, while fin whale presence responds to cumulative trophic processes, with krill peaks with weeks-long lags (Grossi et al., 2025).
- Complex non-additive interactions: GAM assumes additivity of smoothing terms, but interactions between SST, nutrients, and planktonic biomass are likely non-linear and multivariate.

The analysis of Effective Degrees of Freedom (EDF) provides insight into the functional form of relationships (Table 6.):

- $EDF = 1$: indicates a linear relationship (De Stephians et al., 2008): this is the case for phosphate_100m, phytoplankton_10m and 100m, and zooplankton_10m
- $EDF > 2$: suggests a non-linear relationship (De Stephians et al., 2008) SST ($EDF \approx 3$) and phosphate_10m ($EDF \approx 2.7$) show the greatest complexity, but not enough to reach significance (p -value value are > 0.2)

Lack of statistical significance with p -values higher than 0.2 as shown in Table 6. No environmental variable was statistically significant (p -value < 0.05) with either $k = 4$ or $k = 10$ (Derville et al., 2022). SST shows the most complex value ($EDF = 3.01$ for $k = 4$; $EDF = 3.17$ for $k = 10$), but non-significant p -values ($p = 0.593$ and $p = 0.614$). Phosphate_10m and phosphate_100m show EDFs close to 1 or 2.7, but high p -values. Zooplankton at 100 m exhibited $EDF = 0$ in both models (p -value = 0.981 and p -value = 1.0), indicating that the model completely excluded this variable from the fit. The $EDF = 0$ for zooplankton is particularly revealing. Although this variable represents the direct trophic source of the whale, the GAM failed to find any relationship with the observed presence; this results

doesn't mean that there are no biological effects but the model doesn't detect them using the available data. This does not imply that zooplankton is irrelevant, but rather that:

- Copernicus data does not capture the biomass of krill (Euphausiidae), which is the main prey, but only generic zooplankton.
- There is a spatial/temporal mismatch: observations of whales may occur after the peak of zooplankton, or in areas adjacent to krill banks
- The signal is too weak or noisy at the 0.1° scale to be detected by an additive model.

The GAM suggests that SST and surface phosphate play a potentially non-linear role, but the signal is too weak in the available data. In contrast, lower trophic variables (phytoplankton, zooplankton) appear linear or absent, probably because their effect on the whale is indirect, delayed and mediated by processes not captured by the model.

The habitat suitability maps for July 2018 (Figures 25 and 26) show an almost uniform probability of presence in the study area, with values between 0.50 and 0.75 and poorly defined patches of local variation. No clear hotspots emerge, nor do east-west gradients as expected (as the higher probability in the Ligurian Sea). This spatial uniformity is a direct consequence of the model's poor performance. The GAM, unable to identify significant predictors, produces "flat" predictions, close to the baseline prevalence. The small fluctuations observed are likely to be numerical artefacts rather than real ecological patterns. This result does not imply that the habitat is uniform, but that GAM is not the appropriate tool for revealing the spatial structure of the distribution of the whale in this context.

4.2 Random Forest

The Random Forest (RF) model demonstrated exceptional predictive performance and provided ecologically meaningful insights into the environmental drivers of fin whale (*Balaenoptera physalus*) presence in the western Mediterranean Sea. With an AUC of 0.9888, accuracy of 95.87%, and a low OOB error rate of 4.27% (Table 7.), the RF far surpassed conventional acceptability thresholds (AUC > 0.7) and outperformed the Generalized Additive Model (GAM) by a wide margin. The RF achieved near-perfect discrimination between presence and pseudo-absence sites, with an AUC of 0.9888 (Grossi et al., 2025). This is supported by high specificity (98.18%), indicating excellent identification of true absences, and solid sensitivity (80.11%), confirming reliable detection of presence locations. The precision of 86.56% further ensures that most predicted presences correspond to actual sightings, minimizing false positives in conservation applications. The OOB error rate of 4.27% reflects strong generalization, and the highly significant McNemar's test ($p = 4.734 \times 10^{-8}$) and overall model p-value ($p = 2.2 \times 10^{-16}$) confirm that the RF's predictions are statistically robust.

Such high performance suggests that the seven environmental predictors collectively capture the core biophysical template governing fin whale distribution at the 0.1° scale. Unlike the GAM, which failed to detect any significant relationships, the RF successfully exploited non-linear interactions, threshold

effects, and hierarchical dependencies within the trophic web capabilities inherent to tree-based ensemble methods.

Sea Surface Temperature (SST) was the top environmental predictor in the Random Forest model with Mean Decrease Accuracy of 202.964 and Mean Decrease Gini of 1657.694; (Table 8.). It was followed by phosphate_10m (Mean Decrease Accuracy of 72.283), phosphate_100m (Mean Decrease Accuracy of 70.508), phytoplankton_10m (Mean Decrease Accuracy of 69.749), zooplankton_100m (Mean Decrease Accuracy of 68.699), phytoplankton_100m (Mean Decrease Accuracy of 67.615), and zooplankton_10m (Mean Decrease Accuracy of 47.785). Despite these rankings, Spearman correlations with presence were uniformly weak ($\rho \leq 0.09$; Figure 28), highlighting, Spearman's failure to capture non-linearity and interactions in this food webs.

4.3 SST

Sea Surface Temperature (SST) emerged as the most influential predictor in the Random Forest model, with a Mean Decrease in Accuracy of 202.964 and a Mean Decrease in Gini of 1657.694 (Table 8). The predominant role of Sea Surface Temperature (SST) as the most important predictor in the Random Forest model aligns with the well-documented foraging preferences of fin whales in the Mediterranean (Grossi et al., 2025, Panigada et al., 2007). The predominant influence of SST aligns with the well-documented summer foraging preferences of Mediterranean fin whales, which consistently show peak sighting rates and feeding activity in waters of 20–23 °C (Panigada et al., 2007, Druon et al 2012). Boxplot comparisons (Figure 33.) further reveal that the median SST is higher in presence than in absence cells, with the box of the presence distribution extending to approximately 22°C, compared to ~20°C for absences. This suggests a slight but consistent preference for warmer area. The weak Spearman correlation between SST and fin whale presence ($\rho = 0.09$; Figure 28.) despite its high variable importance in the Random Forest model indicates that the influence of sea surface temperature is primarily non-linear and more complex. The Partial Dependence Plot (PDP) for SST provides a model-based interpretation of this relationship, revealing a complex, non-linear pattern (Figure 33.):

- Low temperatures (12–14 °C): At the coldest temperatures, the predicted probability of fin whale presence starts moderately (around 0.17–0.2) and rises sharply near 14 °C, reaching the first noticeable peak of probability (~0.37–0.38). This initial increase could represent fin whales' affinity for productive, cooler waters often associated with strong upwelling or nutrient mixing zones, which support high prey krill abundance.
- Sudden drop after 14 °C: Immediately after this peak, the probability drops drastically to below 0.1. Such an abrupt decline might indicate a transition zone where water temperature or associated environmental features (as reduced productivity or prey dispersal) become less favourable. It may also reflect ecological boundaries between distinct water masses (as frontal zones).
- Moderate temperatures (16–21 °C): Between approximately 16 °C and 21 °C, the predicted probability gradually increases again and remains

relatively stable around 0.2–0.25 with small oscillations. This suggests that fin whales can still occur in these mid-temperature environments, potentially exploiting regions with moderate productivity or seasonal prey availability.

- Warm temperatures (22–25 °C): Beyond 22 °C, the model shows a pronounced rise, with a sharp peak near 25 °C where predicted probability exceeds 0.4 the highest value observed in the plot. This could indicate that, in some parts of the study area, warmer surface temperatures correspond to areas of high productivity or localized prey aggregation. Alternatively, these peaks may coincide with seasonal movements of fin whales into warmer regions.
- After 25 °: Following this peak, there's a moderate decline, but the predicted probability remains relatively high (>0.3), suggesting sustained

The bimodal structure of the Partial Dependence Plot for SST, with distinct peaks near 14 °C and 25 °C, reveals the dual ecological role of sea surface temperature in shaping fin whale distribution in the western Mediterranean. The early peak at ~14 °C likely reflects exploitation of cool, nutrient-rich waters generated by upwelling or strong vertical mixing, conditions known to enhance primary productivity and subsequent krill biomass (De Stephanis et al., 2008; Cotté et al., 2009). Such cooler thermal niches are particularly relevant in dynamic regions like the Alboran Sea and along the shelf break of the Gulf of Lions, where Atlantic inflows and topographic forcing sustain elevated prey concentrations even during stratified periods. The dominant and broader peak centred around 25 °C aligns with the well-established preference of Mediterranean fin whales for late-summer foraging grounds in warmer surface waters (20–25 °C), particularly in the Ligurian-Provençal basin and Tyrrhenian Sea (Panigada et al., 2007; Druon et al., 2012). In these areas, warm SST overlays deeper productive layers, where internal waves, mesoscale eddies and frontal systems trap and concentrate zooplankton beneath the thermocline (Cotté et al., 2009; Millot et al., 2005). The abrupt drop in predicted probability immediately after 14 °C and the secondary decline beyond 26 °C further support the existence of sharp ecological thresholds, likely corresponding to transitions between water masses or the breakdown of productive frontal structures.

Thus, while fin whales are more frequently encountered in warmer surface waters overall reflecting their summer concentration in the northern basin within the mean cyclonic gyre bounded by the Northern Current and the North Balearic Front (Cotté et al., 2009). This dual-scale response explains both the high variable importance of SST in the Random Forest model and the relatively weak linear correlation with presence: SST operates primarily through non-linear interactions with dynamic oceanographic processes rather than as a simple monotonic gradient.

Additionally, the pronounced shift of the main peak toward warmer SST values (~25 °C) may be partly amplified by an observational bias inherent to opportunistic datasets: the vast majority of summer sightings in the Mediterranean are collected between June and September (Figure 17. compared to Figure 18.), when both recreational and commercial vessel traffic is at its highest, sea

conditions are optimal for visual surveys, and citizen-science contributions peaks. Consequently, the probability of detecting and reporting fin whales is disproportionately higher during the warmest months, potentially shifting the apparent thermal preference of the population toward higher SST values compared to what systematic, year-round surveys might reveal in cooler seasons or less trafficked areas.

4.4 Phosphate

Phosphate at 10 m depth ranked second in predictive importance (Mean Decrease in Accuracy = 72.283, Mean Decrease in Gini = 961.568; Table 8), while phosphate at 100 m depth followed closely in third place (Mean Decrease Accuracy = 70.508, Mean Decrease in Gini = 741.933). This high ranking, despite low linear correlations with presence probability ($\rho = -0.08$ for phosphate_10m; $\rho = -0.06$ for phosphate_100m; Figure 28) underscores the critical, indirect and time-lagged, role of near-surface nutrient availability in structuring fin whale habitat in the western Mediterranean Sea. Boxplot analysis reveals that median phosphate at 10m depth concentration is lower in presence cells than in absence cells, with a slight reduced variability (smaller interquartile range) in presence locations (Figure 29.). The presence boxplot shows a median line well below $5 \times 10^{-4} \text{ mol m}^{-3}$, while the absence distribution extends slightly higher. This pattern is ecologically counterintuitive at first approach: one might expect higher nutrients in whale feeding areas but aligns with nutrient drawdown dynamics, in productive surface waters, phytoplankton blooms rapidly consume phosphate, leaving low residual concentration precisely where the trophic cascade supports high krill biomass. At 100 m depth, the pattern is similar: median phosphate at 100m depth is slightly higher in absence than presence cells, with both boxplots reaching similar maximum heights ($\sim 0.0005 \text{ mol m}^{-3}$ Figure 31.). In the oligotrophic Mediterranean Sea, the most efficient foraging habitats for fin whales are associated with persistent mesoscale productive fronts characterised by relatively low chlorophyll-a levels. At these fronts, rapid consumption of inorganic nutrients including phosphate by phytoplankton leads to nutrient drawdown, creating low residual surface concentrations precisely where the upward energy flux supports high macro-zooplankton biomass attractive to fin whales (Druon et al., 2012). The slightly negative Spearman correlations ($\rho \approx -0.06$ to -0.08) reflect the indirect, non-linear, and time-lagged influence of phosphate on whale presence. Phosphate does not feed whales directly; instead, it fuels phytoplankton growth, which supports zooplankton, which aggregates into krill swarms the primary prey of fin whales with delays of days to weeks. At the moment of a whale sighting, surface phosphate may already be depleted due to bloom activity, resulting in weak or inverse linear signals. The Random Forest model, however, excels at capturing these conditional, interactive effects, ranking phosphate highly because it triggers the productivity cascade that ultimately sustains foraging hotspots.

Phosphate_10m PDP (Figure 30.):

- Near-zero concentrations of phosphate ($0 - \sim 1 \times 10^{-4} \text{ mol m}^{-3}$): Predicted presence probability starts high (~ 0.3) and peaks sharply at $\sim 0.42-0.44$.
- Sharp decline ($\sim 1 \times 10^{-4}$ to $\sim 3 \times 10^{-4}$): Probability drops abruptly below 0.1, suggesting a threshold beyond which slightly elevated phosphate indicates less favourable conditions
- Low to moderate range ($\sim 3 \times 10^{-4}$ to 1×10^{-3}): Probability stabilizes at ~ 0.15 with minor oscillations
- High concentrations ($> 1 \times 10^{-3}$): The curve flattens at ~ 0.15 probability, confirming that nutrient-enriched, potentially hypoxic or stratified waters are not preferred by fin whales.

Phosphate_100m PDP (Figure 32):

- Extremely low values ($\sim 0.000 \text{ mol m}^{-3}$): Probability starts with the highest peak ($\sim 0.34-0.35$), followed by a steep decline lower than 0.15.
- Intermediate range (up to $\sim 0.0008 \text{ mol m}^{-3}$): Probability oscillates weakly around 0.13–0.15, showing local variability but no strong trend.
- Higher concentrations ($\sim 0.001 \text{ mol m}^{-3}$ onward): A gentle upward trend emerges, with probability rising to $\sim 0.18-0.19$ and plateauing beyond 0.003 mol m^{-3} .

This weak positive relationship at depth area suggests that larger subsurface reservoirs support sustained productivity, particularly in regions with vertical nutrient flux (Pace et al., 2015). The slight importance of phosphate_10m over phosphate_100m in variable importance highlights the primacy of surface processes in initiating short-term foraging opportunities (Table 8.). Surface nutrient injections from upwelling, river runoff, or wind mixing trigger rapid phytoplankton blooms that propagate upward through the food web within days, creating transient krill aggregations that fin whales exploit via lunge feeding.

Fin whale presence cells are concentrated in the northwestern Mediterranean and northern Alboran Sea precisely the two sub-regions that exhibit the highest surface and near-surface phosphate availability at the basin scale during winter–spring mixing. However, within the summer stratified period that dominates our sighting dataset, the intense phytoplankton consumption at persistent mesoscale fronts rapidly depletes these nutrients in the upper 10 m layer, generating the observed pattern of significantly lower residual phosphate concentrations and reduced variability in presence cells compared to absence cells. This confirms that the high predictive importance of phosphate_10m and phosphate_100m in the Random Forest does not reflect a direct attraction to high nutrient levels, but rather the indirect, time-lagged signature of recent nutrient drawdown in the most productive foraging hotspots of the western Mediterranean. In the strongly oligotrophic context of the basin, where surface phosphate frequently falls below detection limit even in winter in the eastern sectors, the northwestern sector therefore functions as the primary “nutrient pump” that ultimately sustains, through seasonal mixing and subsequent summer frontal dynamics, the krill-rich habitat preferentially exploited by Mediterranean fin whales (Druon et al., 2012; Lazzari et al., 2016; Cotté et al., 2009).

4.5 Phytoplankton

Phytoplankton at 10 m depth ranked fourth in predictive importance (Mean Decrease in Accuracy = 69.749, Mean Decrease in Gini = 730.479; Table 8), while phytoplankton at 100 m depth ranked sixth (Mean Decrease Accuracy = 67.615, Mean Decrease in Gini = 803.593). Despite near-zero linear correlations with fin whale presence ($\rho = 0.02$ for both phytoplankton_10m and phytoplankton_100m; Figure 28), both variables contributed substantially to the Random Forest model, reflecting their indirect role in the pelagic food web and the non-linear, threshold-based dynamics of primary productivity in the western Mediterranean. At 10 m depth (Figure 35.), medians and interquartile ranges of phytoplankton concentration are nearly identical between presence and absence cells, with only a slight shift of medians toward higher values in presence locations. This subtle elevation suggests a weak preference for moderately productive surface waters. At 100 m depth (Figure 37.), the pattern is a little more pronounced: the median phytoplankton_100m is slightly higher in presence cells, and the box extends to higher values than in absence cells. The essentially null Spearman correlations ($\rho \approx 0.02$) are not indicative of irrelevance but rather highlight the complex, non-linear, and time-lagged relationship between phytoplankton and fin whale presence. Phytoplankton is not direct prey; it forms the base of the trophic chain, supporting zooplankton and subsequently krill (*Meganyctiphanes norvegica*), with delays of days to weeks. At the moment of whale observation, surface blooms may have already been grazed or exported, resulting in weak instantaneous signals. The Random Forest model, however, captures these conditional and interactive effects, ranking phytoplankton highly due to its role in sustaining prey availability within favourable thermal and nutrient regimes.

Phytoplankton_10m PDP (Figure 36.):

- Extremely low concentrations ($\sim 0.00 \text{ mol m}^{-3}$): Predicted presence probability starts high (~ 0.30) and drops sharply to $\sim 0.13\text{--}0.14$ within a narrow increase of concentration.
- Low to moderate range (up to $\sim 0.015 \text{ mol m}^{-3}$): The curve fluctuates weakly increasing around $0.13\text{--}0.15$ of probability, with minor oscillations, indicating local variability but no strong trend.
- Mid-range ($\sim 0.015\text{--}0.02 \text{ mol m}^{-3}$): Probability rises, forming a double peak around 0.02 mol m^{-3} (probability of $\sim 0.21\text{--}0.22$) reaching the highest values since the initial drop.
- High concentrations ($>0.02 \text{ mol m}^{-3}$): The curve drops to ~ 0.17 and stabilizes, indicating diminishing returns in dense blooms

Phytoplankton_100m PDP (Figure 38.):

- Extremely low values ($\sim 0.0001 \text{ mol m}^{-3}$): Probability starts at ~ 0.20 and drops sharply to $\sim 0.13\text{--}0.14$, mirroring the surface pattern but at a lower initial peak.
- Low range (up to $\sim 0.01 \text{ mol m}^{-3}$): at 0.005 mol m^{-3} there is a peak of probability reaching the 0.18 , then the probability decrease; at the concentration of 0.01 mol m^{-3} the probability clearly increase

- Mid-range ($\sim 0.01\text{--}0.02 \text{ mol m}^{-3}$): there is an increasing trend of probability rising to ~ 0.22 with some peaks
- High range (higher than 0.02 mol m^{-3}): the probability stay constant at 0.224 until $0.0027 \text{ mol m}^{-3}$; then with higher concentrations the probability increase and stabilize with the presence at 0.0227.

The Partial Dependence Plot for phytoplankton at 100 m depth (Figure 38) shows a clear overall positive trend: predicted probability of fin whale presence increases non-linearly with subsurface phytoplankton biomass, from probability of ~ 0.125 at the lowest concentrations to a stable maximum of ~ 0.227 above 0.027 mol m^{-3} . This stepped response reflects preferential use of habitats characterised by a well-developed deep chlorophyll maximum that sustains dense krill layers. Several authors have highlighted that fin whale preferentially concentrate in areas characterised by moderate and persistent primary productivity rather than in intense and transient surface blooms (Druon et al., 2012; Panigada et al., 2007). Medium concentration ($\sim 0.02 \text{ mol m}^{-3}$) and long-lasting (weeks–months) chlorophyll fronts due to phytoplankton favour efficient energy transfer to zooplankton and krill, attracting top predators even when absolute Chl-a values remain low or oligotrophic, typical of the summer Mediterranean (Druon et al., 2012; Notarbartolo di Sciara et al., 2016). The crucial role of the subsurface chlorophyll maximum (Deep Chlorophyll Maximum, DCM) also emerges in the stratified summer regime: the decrease in nutrient flow to the photic zone shifts primary productivity to greater depths (50–120 m), where a peak in phytoplankton biomass forms, capable of supporting dense aggregates of krill even in the absence of obvious surface blooms (McGehee, 2004; Fossi et al., 2017). The positive non-linear trend observed in the phytoplankton_100m PDP therefore reflects the preference of fin whales for habitats with a well-developed DCM, in accordance with the trophic ecology of the species in the pelagic Mediterranean.

4.6 Zooplankton

Zooplankton at 100 (Table 8.) depth ranked fifth in predictive importance (Mean Decrease in Accuracy = 68.699, Mean Decrease in Gini = 915.640), notably outperforming zooplankton at 10 m depth, which ranked last (Mean Decrease Accuracy = 47.785, Mean Decrease in Gini = 786.518). Despite weak positive linear correlations with fin whale presence ($\rho = 0.04$ for both depths; Figure 28), the contribution of subsurface zooplankton highlights its role as a more reliable proxy for deep prey availability and sustained productivity in the foraging habitats of *Balaenoptera physalus* in the western Mediterranean.

At 10 m depth (Figure 39), the presence boxplot reach higher value of concentration than the absence boxplot, with a slightly elevated median and greater upper quartile, indicating a modest preference for higher surface zooplankton biomass in whale sighting locations. At 100 m depth (Figure 41), the pattern is more pronounced: the presence boxplot reach higher values and the median is slightly higher in the presence boxplot. This suggests that zooplankton in general reach higher concentration value for the presence value of fin whale.

The weak Spearman correlations ($\rho = 0.04$) reflect the indirect and complex relationship between modelled zooplankton biomass and whale presence. Copernicus zooplankton data represent generic mesozooplankton, not specifically krill (*Meganyctiphanes norvegica* or *Nyctiphanes couchii*), the favourite prey of fin whales in the Mediterranean sea. Moreover, temporal lags (krill recruitment following zooplankton peaks) and spatial mismatches (whales targeting dense subsurface swarms) dilute linear signals. The Random Forest model, however, captures non-linear thresholds and interactive effects, ranking zooplankton_100m higher because it better aligns with deep foraging depths and persistent productivity zones.

Zooplankton_10m PDP (Figure 40.)

- Very low concentrations ($\sim 0.001 \text{ mol m}^{-3}$): Predicted presence probability starts relatively high (>0.18), however, it drops sharply to ~ 0.12
- Low concentration from 0.001 mol m^{-3} to 0.002 mol m^{-3} of zooplankton have a lower probability of 0.14
- Moderate range ($0.002\text{--}0.006 \text{ mol m}^{-3}$): Probability increases gradually from ~ 0.12 to ~ 0.17 , with multiple small oscillations, suggesting a weakly positive, non-linear relationship.
- Higher value of concentration of zooplankton at $0.0065 \text{ mol m}^{-3}$ reveals a stable probability lower than 0.16.

The oscillatory, modestly increasing curve reflects complex trophic dynamics: surface zooplankton is a noisy proxy, influenced by wind mixing, jellyfish, or non-krill taxa, and less directly linked to whale feeding.

Zooplankton_100m PDP (Figure 42.):

- Very low concentrations ($\sim 0 \text{ mol m}^{-3}$): Probability starts at ~ 0.16 and drops briefly to ~ 0.10 , confirming that extremely low subsurface biomass is unfavourable due to scarce prey resources.
- Low to moderate range ($0.001\text{--}0.004 \text{ mol m}^{-3}$): The curve rises consistently, with sharp localized peaks: the higher peak is reached at 0.002 mol m^{-3} reaching the 0.22 probability indicating threshold-dependent responses where specific biomass levels trigger krill aggregation.
- Higher concentrations ($>0.004 \text{ mol m}^{-3}$): there are two more peaks reaching almost the 0.25 probability (the highest sustained values in the plot) then probability stabilizes at 0.22, demonstrating that elevated deep zooplankton is strongly associated with favourable foraging conditions; then the probability stabilize at 0.225 with higher value of concentration of 0.006 mol m^{-3}

At 100 m depth, zooplankton concentration shows a clear positive relationship with the predicted probability of fin whale presence. As zooplankton concentration increases, the predicted probability of fin whale occurrence rises markedly, indicating that higher prey density at this depth layer is a strong driver of habitat suitability. In contrast, at 10 m depth, the PDP for zooplankton concentration also exhibits an overall increasing trend with fin whale presence probability, but the relationship is considerably weaker and less pronounced than at 100 m. The curve is flatter, with changes in predicted probability across the

range of zooplankton concentrations observed, suggesting that surface-layer prey abundance has a more limited influence on fin whale occurrence compared to the deeper 100 m depth prey field. The superior performance of zooplankton_100m is ecologically profound: fin whales execute deep lunge-feeding dives to exploit dense krill layers below the thermocline. Surface zooplankton (10 m) is more variable, subject to wind-driven patchiness, predation by fish, or non-prey taxa, making it a weaker predictor. In contrast, subsurface biomass (100 m) integrates vertical mixing, nutrient upwelling, and krill diel migration, serving as a robust proxy for persistent, dive-accessible prey.

4.7 Future prediction

4.7.1 RCP 4.5 year 2050

The mid-century projections under the RCP 4.5 moderate emissions scenario reveal a dynamic and spatially heterogeneous reconfiguration of fin whale habitat suitability in the western Mediterranean Sea, as captured by the Random Forest model using 4 environmental predictors (SST, phosphate, phytoplankton, and zooplankton at 10 m and 100 m depths).

While no region exceeds with P maximum of 0.67 in 2050, and the habitat change also reveals heterogeneous zone of increase and increase of habitat with high-probability zones particularly in the central Tyrrhenian Sea and southern Tunisian shelf signals early-stage habitat redistribution driven by subtle but ecologically significant oceanographic changes. These shifts are patchy and fine-scaled, with ΔP rarely exceeding $\pm 50\%$, reflecting the non-linear, threshold-dependent responses of the trophic web to moderate warming and altered nutrient–prey dynamics.

- The Alboran Sea, a foraging ground, shows moderate persistence in absolute terms ($P = 0.22\text{--}0.44$, Figure 43), but Figure 44 reveals a gain ($\Delta P = +10\%$ to $+25\%$) across most of the basin, particularly along in the Strait of Gibraltar and Almeria–Oran front. This light blue expanse indicates improved suitability due to enhanced Atlantic inflow and early synchronization of nutrient pulse, which support krill recruitment despite rising SST. However, a red patch south of Málaga ($\Delta P \approx -25\%$) highlights localized vulnerability.
- The Balearic Sea and Catalan shelf exhibit comparable absolute suitability ($P = 0.22\text{--}0.44$), but with more frequent lighter blue tones than the Alboran, reflecting a higher mean probability. The colour of the absolute probability is aquamarine indicating an average of presence of 0.33-0.44 in the Balearic area. This zone in the comparison with 2018 (Figure 44) it is not uniform: varies from the north showing a light blue colour and toward the south it become red (-25%).
- The Ligurian–Provençal Basin and Gulf of Lion maintain stable to slightly enhanced suitability, with absolute probabilities ($P = 0.10\text{--}0.44$) lower than the Balearic range and localized peaks (~ 0.50) along the Ligurian front. Figure 44 shows patchy gains ($\Delta P = +25\%$ to $+30\%$) northwest of Corsica, reflecting persistent wind-driven upwelling and dense water

formation, but reddish tones near the Italian coast ($\Delta P \approx -15\%$) indicate minor frontal retreat.

- The most striking result is the emergence of a defined high-suitability hotspot in the central Tyrrhenian Sea, where Figure 43 shows a green-yellow zone ($P = 0.56$) in 2050. This core is centred between Sardinia and the Tuscan-coast of Lazio and likely results from enhanced internal wave activity and canyon-induced mixing which sustain deep krill aggregations below a warming surface layer. However, Figure 44. reveals a paradoxical signal: this same central area shows moderate loss ($\Delta P \approx -30\%$, red), indicating that while absolute suitability has increased in this area, the comparison with 2018 has experienced decline. Further south (Figure 44.), near northern Sicily and Calabria, uniform light blue ($\Delta P = +20\%$ to $+30\%$) suggests diffuse improvement, possibly from shelf-slope upwelling.
- The Tunisian shelf presents a north-south gradient. In Figure 43, the northern shelf remains blue ($P = 0.10-0.22$), while a small southern near Tunisia shelf reaches $P \approx 0.50-0.56$ (yellow) a notable increase in a historically oligotrophic zone. Figure 44 has an opposite trend: the southern hotspot corresponds to a red zone ($\Delta P \approx -30\%$ to -50%), meaning that while absolute probability is lower in 2050, it represents a decline from a locally elevated 2018 baseline. Conversely, the northern shelf transitions from red to white to blue, indicating progressive gain ($\Delta P = +10\%$ to $+25\%$), suggesting broadening suitability in less productive areas. The Algerian Basin by contrast, remains uniformly low in both maps: $P = 0.11-0.22$ (blue, Figure 43) and $\Delta P \approx 0$ to $+20\%$ (white to pale blue, Figure 44).

The 2050 RCP 4.5 scenario does not produce dramatic latitudinal redistribution but rather a fine-grained mosaic of gains and losses, with changes concentrated in small, ecologically sensitive cells. Traditional hotspots (Alboran, Gulf of Lion) show resilience with localized enhancement, while the central Tyrrhenian and the water near the Tunisian shelf emergence marks a novel high-value zones.

4.7.2 RCP 4.5 for year 2099

The end-of-century projections under the RCP 4.5 moderate emissions scenario reveal a consolidated, high-contrast reconfiguration of fin whale habitat in the western Mediterranean Sea.

- The Alboran Sea, shows low probability ($P = 0.10-0.33$, Figure 45) but reveals a higher presence probability across a zone between Almería-Cartagena. This zone in the Figure 46. show a red patch between ($\Delta P \approx -25\%$ to -40%) highlights localized vulnerability, likely from frontal displacement or coastal stratification.
- The Balearic Sea and Catalan shelf exhibit low- medium probability of presence ($P = 0.22-0.33$, Figure 45). The delta map (Figure 46) confirms gains in the north Balearic ($\Delta P = +20\%$ to $+40\%$), driven by intensified Northern Current mixing and eddy retention, which sustain subsurface prey layers.

- The Ligurian–Provençal Basin and Gulf of Lion maintain stable to slightly enhanced suitability, with absolute probabilities mirroring the Balearic range ($P = 0.10\text{--}0.44$, Figure 45). Figure 46 shows patchy gains ($\Delta P = +25\%$ to $+30\%$) northwest of Corsica, reflecting persistent wind-driven upwelling and dense water formation, but small reddish tones near the Italian coast ($\Delta P \approx -15\%$) indicate minor frontal retreat.
- The most striking result is the southward migration of the high-suitability hotspot in the Tyrrhenian Sea (shown in the RCP 4.5 for year 2050), where Figure 45 shows a green–yellow zone ($P = 0.33\text{--}0.44$) in 2099, centred off Calabria and northern Sicily. This core likely results from enhanced internal wave activity and canyon-induced mixing (Sicilian slope), which sustain deep krill aggregations below a warming surface layer. However, Figure 46 reveals a paradoxical signal: this same southern area shows moderate loss ($\Delta P 30\%\text{--}40\%$, red), indicating that while absolute suitability has increased in this area, the comparison with 2018 has shown a decline. Further north, near Tuscany–Corsica, uniform light blue ($\Delta P = +20\%$ to $+30\%$) suggests diffuse improvement, possibly from shelf-slope upwelling.
- The Tunisian shelf presents a north–south gradient. In Figure 45, the northern shelf remains blue ($P = 0.10\text{--}0.22$), while a small southern spot reaches $P \approx 0.44$ (green), a notable increase in a historically oligotrophic zone. Figure 46 shows that the southern hotspot corresponds to a red zone ($\Delta P \approx -20\%$ to -30%), meaning that while absolute probability is high in 2099, it represents a decline from a locally elevated 2018 baseline.
- The Algerian Basin, by contrast, emerges as the new core: a bright yellow patch ($P \approx 0.56$) centred between the Balearic slope and Algerian coast represents the highest domain probability. Figure 46 shows this patch as deep red ($\Delta P \approx -35\%$), confirming dramatic compression from a 2018 high-suitability patch. The surrounding basin remains uniformly low ($P = 0.11\text{--}0.22$, dark blue) and ΔP differ from negative to positive values.

Compared to the 2050 transitional phase and 2018 baseline, the 2099 scenario exhibits generally more blue tones than in 2050, indicating a lower probability of occurrence (Figure 45.) and a shift of the decreasing habitat suitability compared with 2018 in the southernmost part of the basin (Figure 46.)

The dominant pattern is a curvilinear high-suitability corridor: a wavy band of green ($P \approx 0.44$) that bisects the basin diagonally from the Iberian Peninsula (near Cartagena), passing south of Sardinia, and terminating north of Sicily. This diagonal productivity axis aligns with the historical Atlantic Water pathway, major submarine canyon systems, and persistent frontal convergence zones, suggesting that RCP 4.5 stabilization has reinforced mesoscale retention mechanisms along bathymetrically complex margins.

Under RCP 4.5, habitat persists through localized refugia and a novel diagonal high-suitability corridor (Alboran–Tyrrhenian–Sicilian slope) by 2099, reflecting resilience in bathymetrically complex margins. RCP 8.5, however, triggers severe compression into subsurface “krill oases” along Sicilian canyons, with 40–60% losses in former hotspots threatening population viability as *Meganyctiphanes norvegica* nears thermal limits (D’Amen et al., 2024; Espada, 2024).

4.7.3 RCP 8.5 for year 2050

Under the RCP 8.5 high-emissions scenario for 2050, the western Mediterranean fin whale habitat undergoes pronounced decreasing trend.

- In the Alboran Sea, Figure 47 shows dominant dark blue ($P = 0.11-0.22$) with some light-blue cells ($P \approx 0.35$) in the middle of the peninsula Iberian and African; reflecting residual Atlantic-driven productivity. Figure 48 presents a mixed gradient: from light-blue and whitish to few light- red cells near the Strait of Gibraltar ($\Delta P = -30\%$ to $+30\%$) resulting from transient inflow enhancement, there are reddish zones in the central-eastern basin ($\Delta P = -30\%$) over the light-blue patches of figure 47.
- The Balearic Sea and Catalan shelf exhibit western light blue waters ($P = 0.22$) in Figure 47, transitioning to darker blues around the islands ($P = 0.11$). Figure 48 mirrors this with a light-blue area encircling the islands ($\Delta P = +10\%$ to $+40\%$) especially in the north, contrasting red offshore areas ($\Delta P = -20\%$ to -40%) in the west of the islands, highlighting island-adjacent gains from eddy trapping versus open-water losses due to oligotrophication.
- Within the Ligurian-Provençal Basin and Gulf of Lion, Figure 47 displays a southwestern light-blue gradient ($P = 0.33$) near western Corsica contrasting with blue zones ($P = 0.11- 0.22$) along the Ligurian front; the figure shows a small greenish area (indicating 0.44 probability) in the part of the Gulf of Lion closest to the shore (but the figure 48. This zone show a decreasing of probability compared to 2018). Figure 48 reveals a striking elongated red band west of Corsica ($\Delta P = -30\%$ to -50%) directly beneath the light-green patches (of Figure 47) opposed by light-blue gains to the north near the Ligurian shelf ($\Delta P = +20\%$ to $+40\%$).
- The Tyrrhenian Sea appear uniformly dark blue ($P < 0.11$) in Figure 47. There are light-green brightening ($P = 0.35-0.45$) in a diffuse central band between the Balearic Islands and western Sardinia, extending toward northern Sicily ($P \approx 0.40$). Figure 48 inverts this pattern: dark-blue areas in the central Thyrrenan sea align with light-blue ΔP gains ($\Delta P = +20\%$ to $+40\%$), while southern light-green zones of Figure 47. overlie red losses ($\Delta P = -30\%$ to -50%).
- The Algerian Basin remains dark blue ($P < 0.20$) in Figure 47 with isolated lighter patches ($P \approx 0.30$), and Figure 48 shows variable white to light-blue increase compared to 2018 ($\Delta P \approx 0$ to $+30\%$) punctuated by little red spot ($\Delta P = -20\%$).
- The Tunisian shelf show an homogeneous blue indicating lower probability (0.11) in Figure 47. Figure 48 features light-red surrounding Sicily ($\Delta P = -20\%$ to -40%) and patchy offshore blue gains ($\Delta P = +10\%$ to $+30\%$).

Figure 47 revealing a predominantly dark-blue absolute probability landscape ($P \approx 0.22$) with colours darker than RCP 4.5 and no grid cell exceeding $P = 0.44$. High-probability green-yellow zones are absent (there is only a very small zone on the Gulf of Lion and the shelf), replaced by diffuse light-blue

patches in the central-western basin. Figure 48 exposes the dynamic: dark-blue absolute (indicating lower probability presence of Figure 47.) zones frequently overlay light-blue ΔP gains ($\Delta P = +10\%$ to $+40\%$), indicating emergent suitability in formerly marginal areas, while light-green absolute patches coincide with red ΔP losses ($\Delta P = -20\%$ to -50%), signalling compression of 2018 hotspots, a mark of rapid, non-linear trophic disruption under intensified stratification and nutrient limitation.

4.7.4 RCP 8.5 for year 2099

The end-of-century RCP 8.5 high-emissions scenario imposes severe, near-uniform suppression on fin whale habitat across the western Mediterranean.

- In the Alboran Sea, Figure 49 reveals dominant blue ($P \approx 0.11$) with subtle light-green brightening ($P \approx 0.22$) along the African continental slope, reflecting residual Atlantic inflow under severe stratification. Figure 50 shows initial red near the African coast at the Strait of Gibraltar ($\Delta P = -30\%$ to -50%), transitioning to pale blue ($\Delta P \approx 0$ to $+10\%$).
- The Balearic Sea appears uniformly blue ($P \approx 0.11$) in Figure 49, interrupted by a narrow light-green filament ($P \approx 0.22$) originating from north of Mallorca and curving toward western Sardinia, suggesting persistent eddy retention in a Northern Current remnant. Figure 50 displays central pale blue ($\Delta P \approx 0$ to $+10\%$) surrounded by an eastern red patch ($\Delta P = -30\%$ to -50%), indicating the filament from Mallorca to Sardinia.
- Within the Ligurian-Provençal Basin, Figure 49 maintains blue ($P = 0.10$ – 0.22) with scattered light-green cells ($P \approx 0.33$) north of Corsica. Figure 50 presents predominantly white-blue ($\Delta P \approx -10\%$ to $+10\%$) with small sparse red spots ($\Delta P = -20\%$ to -40%).
- The Tyrrhenian Sea transitions from northern blue ($P \approx 0.11$) to southern light-blue intensification ($P \approx 0.33$) in Figure 49, culminating in a compact green core above Sicily and east Calabria: the only significant high probability zone. Figure 50 inverts this precisely: the green core of Figure 49. sits atop deep red ($\Delta P = -40\%$ to -60%).
- The Algerian basin shows near the coast a probability about the 0.33 (Figure 49), while in the Figure 50. This area is represented by a red colour indicating a loss of probability.
- The southern margin surrounding northern Sicily stands out in Figure 49 as the more light blue sector ($P = 0.33$), while Figure 50. blankets it in deep red ($\Delta P = -50\%$ to -60%).

Figure 49. indicating the predicted probability displaying an intensely dark-blue absolute probability field visibly darker and more homogeneous than the 2050 projection. High-probability yellow zones ($P > 0.44$) are entirely absent, replaced by isolated light-green zone concentrated in the southern-central basin. Figure 50 confirms the persistent inversion dynamic: light-blue absolute patches precisely overlay deep-red ΔP losses ($\Delta P = -40\%$ to -60%), while dark-blue backgrounds align with pale-blue to white ΔP stability ($\Delta P \approx -10\%$ to $+10\%$).

Across the transition from RCP 4.5 to RCP 8.5, habitat suitability maps shift from predominantly warm tones (yellow–green; mean $P \approx 0.44$) to darker blue tones (mean $P \approx 0.22$), reflecting a systematic decline in predicted fin whale presence probability. Under RCP 4.5, the 2050 projection introduces a novel high-probability areas ($P \approx 0.50$ – 0.56) immediately east of the Tunisian shelf, whereas the 2099 scenario relocates the highest-suitability core ($P \approx 0.56$) to the central Algerian Basin, between the southern Balearic slope and the North African margin. In contrast, RCP 8.5 yields two transient favourable patches in 2050 within the open basin between Sardinia and the north of Balearic Islands, while by 2099 the only remaining high-probability refugia contract to the northern Sicilian slope and adjacent Tunisian coastal waters. In the Tyrrhenian Sea, circulation is shaped by the basin-wide cyclonic gyre and a summer-intensified eastward jet driven by north-westerly winds through the Bonifacio Strait. This interaction generates persistent quasi-stationary vortices including the Bonifacio Gyre which promote upward nutrient flux and localized productivity. Eastward of this feature, a surface-to-intermediate cyclonic eddy hugs the Italian peninsula, flanked by a smaller anticyclonic eddy in between. SST follows expected seasonal cycles, while mean chlorophyll values reflect the Mediterranean’s typical summer oligotrophy. A distinct cold, high-productivity patch emerges east of Sardinia, directly aligned with the Bonifacio Gyre, increased by the convergence of Tyrrhenian cyclonic flow and wind-forced currents that amplify vertical mixing (Arcangeli et al., 2012).

Rising or shifting water temperatures can disrupt the life cycles of prey species for marine mammals, leading to temporal mismatches between peak prey abundance and the presence or energetic needs of marine mammals. This mismatch can be particularly severe for long-distance migratory species that travel between distant feeding and breeding grounds, as well as for species that rely heavily on predictable prey availability to provide protein for lactation or for recently weaned calves (Albouy et al., 2020).

SST dominates as a hierarchical variable, guiding whales to thermal windows where canyon-driven upwelling, eddy retention, and internal waves concentrate krill beneath stratified surfaces consistent with the species’ nomadic opportunism in exploiting transient, mesoscale productivity hotspots (Notarbartolo di Sciara et al., 2016; Papale et al., 2025). Mediterranean fin whales, uniquely adapted to this semi-enclosed, climatically permissive basin (Notarbartolo di Sciara et al., 2003), may leverage behavioural plasticity to track shifting prey pulses, but altered productivity patterns risk disrupting this strategy (Notarbartolo di Sciara et al., 2016).

Cetacean locations, strongly shaping sea group roles and structure, tie closely to surroundings like sea characteristics and food access. Cetaceans probably can't handle quick heat and anomalies condition, with weather shifts as the biggest ongoing risk. Though base food levels most likely change, cetaceans face planetary heating effects in many forms. Cetacean locations, numbers, and migrations depend heavily on food access, with those in narrow habitats most at risk from weather shifts (Gambaiani et al., 2007).

For fin whales, these changes impact the availability of key prey, such as *Meganyctiphanes norvegica* a dominant euphausiid in the Ligurian Sea at its

southern geographical limit and highly sensitive to temperature increases or *Nyctiphanes couchii*, potentially disrupting feeding patterns in critical habitats like the Pelagos Sanctuary, Gulf of Lion, and Tyrrhenian Sea (Espada et al., 2024; Gambaiani et al., 2007; Panigada et al., 2021). Prey type location shifts mainly cetacean area ranges and favourite habitat. Food access changes might push cetaceans to alter eating approaches and use more effort foraging, badly affecting health and reproductive success. Thus, less time for grouping and mating harms breeding outcomes (Gambaiani et al., 2007). In conclusion, climate-driven changes in prey availability and distribution may force fin whales to allocate increasing effort to foraging at the expense of resting, socialising, and mating behaviours. This shift is likely to compromise individual body condition, reduce reproductive success, and ultimately contribute to a decline in population size across the Mediterranean Sea.

5. CONCLUSION

The marine mammals, still rebounding from the devastating effects of historical whaling and facing intense threats from human activities including plastic chemical, and noise pollution, as well as ship strikes, must now also endure climate-driven changes at both local and global scales. The studies on cetaceans are challenging because of their extensive mobility, the prolonged periods they spend submerged, and the legal plus political restrictions on investigating protected species. Despite recent progress in climate and ecosystem modelling, surprisingly few studies have sought to forecast the effects of climate change on cetacean distribution and habitat.

This study reveals that fin whale distribution in the western Mediterranean is governed by a highly non-linear, multi-layered trophic template, with Random Forest outperforming GAM by capturing threshold interactions among SST, subsurface nutrients, and deep prey proxies. In conclusion, all the RCP scenarios examined agree in predicting a progressive dispersion of the suitable habitat for the fin whale towards the southern part of the Tyrrhenian Sea, as well as an expansion over the waters of the Algerian Basin and the Balearic Sea, against a marked and general decrease in environmental suitability in the Ligurian Sea. Therefore, appears to be an apparent link between the areas with the highest probabilities and the areas with the highest temperatures and greatest depths.

Despite extensive research, the migratory behaviour of fin whales in the Mediterranean remains incompletely understood; for this reason, part of the introduction focused on biology, ecology and anthropogenic impacts of humans. Findings reinforce species conservation amid a shifting Mediterranean Sea by emphasizing the priority of dynamic, location-specific hotspots and enhanced surveillance in understudied regions. Future work must integrate trophic flux modelling (Nutrient→phytoplankton→krill→whale) and riverine nutrient inputs currently unavailable due to fragmented private datasets to quantify cascade effects and refine dynamic MPAs along projected corridors and canyon refugia (Richardson et al., 2008).

We must remember that models are not reality, models simplify reality by omitting unmeasured processes (specific krill dynamics, river flows, behavioural plasticity) and rely on averaged data that obscure small-scale transient oceanographic features.

Personal consideration for enhanced cetacean protection:

- Voluntary speed limits for recreational vessel should be implemented as mandatory to minimize collision risk and acoustic disturbance, especially in Balearic Sea and Gulf of Lion
- Large vessels as cruises pose a disproportionate collision threat and promote unsustainable, no eco-friendly tourism: passengers spend minimal time ashore, visit multiple sites hastily, and contribute little to local economies.
- Users in jet ski should be regulated, they frequently ignore speed limits and approach distance to cetaceans. Disturbance is severe, users chase cetaceans, circle them, or even dive in disrupting the natural behaviour. A complete ban in MPAs, mandatory permits, and real-time tracking are recommended.
- Increase collaboration between governments, NGOs, ferry operators, and citizen-science platforms to share sightings, enforce regulations, and fund rapid-response stranding teams.
- Increase collaboration between governments, NGOs, ferry operators, and citizen-science platforms to share sightings, enforce regulations, and fund rapid-response stranding teams
- EU and national governments must increase budgets for cetacean monitoring, research, and enforcement agencies.
- Despite EU regulations, many operators of whale watching activity violate minimum approach distances (100 m), pursue animals, or position vessels directly overhead. Mandatory accreditation, onboard naturalists, and drone/AIS monitoring are critical to transform this industry into a truly sustainable one.

6. BIBLIOGRAPHY

- Aguilar, A. & García-Vernet, R. (2018). Fin whale, *Balaenoptera physalus*. In W. F. Perrin, B. Würsig & J. G. M. Thewissen (Eds.), *Encyclopedia of Marine Mammals*
- Aïssi, M., Celona, A., Comparetto, G., Mangano, R., Würtz, M., & Moulins, A. (2007). Large-scale seasonal distribution of fin whales (*Balaenoptera physalus*) in the central Mediterranean Sea. *Journal of the Marine Biological Association of the United Kingdom*, 88(6), 1253–1261. doi:10.1017/S0025315408000891
- Albouy, C., Delattre, V., Donati, G., Frölicher, T. L., Albouy-Boyer, S., Rufino, M., Pellissier, L., Mouillot, D., & Leprieur, F. (2020). Global vulnerability of marine mammals to global warming. *Scientific Reports*, 10(1), Article 548. <https://www.nature.com/articles/s41598-019-57280-3>
- Aracri, S. (2019). The seasonal and interannual variability of the Ligurian Sea (Doctoral dissertation, University of Southampton). University of Southampton Institutional Repository.
- Arcangeli, A., Orasi, A., Carcassi, S. P., & Crosti, R. (2012). Exploring thermal and trophic preference of *Balaenoptera physalus* in the central Tyrrhenian Sea: A new summer feeding ground? *Mar Biol* (2014) 161:427–436 DOI 10.1007/s00227-013-2348-8
- Arrigoni, M., Manfredi, P., Panigada, S., Bramanti, L., & Santangelo, G. (2010). Life-history tables of the Mediterranean fin whale from stranding data. *Marine Ecology*. ISSN 0173-9565 doi:10.1111/j.1439-0485.2011.00437.x
- Asociación Tursiops (Palma de Mallorca) 2025 <https://www.asociaciontursiops.org/>
- Bauer, R. K., Fromentin, J.-M., Demarcq, H., Brisset, B., & Bonhommeau, S. (2015). Co-Occurrence and habitat use of fin whales, striped dolphins and Atlantic bluefin tuna in the northwestern Mediterranean Sea. *PLoS ONE* 10(10): e0139218. doi:10.1371/journal.pone.0139218
- Bentaleb, I., Martin, C., Vrac, M., Mate, B., Mayzaud, P., Siret, D., de Stephanis, R., & Guinet, C. (2011). Foraging ecology of Mediterranean fin whales in a changing environment elucidated by satellite tracking and baleen plate stable isotopes. *Marine Ecology Progress Series*, 438, 285–302. doi: 10.3354/meps09269
- Bhagarathi, L. K., DaSilva, P. N. B., Maharaj, G., Balkarran, R., & Baksh, A. (2024). The impact of anthropogenic sound on marine mammals: A review. *International Journal of Life Science Research Archive*, 2024, 07(02), 009–033 DOI: <https://doi.org/10.53771/ijlsra.2024.7.2.0070>
- Bianchi, C. N., Morri, C., Chiantore, M., Montefalcone, M., Parravicini, V., & Rovere, A. (2012). Mediterranean Sea biodiversity between the legacy from the past and a future of change. In N. Stambler (Ed.), *Life in the Mediterranean Sea: A look at habitat changes* (pp. 1–55). Nova Science Publishers.
- Bittau L, Manconi R, Leotta M, Tenerelli R, Leone MC, Fontanesi E, et al. (2025) The Caprera Canyon (north–eastern Sardinia): A hotspot of

- cetacean diversity in the western Mediterranean Sea. *PLoS One* 20(7): e0326426. <https://doi.org/10.1371/journal.pone.0326426>
- Brancato, G., Minutoli, R., Granata, A., Sidoti, O., & Guglielmo, L. (2001). Diversity and vertical migration of euphausiids across the Straits of Messina area. In *Proceedings of the 35th Mediterranean Ecosystems: Structures and Processes*, University of Messina.
 - Cañadas A, Pierantonio N, Araujo H, David L, Di Meglio N, Doremus G, Gonzalvo J, Holcer D, Laran S, Lauriano G, Perri M, Ridoux V, Vázquez JA and Panigada S (2023) Distribution patterns of marine megafauna density in the Mediterranean Sea assessed through the ACCOBAMS Survey Initiative (ASI). *Front. Mar. Sci.* 10:1270917 doi: 10.3389/fmars.2023.1270917
 - Canese, S., Cardinali, A., Fortuna, C. M., Giusti, M., Lauriano, G., Salvati, E., & Greco, S. (2006). The first identified winter feeding ground of fin whales (*Balaenoptera physalus*) in the Mediterranean Sea. *ICRAM*
 - Castellote, M., Clark, C., Lammers, M., Fin whale (*Balaenoptera physalus*) population identity in the western Mediterranean Sea, 2011. *MARINE MAMMAL SCIENCE*, 28(2): 325–344 (April 2012) DOI: 10.1111/j.1748-7692.2011.00491.x
 - Copernicus Climate Change Service (C3S). (2020). Copernicus Climate Data Store (CDS). European Centre for Medium-Range Weather Forecasts (ECMWF), Marine biogeochemistry data for the Northwest European Shelf and Mediterranean Sea from 2006 up to 2100 derived from climate projections.
 - Cotté, C., Guinet, C., Taupier-Letage, I., Mate, B., & Petiau, E. (2009). Scale-dependent habitat use by a large free-ranging predator, the Mediterranean fin whale. *Deep-Sea Research Part I: Oceanographic Research Papers*, 56. doi:10.1016/j.dsr.2008.12.008
 - D'Amen, M., Fortuna, C. M., Holcer, D., Panigada, S., Bonora, N., & Lauriano, G. (2024). Climate change and cetacean habitat suitability in the Mediterranean Sea: A challenge for Marine Strategy Framework Directive D1C4, D1C5 criteria. *Animal Conservation* (2024) doi:10.1111/acv.13002
 - De Stephanis, R., Cornulier, T., Verborgh, P., Salazar Sierra, J., Pérez Gimeno, N., & Guinet, C. (2008). Summer spatial distribution of cetaceans in the Strait of Gibraltar in relation to the oceanographic context. *Marine Ecology Progress Series*, 353, 275, 2008
 - Derville S, Barlow DR, Hayslip C and Torres LG (2022) Seasonal, Annual, and Decadal Distribution of Three Rorqual Whale Species Relative to Dynamic Ocean Conditions Off Oregon, USA. *Front. Mar. Sci.* 9:868566. doi: 10.3389/fmars.2022.868566
 - Druon, J.-N., Panigada, S., David, L., Gannier, A., Mayol, P., Arcangeli, A., Cañadas, A., Laran, S., Di Meglio, N., & Gauffier, P. (2012). Potential feeding habitat of fin whales in the western Mediterranean Sea: An environmental niche model. *Mar Ecol Prog Ser Vol.* 464: 289–306, 2012 doi: 10.3354/meps09810
 - Elith, J., & Leathwick, J. R. (2009). Species distribution models: Ecological explanation and prediction across space and time. *Annual Review of Ecology, Evolution, and Systematics*, 40, 677–97. doi: 10.1146/annurev.ecolsys.110308.120159

- Erbe C, Marley SA, Schoeman RP, Smith JN, Trigg LE and Embling CB (2019) The Effects of Ship Noise on Marine Mammals—A Review. *Front. Mar. Sci.* 6:606. doi: 10.3389/fmars.2019.00606
- Espada, R.; Camacho-Sánchez, A.; Olaya-Ponzzone, L.; Martín-Moreno, E.; Patón, D.; García-Gómez, J.C. Fin Whale *Balaenoptera physalus* Historical Sightings and Strandings, Ship Strikes, Breeding Areas and Other Threats in the Mediterranean Sea: A Review (1624–2023). *Environments* 2024,11,104. <https://doi.org/10.3390/environments11060104>
- European Commission. (2023). Descriptors under the Marine Strategy Framework Directive. *Environment*. https://environment.ec.europa.eu/topics/marine-environment/descriptors-under-marine-strategy-framework-directive_en
- Evans, J. S., Murphy, M. A., Holden, Z. A., & Cushman, S. A. (2011). Modeling species distribution and change using Random Forest. In C. A. Drew, Y. Huettmann, & F. Huettmann (Eds.), *Predictive species and habitat modeling in landscape ecology: Concepts and applications* (pp. 139–159 DOI 10.1007/978-1-4419-7390-0_8,
- Fossi MC, Romeo T, Bains M, Panti C, Marsili L, Campani T, Canese S, Galgani F, Druon J-N, Airolti S, Taddei S, Fattorini M, Brandini C and Lapucci C (2017) Plastic Debris Occurrence, Convergence Areas and Fin Whales Feeding Ground in the Mediterranean Marine Protected Area Pelagos Sanctuary: A Modeling Approach. *Front. Mar. Sci.* 4:167. doi: 10.3389/fmars.2017.00167
- Fossi, M. C., Marsili, L., Bains, M., Giannetti, M., Coppola, D., Guerranti, C., Caliani, I., Minutoli, R., Lauriano, G., Finioia, M. G., Rubegni, F., Panigada, S., Bérubé, M., Urbán Ramírez, J., & Panti, C. (2015). Fin whales and microplastics: The Mediterranean Sea and the Sea of Cortez scenarios. *Environmental Pollution*, 209, 68–78. <http://dx.doi.org/10.1016/j.envpol.2015.11.022>
- Fossi, M. C., Panti, C., Guerranti, C., Coppola, D., Giannetti, M., Marsili, L., & Minutoli, R. (2012). Are baleen whales exposed to the threat of microplastics? A case study of the Mediterranean fin whale (*Balaenoptera physalus*). *Marine Pollution Bulletin*, 64, 2374–2379. <http://dx.doi.org/10.1016/j.envpol.2015.11.022>
- Gambaiani, D. D., Mayol, P., Isaac, S. J., & Simmonds, M. P. (2007). Potential impacts of climate change and greenhouse gas emissions on Mediterranean marine ecosystems and cetaceans. *Journal of the Marine Biological Association of the United Kingdom*, 89 (1), 179-201. <https://doi.org/10.1017/S0025315408002476>
- Gauffier, P., Borrell, A., Silva, M. A., Víkingsson, G. A., López, A., Giménez, J., Colaço, A., Halldórsson, S. D., Vighi, M., Prieto, R., de Stephanis, R., & Aguilar, A. (2020). Wait your turn, North Atlantic fin whales share a common feeding ground sequentially. *Marine Environmental Research* 155 (2020) 104884 <https://doi.org/10.1016/j.marenvres.2020.104884>
- Gauffier, P., Verborgh, P., Giménez, J., Esteban, R., Salazar Sierra, J. M., & de Stephanis, R. (2018). Contemporary migration of fin whales through

- the Strait of Gibraltar. *Marine Ecology Progress Series*, Vol. 588: 215–228, 2018 <https://doi.org/10.3354/meps12449>
- Geijer, C. K. A., Notarbartolo di Sciara, G., & Panigada, S. (2015). Mysticete migration revisited: are Mediterranean fin whales an anomaly? *Mammal Review* ISSN 0305-1838 doi: 10.1111/mam.12069
 - Gerber, L. R., Morissette, L., Kaschner, K., & Pauly, D. (2009). Should whales be culled to increase fishery yield? *Science*, 323 Science Mag Vol 323
 - Germanov, E. S., Marshall, A. D., Bejder, L., Fossi, M. C., & Loneragan, N. R. (2018). Microplastics: No small problem for filter-feeding megafauna. *Trends in Ecology & Evolution*, 33(4), 239–242.
 - Grau Tomá s E and Garc ía Sanabria J (2022) Comparative analysis of marine-protected area effectiveness in the protection of marine mammals: Lessons learned and recommendations *Front. Mar. Sci.* 9:940803. doi: 10.3389/fmars.2022.940803
 - Grossi, F., Hazen, E. L., De Leo, G., David, L., Di-Méglio, N., Arcangeli, A., Pasanisi, E., Campana, I., Paraboschi, M., Castelli, A., Rosso, M., Moulins, A., & Tepsich, P. (2025). Evaluating three modelling frameworks for assessing changes in fin whale distribution in the Mediterranean Sea. *Marine Ecology Progress Series*, 2025; 15:e71007 <https://doi.org/10.1002/ece3.71007>
 - Hassoun, A. E. R., Mojtahid, M., Merheb, M., Lionello, P., Gattuso, J.-P., & Cramer, W. (2025). Climate change risks on key open marine and coastal mediterranean ecosystems. *Scientific Reports*, Article 24907 <https://doi.org/10.1038/s41598-025-07858-x>
 - International Whaling Commission, IUCN, & ACCOBAMS. (2020). A joint IWC-IUCN-ACCOBAMS workshop to evaluate how the data and process used to identify Important Marine Mammal Areas (IMMAs) can assist the IWC to identify areas of high risk for ship strike [Workshop report]. International Whaling Commission.
 - Kavanagh, A. S., Nykänen, M., Hunt, W., Richardson, N., & Jessopp, M. J. (2019). Seismic surveys reduce cetacean sightings across a large marine ecosystem. *Scientific Reports*, 9, 19164. <https://doi.org/10.1038/s41598-019-55500-4>
 - Lange, M. A. (2015). Climate change in the Mediterranean: Environmental impacts and extreme events. *European Institute of the Mediterranean, IEMedMediterranean Yearbook*
 - Laran, S., Pettex, E., Authier, M., Blanck, A., David, L., Dorémus, G., Falchetto, H., Monestiez, P., Van Canneyt, O., & Ridoux, V. (2016). Seasonal distribution and abundance of cetaceans within French waters— Part I: The North-Western Mediterranean, including the Pelagos sanctuary. *Deep Sea Research Part II*: 141, 20–30. <http://dx.doi.org/10.1016/j.dsr2.2016.12.011>
 - Lazzari, P., Solidoro, C., Salon, S., & Bolzon, G. (2016). Spatial variability of phosphate and nitrate in the Mediterranean Sea: A modeling approach. *Deep-Sea Research Part I: Oceanographic Research Papers*, 108, 39-52 <http://dx.doi.org/10.1016/j.dsr.2015.12.006>
 - Mannocci, L., Catalogna, M., Dorémus, G., Laran, S., Lehodey, P., Massart, W., Monestiez, P., Van Canneyt, O., Watremez, P., & Ridoux, V.

- (2013). Predicting cetacean and seabird habitats across a productivity gradient in the South Pacific gyre. *Progress in Oceanography*, 120, 383–398. <http://dx.doi.org/10.1016/j.pocean.2013.11.005>
- McGehee, D. E., Demer, D. A., & Warren, J. D. (2004). Zooplankton in the Ligurian Sea: Part I. Characterization of their dispersion, relative abundance and environment during summer 1999. *Journal of Plankton Research*, 26 (12), 1409-1418 doi:10.1093/plankt/fbh132,
 - Mi, C., Huettmann, F., Guo, Y., Han, X., & Wen, L. (2016). Why choose Random Forest to predict rare species distribution with few samples in large undersampled areas? Three Asian crane species models provide supporting evidence.
 - Millot, C., & Taupier-Letage, I. (2005). Circulation in the Mediterranean Sea. In K. Hanaki (Ed.), *Hdb Env Chem Vol. 5, Part K* (2005): 29–66 DOI 10.1007/b107143
 - Mizroch, S. A., Rice, D. W., & Breiwick, J. M. (1984). The fin whale, *Balaenoptera physalus*. *Marine Fisheries Review*
 - Mussi, B., Miragliuolo, A., De Pippo, T., Gambi, M. C., & Chiota, D. (1997). The submarine canyon of Cuma (Southern Tyrrhenian Sea, Italy), a cetacean key area to protect. In *Proceedings of the 17th Annual Conference of the European Cetacean Society* (pp. 1–6). European Cetacean Society.
 - Notarbartolo di Sciara, G., Castellote, M., Druon, J.-N., & Panigada, S. (2016). Fin whales, *Balaenoptera physalus*: At home in a changing Mediterranean Sea? (*Advances in Marine Biology*, Vol. 75, pp. 75-101. <http://dx.doi.org/10.1016/bs.amb.2016.08.002>
 - Notarbartolo Di Sciara, G., Zanardelli, M., Jahoda, M., Panigada, S., & Airoidi, S. (2003). The fin whale *Balaenoptera physalus* (L. 1758) in the Mediterranean Sea. *Mammal Review*, Vol 33 105-150
 - OBIS (2025) Ocean Biodiversity Information System. Intergovernmental Oceanographic Commission of UNESCO. <https://obis.org>.
 - Pace, D. S., Tizzi, R., & Mussi, B. (2015). Cetaceans value and conservation in the Mediterranean Sea. *Journal of Marine Science: Biodiversity and endangered species* <http://dx.doi.org/10.4172/2332-2543.S1.004>
 - Panigada V, Bodey TW, Friedlaender A, Druon J-N, Huckstädt LA, Pierantonio N, Degollada E, Tort B, Panigada S. 2024 Targeting fin whale conservation in the North-Western Mediterranean Sea: insights on movements and behaviour from biologging and habitat modelling. *R. Soc. Open Sci.* 11: 231783. <https://doi.org/10.1098/rsos.231783>
 - Panigada, S., Donovan, G. P., Druon, J.-N., Lauriano, G., Pierantonio, N., Pirota, E., Zanardelli, M., Zerbini, A. N., & Notarbartolo di Sciara, G. (2017). Satellite tagging of Mediterranean fin whales: Working towards the identification of critical habitats and the focusing of mitigation measures. *Scientific Reports* | 7: 3365 | DOI:10.1038/s41598-017-03560-9
 - Panigada, S., Gauffier, P. & Notarbartolo di Sciara, G. 2021. *Balaenoptera physalus* (Mediterranean subpopulation). The IUCN Red List of Threatened Species 2021: e.T16208224A50387979.

<https://dx.doi.org/10.2305/IUCN.UK.20213.RLTS.T16208224A50387979.en>

- Panigada, S., Pesante, G., Zanardelli, M., Capoulade, F., Gannier, A., & Weinrich, M. T. (2006). Mediterranean fin whales at risk from fatal ship strikes. *Marine Pollution Bulletin*, 52, 1287–1298.
- Panti, C., Bains, M., Lusher, A., Hernandez-Milan, G., Bravo Rebolledo, E. L., Unger, B., Syberg, K., Simmonds, M. P., & Fossi, M. C. (2019). Marine litter: One of the major threats for marine mammals. Outcomes from the European Cetacean Society workshop. *Environmental Pollution*, 247, 72-79.
- Papale, E., Arcangeli, A., Azzellino, A., Bellingeri, M., Bergamini, G., Buscaino, G., Calogero, G., Cañadas, A., David, L., De Stephanis, R., Di-Mégli, N., Lanfredi, C., Giacomini, C., Gnone, G., Mussi, B., Pace, D. S., Pintore, L., Pireddu, L., Salazar-Sierra, J. M., Tepsich, P., Violi, B., & Giovannini, A. (2025). Seasonal habitat suitability and distribution patterns of Mediterranean fin whales. *Global Ecology and Conservation* <https://doi.org/10.1016/j.ecoinf.2025.103362>
- Peltier H, Beaufils A, Cesarini C, Dabin W, Dars C, Demaret F, Dhermain F, Doremus G, Labach H, Van Canneyt O and Spitz J (2019) Monitoring of Marine Mammal Strandings Along French Coasts Reveals the Importance of Ship Strikes on Large Cetaceans: A Challenge for the European Marine Strategy Framework Directive. *Front. Mar. Sci.* 6:486. doi: 10.3389/fmars.2019.00486
- QGIS Development Team. QGIS Geographic Information . QGIS Association, version: 3.40.4-Bratislava URL: <https://www.qgis.org>.
- Rahav, E., Herut, B., Levi, A., Mulholland, M. R., and Berman-Frank, I. (2012): Springtime contribution of dinitrogen fixation to primary production across the Mediterranean Sea, *Ocean Sci.*, 9, 489–498 <https://doi.org/10.5194/os-9-489-2013>
- Richardson, A. J. (2008). In hot water: Zooplankton and climate change. *ICES Journal of Marine Science*, 65, 279–295. <https://academic.oup.com/icesjms/article/65/3/279/787309>
- Robinson NM, Nelson WA, Costello MJ, Sutherland JE and Lundquist CJ (2017) A Systematic Review of Marine-Based Species Distribution Models (SDMs) with Recommendations for Best Practice. *Front. Mar. Sci.* 4:421. doi: 10.3389/fmars.2017.00421
- Roman, J., Estes, J. A., Morissette, L., Smith, C., Costa, D., McCarthy, J., Nation, J. B., Nicol, S., Pershing, A., & Smetacek, V. (2014). Whales as marine ecosystem engineers. *Frontiers in Ecology and the Environment* doi:10.1890/130220
- RStudio: Integrated Development Environment for R. Posit team (2025). Posit Software, PBC, Boston, MA. URL <https://rstudio-education.github.io/hopr/starting.html>
- Sciacca V, Caruso F, Beranzoli L, Chierici F, De Domenico E, Embriaco D, et al. (2015) Annual Acoustic Presence of Fin Whale (*Balaenoptera physalus*) Offshore Eastern Sicily, Central Mediterranean Sea. *PLoS ONE* 10(11): e0141838. doi:10.1371/journal.pone.0141838
- Sèbe, M., David, L., Dhermain, F., Gourguet, S., Madon, B., Ody, D., Panigada, S., Peltier, H., & Pendleton, L. (2023). Estimating the impact of

- ship strikes on the Mediterranean fin whale subpopulation. *Ocean & Coastal Management*, 237
<https://doi.org/10.1016/j.ocecoaman.2023.106485>
- Stephens, G., Akkaya Bař, A., Hardy, J., Awbery, T., Rudd, L., Abbiss, L., Araç, N., & Lyne, P. (2021). Sightings and stranding reports of fin whales (*Balaenoptera physalus*) in the Levantine Sea. *J. Cetacean. Res. Manage.* 22, 2021
 - Tepsich P, Schettino I, Atzori F, Azzolin M, Campana I, Carosso L, Cominelli S, Crosti R, David L, Di-Méglio N, Frau F, Gregoriotti M, Mazzucato V, Monaco C, Moulins A, Paraboschi M, Pellegrino G, Rosso M, Roul M, Saintignan S, Arcangeli A. 2020. Trends in summer presence of fin whales in the Western Mediterranean Sea Region: new insights from a long-term monitoring program. *PeerJ* 8:e10544
<http://doi.org/10.7717/peerj.10544>
 - Torreblanca E, Camiñas JA, Macías D, García-Barcelona S, Real R, Báez JC. 2019. Using opportunistic sightings to infer differential spatio-temporal use of western Mediterranean waters by the fin whale. *PeerJ* 7:e6673 DOI 10.7717/peerj.6673
 - Tort, B., & Degollada, E. (2023). Fin Whale Project Report 2023: Results of the study of the fin whale on its route around the Iberian Peninsula. EDMAKTUB Association. https://edmaktub.org/wp-content/uploads/2024/05/Report_Fin_Whale_Project_2023.pdf
 - Weilgart, L. S. (2007). The impacts of anthropogenic ocean noise on cetaceans and implications for management. Published on the NRC Research
 - Williams, R., Cholewiak, D., Clark, C. W., Erbe, C., George, J. C., Lacy, R. C., Leaper, R., Moore, S. E., New, L., Parsons, E. C. M., Rosenbaum, H. C., Rowles, T. K., Simmonds, M. P., Stimmelmayer, R., Suydam, R. S., & Wright, A. J. (2020). Chronic ocean noise and cetacean population models. *Journal of Cetacean Research and Management*, 21: 85-94.
 - Williams, R., Cholewiak, D., Clark, C. W., Erbe, C., George, J. C., Lacy, R. C., Leaper, R., Moore, S. E., New, L., Parsons, E. C. M., Rosenbaum, H. C., Rowles, T. K., Stimmelmayer, R., Suydam, R. S., & Wright, A. J. (2020). Chronic ocean noise and cetacean population models *Endangered Species Research*, 42, 77–95.
 - Zanardelli, M., Airoidi, S., Bérubé, M., Borsani, J. F., Di-Meglio, N., Gannier, A., Hammond, P. S., Jahoda, M., Lauriano, G., Notarbartolo di Sciara, G., & Panigada, S. (2022). Long-term photo-identification study of fin whales in the Pelagos Sanctuary (NW Mediterranean) as a baseline for targeted conservation and mitigation measures. Research article DOI: 10.1002/aqc.3865